STUDIES ON HETEROGENEOUS CATALYTIC SYNTHESIS OF BIODIESEL AND ADDITIVES FROM BIO-RESOURCES

Thesis Submitted by:

Piasy Pradhan

Doctor of Philosophy (Engineering)

Department of Chemical Engineering

Faculty Council of Engineering & Technology

JADAVPUR UNIVERSITY

Kolkata, India

2018

Dedicated to my beloved

FATHER

CERTIFICATE FROM THE SUPERVISOR

This is to certify that the thesis entitled "**Studies on heterogeneous catalytic synthesis of biodiesel and additives from bio-resources**" submitted by Smt. **Piasy Pradhan**, who got her name registered on 13.7.2011 for the award of Ph.D. (Engineering) degree of Jadavpur University is absolutely based upon her own work under the supervision of Prof. (Dr.) Rajat Chakraborty, Department of Chemical Engineering, Jadavpur University and that neither her thesis nor any part of the thesis has been submitted for any degree/diploma or any other academic award anywhere before.

Prof. (Dr.) Rajat Chakraborty

Department of Chemical Engineering

Jadavpur University

JADAVPUR UNIVERSITY

KOLKATA- 700032, INDIA

INDEX NO. 198/11/E

1. Title of the thesis: Studies on heterogeneous catalytic synthesis of biodiesel and additives from bio-resources.

2. Name, Designation & Institution of the Supervisor:

Prof. (Dr.) Rajat Chakroborty

Professor

Department of Chemical Engineering

Jadavpur University

3. List of Publication:

1. Optimal efficient biodiesel synthesis from used oil employing low-cost ram bone supported Cr catalyst: Engine performance and exhaust assessment; **Piasy Pradhan**, Rajat Chakraborty; Energy 2018; 164: 35-45.

2. Optimization of infrared radiated fast and energy-efficient biodiesel production from waste mustard oil catalyzed by Amberlyst 15: Engine performance and emission quality assessments; **Piasy Pradhan**, Sourojeet Chakraborty, Rajat Chakraborty; Fuel 2016; 173: 60–68.

3. Fly ash supported Ni—Fe solid acid catalyst for efficient production of diesel additive: intensification through far-infrared radiation; **Piasy Pradhan** and Rajat Chakraborty; Asia-Pac. J. Chem. Eng. 2016; 11: 4–13.

4. Prediction of Optimal Conditions in the Methanolysis of Mustard Oil for Biodiesel Production Using Cost-Effective Mg-Solid Catalysts; Rajat Chakraborty, Sukamal Das, **Piasy Pradhan**, and Punam Mukhopadhyay; Ind. Eng. Chem. Res. 2014; 53 (51): 19681–19689. (This work not included in the thesis).

4. List of Patents: None

5. List of Presentations in National/International:

1. Prediction of optimal conditions in methanolysis of mustard oil for biodiesel production using cost effective Mg-Solid catalyst. **Piasy Pradhan**, Rajat Chakraborty, Sukamal Das and Punam Mukhopadhyay; Energy System Modeling and optimization conference (ESMOC 2013); NIT Durgapur

2. Commercially important products derived from power plant fly ash: A review. **Piasy Pradhan** and Rajat Chakraborty; Environment Management on coal based thermal power plant in Indian perspective from 21st to 22nd December, 2013. ISBN 978-93-83360-04-8

3. Evaluation of Reaction Kinetics of Oleic Acid Esterification under In-situ Water Removal. Sourojeet Chakraborty, **Piasy Pradhan** and Rajat Chakraborty; CHEMCON 2013 66th Annual Indian Chemical Engineering Congress 27th to 30th December, 2013.

4. Optimization of Methyl Oleate Synthesis using Flyash supported Ni-Fe acid heterogeneous catalyst. **Piasy Pradhan**, Rajat Chakraborty; CHEMCON 2013 66th Annual Indian Chemical Engineering Congress 27th to 30th December, 2013.

ACKNOWLEDGEMENT

I would like to take the opportunity to convey my sincere gratitude, respect and deep regards to Prof. (Dr.) Rajat Chakraborty, Department of Chemical Engineering, Jadavpur University, for their kind cooperation, able guidance, constant help and encouragement without which it would not have been possible for me to shape this thesis in the present form.

Special thanks to Prof. Tapan Kumar Ghoshal, Emeritus Professor, Electrical Engineering, Centre for Knowledge Based Systems, Jadavpur University, for his valuable suggestions and mental supports during my research work.

I would like to specifically thanks Sourojeet Chakraborty, Sourav Barman, Epica Mondal, Poulami Karan, Labani Biswas, Pritam Chakraborty; those junior colleague helped me a lot in my research period.

I would also like to thanks the non-teaching staffs especially to Asoke Kr. Seal, Tapas Kr. Maity, Susanta Kr. Mondal, Devkumar Ari, Sankar Nath, Nirmal Das and Asim Kr. Bhattacharya of Department of Chemical Engineering, Jadavpur University; for their supports and help.

CONTENTS

LIST OF TABLES

LIST OF FIGURES

CHAPTER: 1

INTRODUCTION

1. INTRODUCTION

Nowadays, the energy crisis is one of the major problems of mankind. Day by day the demands of the fossil fuels are increasing but the reserves of natural resources i.e. coal, petroleum and natural gas are gradually decreasing. To fulfil the ever increasing demand of energy, biodiesel has become a viable alternative to the petro-diesel. Biodiesel, mono alkyl esters of long chain fatty acids can be derived through esterification of free fatty acid (FFA) or by transesterification triglycerides (TG) of different bio-resources (available in vegetable oils and animal fats) with monohydric alcohol (Figure 1.1.). It presents the advantages of low emission of carbon monoxide, particulate matter and unburned hydrocarbons. Besides, biodiesel (B100) also facilitates lowering engine exhaust temperature, thus can help in mitigating global warming. Therefore, in recent years, biodiesel production has been highly promoted which can be achieved either through heterogeneous or homogeneous catalytic route.

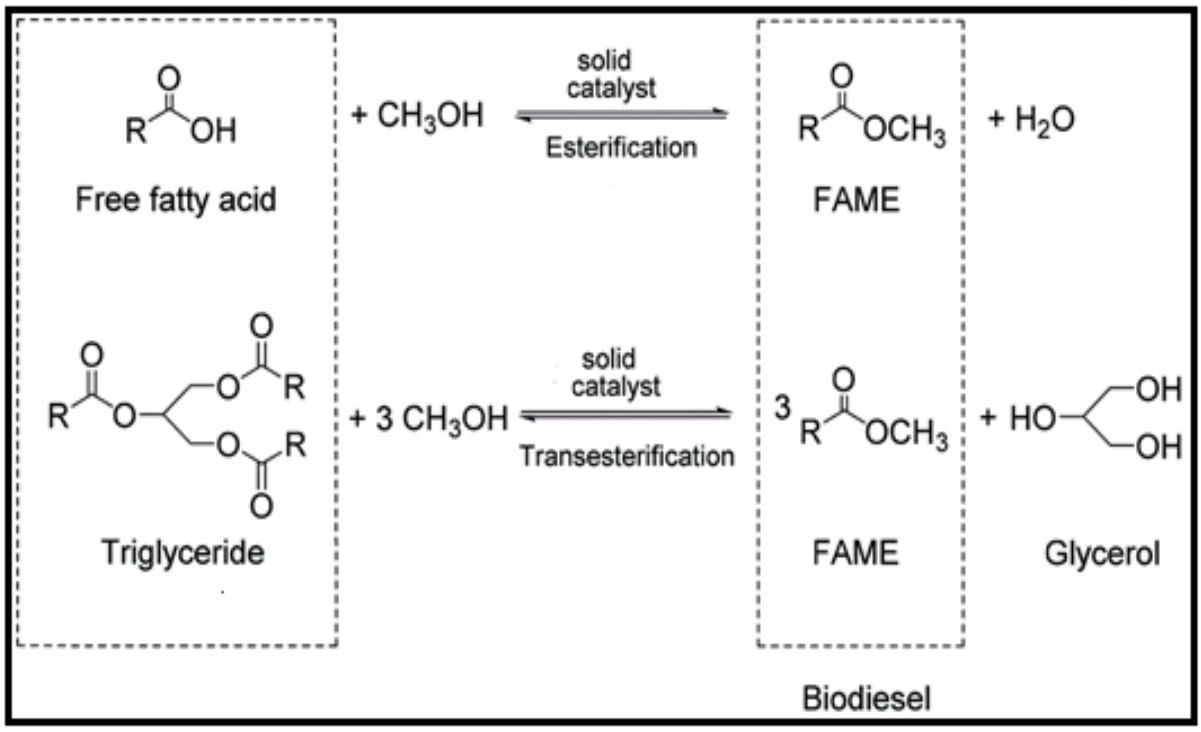

Figure 1.1. Esterification and Transesterification reaction for biodiesel. production.

1.1. Biodiesel

The non-renewable energy resources viz. fossil fuels (coal and crude oil) account for the major amount of the total energy utilization. Notably, the adverse environmental impact of crude oil derived petro-diesel is manifested as global warming and overall climate change. The rapid depletion of non-renewable resource as well as owing to the necessity to mitigate the adverse effects of fossil fuels, researchers have long been searching for alternative renewable and sustainable energy sources. Production of biodiesel from non-food feed stocks in an environment friendly, cost-effective and sustainable manner can provide a long term energy security by supplementing conventional energy resources, thereby, reducing dependence on fossil fuels and meeting increasing energy needs. Hence, sustainable production of biodiesels through energy-efficient, cost-effective and environmentally benign route has become utmost important to global researchers and technologists. In recent days, the scenario of energy resources are depicted in the Figure 1.2.

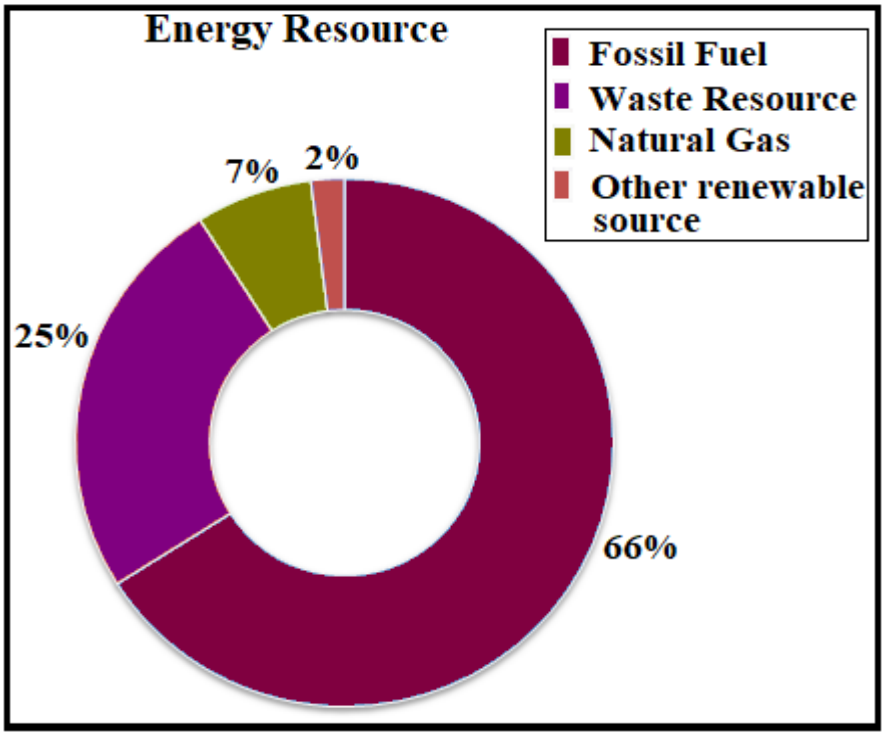

Figure 1.2. Percentages of existing different global energy resources.

Biodiesel is a renewable fuel derived from biomass feed stocks mainly vegetable oil (virgin, refined, unrefined and cooked oil), animal fat and other lipid containing feedstock. However, sustainability of biodiesel productions largely depends on availability of low cost feed stock. Furthermore, an advanced biofuel production is in budding stage as its commercial production and economic viability remains to be demonstrated. As per the global biofuel mandate, the biodiesel demand across several countries by 2022 has been illustrated in Figure 1.3.

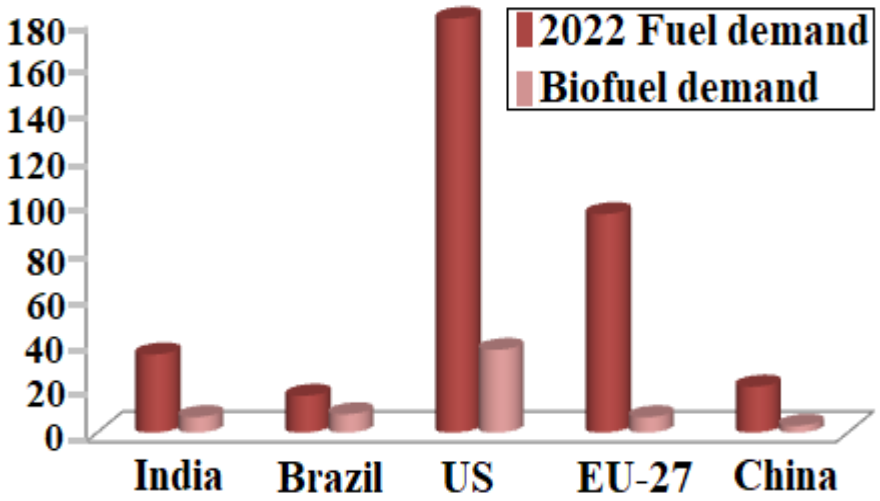

Figure 1.3. Projected Fuel demand and biofuel demand for 2022 in different countries (Biofuels Mandates Around the World : Biofuels Digest).

India, being fourth largest global contributor to carbon emission, has recently started using clean and green fuel. The government of India (GoI) transport policy has targeted EURO-III and IV as reference emission norms for vehicles. Furthermore, in order to meet the objective, on December 24, 2009 the Union Cabinet approved the National Policy on biofuels. The policy encourages use of renewable energy resources as alternate fuel to supplement transport fuels and had proposed an indicative target to replace 20% of petroleum fuel consumption with biofuels (bioethanol and biodiesel) by end of 12th Five-Year Plan (2017).

The GoI had launched the National Biodiesel Mission (NBM) identifying jatropha (*jatropha curcas*) as the most suitable inedible oilseed for biodiesel production. However, the GoI's ambitious plan of producing sufficient biodiesel by 2011/12 (marketing year October/September) to meet its mandate of 20% blending with diesel was unachievable mostly due to unavailability of sufficient feedstock (jatropha seeds) and lack of high-yielding drought-tolerant jatropha cultivars. Hence, most of the biodiesel units operating in India have shifted to alternative feed-stocks such as edible oil waste (unusable oil fractions), animal fat and inedible oils, utilizing almost 30% of their existing capacity to continue year round operations.

1.1.1. Biodiesel production and consumption patterns in India

An annual report on recent biofuel scenario of India was published on 27.6.2017 by Global Agricultural Information Network. From this report a clear scenario of biodiesel production and consumption pattern of India can be observed.

Presently, India has five plants with an installed capacity to generate 10,000 metric ton to 250,000 metric tons (MT) of biodiesel per year. Biodiesel industry based on *Jatropha curcus* feedstock in India seems to be somewhat a failure project. On the contrary, India is using many other feedstocks viz. used cooking oil, animal fats & tallows and other inedible vegetable oils for generation of biodiesel. From the Table 1.1.; we get a clear overview of the feedstock utilization pattern from the year 2009 to 2018. The information provided in Table 1.1. clearly indicates growing trend in use of used cooking oil and other oils (other than *Jatropha curcus*). Remarkably, the growth of utilization of used cooking oil for biodiesel production has been 115% between the year 2009 and 2018.

Table 1.1. Feedstock for biodiesel production (in 1000 MT) in India from year 2009 to 2018

Year	2009	2010	2011	2012	2013	2014	2015	2016	2017	2018
Used cooking oil	35	38	42	48	50	55	60	65	70	75
Animal Fats & Tallow's	3	6	6	7	7	6	5	6	6	8
Other Oils	30	50	58	60	65	65	70	70	70	70

Table 1.2 provides a report of beginning stocks, production, imports, exports, consumption and ending stocks of biodiesel in India over recent years (2009 to 2018).

Table 1.2. Details of biodiesel inventory in India over recent years (2009 to 2018)

Year	2009	2010	2011	2012	2013	2014	2015	2016	2017	2018
Beginning stocks	0	45	36	29	30	23	14	11	11	12
Production	75	99	111	121	128	132	142	148	153	161
Imports	0	0	0	0	0	2	1	3	2	3
Exports	0	0	0	0	8	64	44	53	51	60
Consumption	30	108	118	120	128	79	101	98	104	104
Ending stocks	45	36	29	30	23	14	11	11	12	12

As per Table 1.2., it is evident that the production of biodiesel in India is steadily increasing on year to year basis since 2009; the continual increasing trend of biodiesel production

substantiates the growing demand for biodiesel use as an environment friendly biofuel to reduce carbon footprint.

Figure 1.4. further shows an ever increasing trend of biodiesel capacity use (%) over recent years (from 2009 to 20018) in India. The data depicted in Figure 1.4, thus evidences the positive growth pattern concerning biodiesel requirement in Indian context.

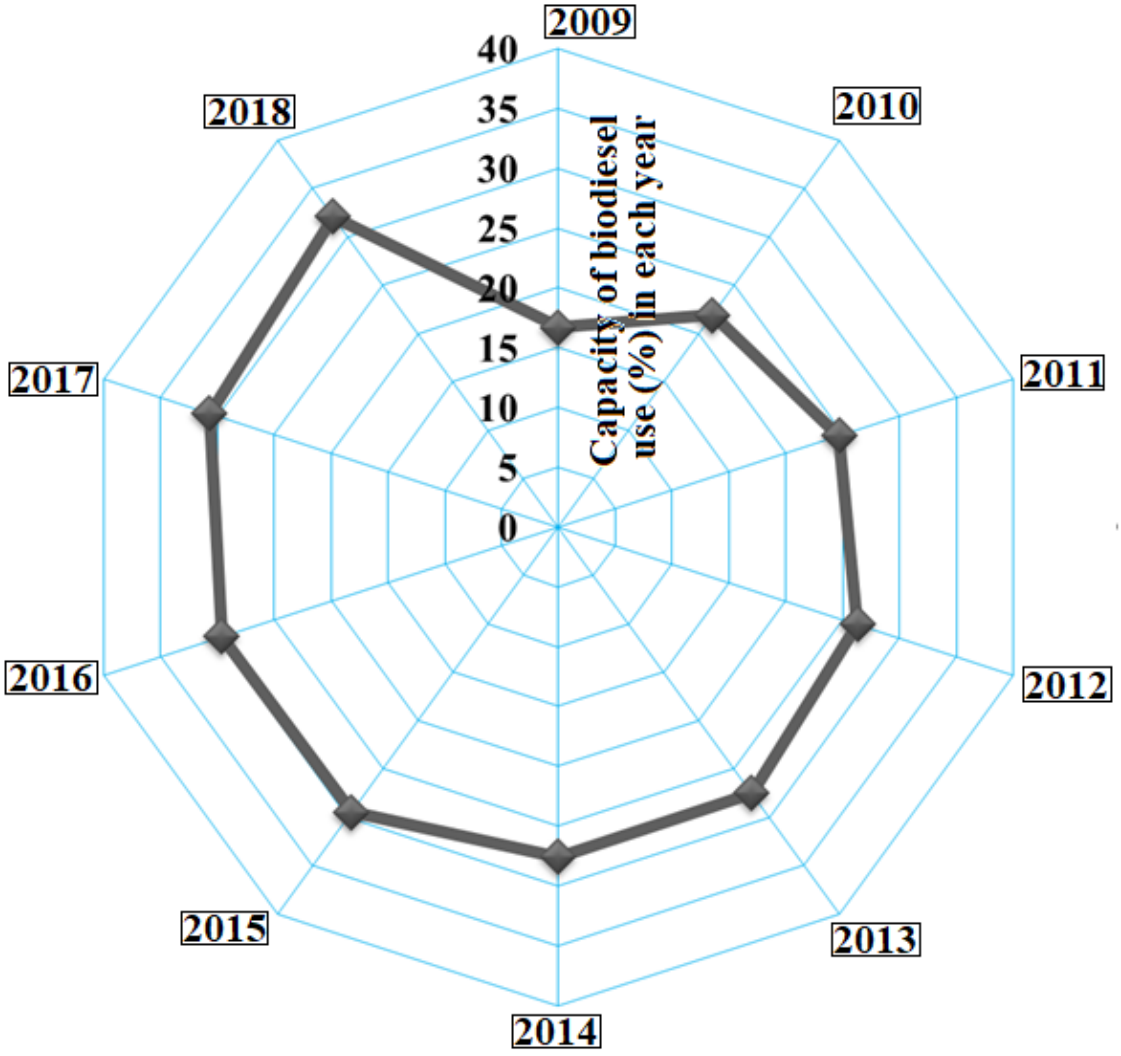

Figure 1.4. Biodiesel capacity utilization (%) growth pattern in India over recent years.

1.1.2. Biodiesel production and consumption patterns in US

US Energy Information Administration prepared and published a report in 2018 about the recent scenario of biodiesel production in US. Notably, canola oil, corn oil, soybean oil, poultry fats and animal tallow have been the major feed stocks for biodiesel production in US over recent years (the details are shown in Table 1.3.).

Table 1.3. Feed biodiesel production in stocks for US over recent years

Year	**2016**	**2017**	**2018** (3 months only: January, February, March)
Canola oil	1130	1452	331
Corn oil	1306	1579	451
Soybean oil	6117	6230	1582
Poultry fats	220	Data not provided	Data not provided
Animal tallow	332	Data not provided	Data not provided

It may be observed from Table 1.3. that soybean oil continues to be the major contributor in the production of biodiesel in US, while uses of poultry and animal fats as feedstock have not been reported for the last two years.

The statistics of production of B100 (i.e 100% biodiesel, unblended with petroleum-diesel), and sales of B100 included in biodiesel blended diesel fuels in US over the last few years are depicted in Table 1.4.

Table 1.4. B100 production and sales of B100 included in biodiesel blended fuels in US

Year	**2016**	**2017**	**2018** (3 months only: January, February, March)
B100 production	1569	1595	396
Sales of B100 included in biodiesel blends	767	923	224

Table 1.4. indicates a promising production and sales profiles concerning biodiesel over recent years in US; these data clearly motivate the researchers and practicing technologists to develop improved technology for economical and environment-friendly sustainable techniques for biodiesel production.

1.1.3. Biodiesel production and consumption patterns in EU

EU biofuels annual 2017 report was published by Global Agricultural Information Network on 21.6.2017. The EU is the world's largest biodiesel producer. For biodiesel (FAME) (fatty acid methyl ester) and hydrogenated vegetable oil (HVO) production, the typical feed-stocks used in EU are rapeseed oil, palm oil, used cooking oil (UCO), animal fats, soybean oil, sunflower oil and other virgin oils (pine oil, tall oil) and fatty acids.

Table 1.5. Feedstock consumption pattern for biodiesel and renewable diesel (HVO) (1,000 MT) in EU

Year	2011	2012	2013	2014	2015	2016	2017	2018
Rapeseed oil	6700	6750	5900	6400	6380	6140	6160	6150
Palm oil	940	1470	2360	2300	2600	2400	2610	2720
UCO	680	760	1100	110	2270	2440	2510	2950
Animal fats	340	350	410	940	965	1110	1140	1220
Soybean oil	950	810	890	850	430	590	620	710
Other (pine oil, tall oil, fatty acids)	50	90	180	170	185	350	355	375
Sunflower oil	10	0	0	0	15	5	5	5
Other virgin veg oil	280	320	310	330	210	250	160	170

From Table 1.5.; one can get a clear overview that, the use of UCO, animal fats and other (pine oil, tall oil, fatty acids) feedstock for biodiesel generation are increasing almost in each year from 2011 to 2018. On the contrary, a reverse declining utilization trend was observed for most of the refined vegetable oil feed-stocks viz. Rapeseed oil, Sunflower oil and Soybean oil in recent years. Thus, this clearly indicates that industrial biodiesel production is increasingly becoming more reliant on bio-waste derived feedstock viz. UCO, animal fat for economic and environment-friendly production of biodiesel.

The summary data on beginning stocks, production, imports, exports, consumption and ending stocks of biodiesel (FAME) and HVO in EU from 2011 to 2018 are provided in Table 1.6.

Table 1.6. Detailed inventory of biodiesel and HVO in EU from 2011 to 2018

Years	**2011**	**2012**	**2013**	**2014**	**2015**	**2016**	**2017**	**2018**
Beginning Stocks	530	575	600	540	590	590	595	620
Production	11344	11829	12417	14316	14436	14724	15295	16120
Imports	3164	3293	1393	632	541	579	570	570
Exports	100	116	416	182	245	408	450	450
Consumption	14363	14981	13454	14716	14732	14890	15390	16210
Ending Stocks	575	600	540	590	590	595	620	650

Table 1.6 provides a well-defined indication of gradual increment in biodiesel production and consumption profiles over recent year in EU. Hence, it may be concluded that there is a steady and increasing demand of biodiesel in EU.

1.2. Diesel Additives

Strict emission regulations in order to reduce the detrimental emanations (viz. CO, HC, PM etc.) from diesel engine have demanded the use of clean burning fuels. GoI has implemented different policies to promote the research on different potential renewable fuels and fuel additives. As per the legislative rules (National policy biofuels, Ministry of New & Renewable Energy), it has become a mandate to use 20% biodiesel blended diesel without compromising the design of the existing diesel engine. Thus, the recent researchers are focusing on the production of biodiesel or fatty acid ester of low molecular weight monohydric alcohol(s) from various waste vegetable resources which could efficiently serve as a potential diesel additive thereby improving the fuel properties along with engine emission and engine performance. Additives for pour point (cold flow properties) improvers for biodiesel/diesel.

1.3. Heterogeneous Catalyst

Homogeneous catalytic processes involve lower cost, higher yield of product and less time. Homogeneous catalysed (base type) biodiesel production has been already commercialized in India by Emami Agrotech Ltd. which is located in Haldia, West Bengal. The plant manufactures biodiesel from palm oil by using sodium methoxide as homogeneous base catalysts. 'Biodiesel Technologies' is another biodiesel producing company in India that utilizes neem oil, palm oil, rapseed oil, rice bain oil, waste vegetable oil, animal tallow for biodiesel production through transesterification reaction, however, no detailed information concerning catalyst has been available. 'Biodiesel Technorats' is yet another biodiesel manufacturer in India; wherein potassium hydroxide has been employed as a homogeneous base catalyst in transesterification reaction to produce biodiesel from jactropha curas. Nevertheless, it is an established fact that homogeneous catalysts encounter difficulty in separation and thus, generate enormous quantity of waste streams and are not reusable, whereas, on the other hand, heterogeneous catalyst is reusable and easily separable and does not pose problems related to biodiesel purification and waste stream generation. However, heterogeneous catalysts involving metal oxides are cost intensive which could increase the production cost of the overall process. Therefore, researchers around the globe have been focusing on utilization of different municipal and industrial waste in order to develop cost-effective heterogeneous catalysts that would make the process economically attractive besides facilitating waste management in a sustainable pathway.

1.3.1. Application of fly ash

Fly ash (FA), a solid waste of thermal power plants generated through coal combustion process at 1200-1700 ℃ temperature, is known as an environmental pollutant. Every year in

India about 75% of the electricity is generated through coal based thermal power plants, which produce more than 60 millions tones FA.

In last few decades, several technologies have been introduced for conversion of FA to value-added products viz., chemical fertilizer, bio-fertilizer, bio-pesticides. Notably, replacement of these chemical pesticides by bio-pesticides derived from FA is a step forward towards achieving sustainable agriculture. Furthermore, FA has also been employed for the manufacture of high quality ceramics and glass with better physical and chemical properties. In recent past, utilization of FA was found as a low-cost support for manufacturing of various efficient catalysts for catalytic reactions (Khatri and Rani, 2008) with desirable thermal stability. The use of such industrial waste materials for production of useful solid catalysts is a very important step towards environmental remediation. FA was successfully utilized to manufacture zeolites, which found usage in water purification, catalytic application and manufacture of advanced materials and nuclear reprocessing. From previous scientific reports, it could be seen that although fly ash supported catalysts were exhibited as capable of performing esterification and transesterification simultaneously to synthesize biodiesel from several low cost feed stocks with high FFAs (Peng et al., 2008); however, the acceptable catalytic activity was achieved at the expense of high reaction temperature (200 °C). Thus, further investigations are required for energy-efficient application of FA derived catalyst for production of useful ester. Kotwal et al., (2009) conducted a work by employing FA for preparation of KNO_3 doped FA, a solid-base heterogeneous catalyst, to produce methyl esters and glycerol through transesterification of sunflower oil.

1.3.2. Application of hydroxyapatite

Hydroxyapatite (HAp) is a naturally occurring mineral form of calcium apatite having the formula $Ca_5(PO_4)_3(OH)$, usually written as $Ca_{10}(PO_4)_6(OH)_2$ denoting that every crystal unit cell comprises of two entities.

Chemically synthesised HAp directly or in calcined form was used as a support for various catalysts has been reported revealing that HAp is an efficient catalyst carriess that clearly magnifies the efficiency of the catalyst and improves its functionality (Rasquinha et a1., 2002).

The HAp-based catalysts can be classified into- natural and chemical HAp. The natural sources of HAp varied widely ranging from fish bones, mammal bones, bird bones and fish scales. About 50% of animal bone is actually made of various forms of HAp (Junqueira and Carneiro, 2005). All the different sources have different impacts on the composition of the catalyst and render different catalytic properties. Chicken bone is one of the primary sources to derive natural HAp. The constituents of the chicken bone are very suitable for imparting useful properties to the catalyst. Among fish, animal and chicken bones, the calcium content of chicken bone was found to be 32.2%, while mammal bone is known to contain 35-36% Ca, indicating that it is better than its chicken counterpart (Phiraphinyo et. al., 2006). Although, the process of removing tissue from chicken bone is much easier, however, the amounts of impurities in fish bones were found to be considerably lower of chicken bone. Natural HAp (NHAp) derived catalysts have been recently applied for manufacture of biodiesel.

Chemical HAp (CHAp) based catalysts have been used for a variety of applications – in various areas of fuel synthesis including biodiesels, methane reforming, synthesis gas generation and hydrogen production. Hydrogen is considered as the fuel of the future as it is the most abundant element in the entire universe and hence, it source quantity is basically

unending. Presently, various processes are being developed which run on hydrogen, ranging from car engines to jet rockets. Hence, preparation of HAp supported catalysts that reduce the cost of hydrogen production and also increases the efficiency of the process will be a breakthrough. The CHAp catalyst is disadvantageous owing to the fact that it requires the use of reagent grade chemicals so as to develop the catalyst. Using NHAp as support for catalysts by utilising waste materials (bone, fish Scale etc.) coupled with use of cheap waste frying oils for biodiesel production can reduce the cost of production of manufacture of such bio fuels; thus, overcoming one of the chief hindrances for the sustainable production of biodiesel. Moreover, these inexpensive catalysts can be used for other purposes too and not only for production of fuels. These uses include dehydration of lactic acid to acrylic acid, oxidation of carbon mono oxide, so as to reduce the poisonous gas, glycerol carbonate production, claisen-schmidt condensation, alcohol oxidation and also the preparation of chalcones (Bai et. al., 2011 and Ghantani et. al., 2013). These processes generally use chemically synthesised HAp supported catalyst.

On the contrary, effective application of municipal wastes (animal bone, scales etc.) for preparation of NHAp could also help mitigating waste management problems (Sebti et. al., 2002 and Chakraborty et. al., 2010).

1.4. Application of infrared radiation

Infrared radiation is a visible electromagnetic wave, which has various applications in different fields. There are three types of infrared radiations i.e. near infrared, mid-wavelength infrared, and far-infrared radiation. Near infrared radiation corresponds to 0.75–1.4 μm wavelength, 214–400 THz frequency, 886–1653 meV photon energy and 3864–2070 K (3,591–1,797 ℃) temperature. It finds application for the determination of the quality of agricultural products (forages, grains, and grain products, oilseeds, coffee, tea, spices, fruits, vegetables, sugarcane, beverages, fats, and oils, dairy products, eggs, meat etc.) (Knipling, 1970; Mongpraneet et al, 2002). Near infrared radiation is also used in remote monitoring, materials science and medical science. Huang et al., 2006 reported that near infrared radiation could also be used for cancer therapy. Multiwalled carbon nanotubes and near-infrared radiation can also be used for treatment of kidney tumors (Burke et al., 2009).

Mid-wavelength infrared radiation is characterised by 3–8 μm wavelength, 37–100 THz frequency, 155–413 meV photon energy, 966–362 K (693–89 ℃) temperature and it is applied in medical science. As the mid–IR radiation could be connected with invisible chemical processes, it became possible to observe the biochemical processes (Waynant et al., 2001). Moreover, Seddon, (2011) reported for the first time mid-infrared medical endoscopy using chalcogenide glasses. However, mid-IR radiation has not been employed as thermal energy source for chemical/biochemical process.

Far-infrared (15–1000 μm wavelength, 0.3–20 THz frequency, 1.2–83 meV photon energy, 193–3 K (-80.15 – -270.15 ℃) temperature) radiation (FIR) is frequently used in medical science (Vatansever and Hamblin, 2012). Interestingly in recent days, FIR has also been applied as a thermal-energy source in reaction engineering to decrease the reaction time. For the first time Chakraborty and Sahu, 2013 reported the positive effects of FIR on

homogeneously catalysed simultaneous trans/esterification process for biodiesel synthesis from waste goat tallow. In last few decades, several intensification techniques viz., ultrasonication, microwave radiation had been applied to intensify the esterification and transesterification process to enhance biodiesel production. It has also been revealed that, microwave radiation is more energy consuming than infrared radiation. Hence, further investigation on application of FIR for intensification of heterogeneously catalysed chemical reaction for production of biodiesel and diesel additives (esters).

References

Bai, R., Wang, S., Mei, F., Li, T. and Li, G., 2011. Synthesis of glycerol carbonate from glycerol and dimethyl carbonate catalyzed by KF modified hydroxyapatite. Journal of Industrial and Engineering Chemistry, 17(4), pp.777-781.

Biofuels Mandates Around the World: Biofuels Digest. The world's most widely read biofuels daily; http://www.biofuelsdigest.com/bdigest.

Burke, A., Ding, X., Singh, R., Kraft, R.A., Levi-Polyachenko, N., Rylander, M.N., Szot, C., Buchanan, C., Whitney, J., Fisher, J. and Hatcher, H.C., 2009. Long-term survival following a single treatment of kidney tumors with multiwalled carbon nanotubes and near-infrared radiation. Proceedings of the National Academy of Sciences, pp.pnas-0905195106.

Chakraborty, R., Bepari, S. and Banerjee, A., 2010. Transesterification of soybean oil catalyzed by fly ash and egg shell derived solid catalysts. Chemical Engineering Journal, 165(3), pp.798-805.

Chakraborty, R. and Sahu, H., 2014. Intensification of biodiesel production from waste goat tallow using infrared radiation: process evaluation through response surface methodology and artificial neural network. Applied energy, 114, pp.827-836.

GAIN Report Number: IN7075, Date: 6/27/2017; Global Agricultural Information Network; Biofuels Annual Report of India 2017. This report contains assessments of commodity and trade issues made by USDA staff and not necessarily statements of official U.S. Government policy.

GAIN Report Number: NL7015 Date: 6/21/2017; EU Biofuels Annual 2017 Report of EU-28. This report contains assessments of commodity and trade issues made by USDA staff and not necessarily statements of official U.S. Government policy.

Ghantani, V.C., Lomate, S.T., Dongare, M.K. and Umbarkar, S.B., 2013. Catalytic dehydration of lactic acid to acrylic acid using calcium hydroxyapatite catalysts. Green chemistry, 15(5), pp.1211-1217.

Huang, X., El-Sayed, I.H., Qian, W. and El-Sayed, M.A., 2006. Cancer cell imaging and photothermal therapy in the near-infrared region by using gold nanorods. Journal of the American Chemical Society, 128(6), pp.2115-2120.

Junqueira, L.C. and Carneiro, J., 2005. Basic histology: text and atlas. McGraw-Hill Professional.

Khatri, C. and Rani, A., 2008. Synthesis of a nano-crystalline solid acid catalyst from fly ash and its catalytic performance. Fuel, 87(13-14), pp.2886-2892.

Knipling, E.B., 1970. Physical and physiological basis for the reflectance of visible and near-infrared radiation from vegetation. Remote sensing of environment, 1(3), pp.155-159.

Kotwal, M.S., Niphadkar, P.S., Deshpande, S.S., Bokade, V.V. and Joshi, P.N., 2009. Transesterification of sunflower oil catalyzed by flyash-based solid catalysts. Fuel, 88(9), pp.1773-1778.

Mongpraneet, S., Abe, T. and Tsurusaki, T., 2002. Accelerated drying of welsh onion by far infrared radiation under vacuum conditions. Journal of Food Engineering, 55(2), pp.147-156.

Peng, B.X., Shu, Q., Wang, J.F., Wang, G.R., Wang, D.Z. and Han, M.H., 2008. Biodiesel production from waste oil feedstocks by solid acid catalysis. Process Safety and Environmental Protection, 86(6), pp.441-447.

Phiraphinyo, P., Taepakpurenat, S., Lakkanatinaporn, P., Suntornsuk, W. and Suntornsuk, L., 2006. Physical and chemical properties of fish and chicken bones as calcium source for mineral supplements. Songklanakarin J. Sci. Technol, 28(2), pp.327-335.

Rasquinha, V.J., Ranawat, C.S. and Mauriello, A.J., 2002. Hydroxyapatite: catalyst or conjuror?. The Journal of arthroplasty, 17(4), pp.113-117.

Sebti, S., Solhy, A., Tahir, R. and Smahi, A., 2002. Modified hydroxyapatite with sodium nitrate: an efficient new solid catalyst for the Claisen–Schmidt condensation. Applied Catalysis A: General, 235(1-2), pp.273-281.

Seddon, A.B., 2011. A prospective for new mid-infrared medical endoscopy using chalcogenide glasses. International Journal of Applied Glass Science, 2(3), pp.177-191.

U.S. Energy Information Administration; Monthly Biodiesel Production Report, Release Date: June 29, 2018. https://www.eia.gov/survey/#eia-22m.

Vatansever, F. and Hamblin, M.R., 2012. Far infrared radiation (FIR): its biological effects and medical applications. Photonics & lasers in medicine, 1(4), pp.255-266.

Waynant, R.W., Ilev, I.K. and Gannot, I., 2001. Mid–infrared laser applications in medicine and biology. Philosophical Transactions of the Royal Society of London A: Mathematical, Physical and Engineering Sciences, 359(1780), pp.635-644.

CHAPTER: 2

LITERATURE REVIEW

2. LITERATURE REVIEW

2.1. Biodiesel Production

Biodiesel is non-petroleum renewable liquid fuel consisting of alkyl esters derived from transesterification of triglycerides (TG) or by the esterification of free fatty acids (FFA) with low molecular weight monohydric alcohol(s). Over recent past, it has become very important to develop alternative, eco-friendly and energy-efficient fuels for the purpose of reducing the enormous demand of coal and petroleum-based fossil fuels. Biodiesel has received considerable acclaim in recent years as a biodegradable, renewable, non-toxic, environment friendly substitute for commercial diesel (Chattopadhyay and Sen, 2013). Biodiesel production can be accomplished either using chemical homogeneous / heterogeneous catalyst or using enzyme (bio-catalyst).

Early extensive research works revealed that chemical homogeneous acid and base catalysts (H_2SO_4, HCl, NaOH, KOH) suffered from several bottlenecks viz., non-reusability, product purification problems, corrosion problem (Freedman et al. 1984; Canakci et al. 1999). Antczak et al., (2009) reported that among enzymatic catalysts, lipase showed superior activity over chemical catalyst for biodiesel production from waste sources (with high moisture content) as it could prevent soap formation. Nevertheless, higher production cost as well as difficulty during processing restricted its uses in commercial production of biodiesel. Therefore, reusable heterogeneous catalysts could be a probable option for production of biodiesel over enzymes or homogeneous catalysts.

2.1.1. Feedstocks for biodiesel production

Various types of feedstocks are used to produce biodiesel through transesterification and esterifation reaction. Edible vegetable oil (EVO) (viz. palm (Crabbe et al., 2001), sunflower

(Granados et al., 2007), rapeseed (Rashid and Anwar, 2008), rice bran oil (Sinha et al., 2008) peanut (Kaya et al., 2009), coconut (Nakpong and Wootthikanokkhan; 2010), soybean (Chakraborty et al., 2010) etc.), non-edible vegetable oil (NEVO) (i.e. *Madhuca indica* (mahua) (Puhan et al, 2005), Linseed, *Pongamia pinnata* (karanja) (Karmee and Chadha, 2005), *jatropha curcas* (Tiwari et al., 2007), Azadirachta indica (neem) (SathyaSelvabala et al., 2010) etc.) and waste derived feedstocks (animal fats and waste cooking oil (WCO)) are the various feedstocks which have been used to produce biodiesel. Besides, monohydric alcohol (e.g. methanol, ethanol, isopropanol etc.) is also important feedstock for biodiesel production which reacts with the different types of oils and animal fats usually in presence of a suitable catalyst.

2.1.2. Edible vegetable oil (EVO)

Globally, edible vegetable oil (EVO) has been extensively used to generate biodiesel through transtesterfication reaction.

Crude palm oil was used to synthesise biodiesel under optimal parametric condition viz. 9 h reaction time, 95 °C temperature and a high 40:1 methanol/oil molar ratio. Though 97% FAME yield was reported by Crabbe et al., (2001) but the long process involved reaction time, relatively higher reaction temperature and methanol/oil molar ratio. Figure 2.1. demonstrates the FAME yield as a function of reaction time. Three different temperatures (70 °C, 80 °C and 95 °C) were maintained for 24 h while employing a reaction mix consisting of 40:1 methanol to oil molar ratio and 5% H_2SO_4 acid catalyst for biodiesel generation. The plots depict the optimal conditions of the produced biodiesel through transesterification.

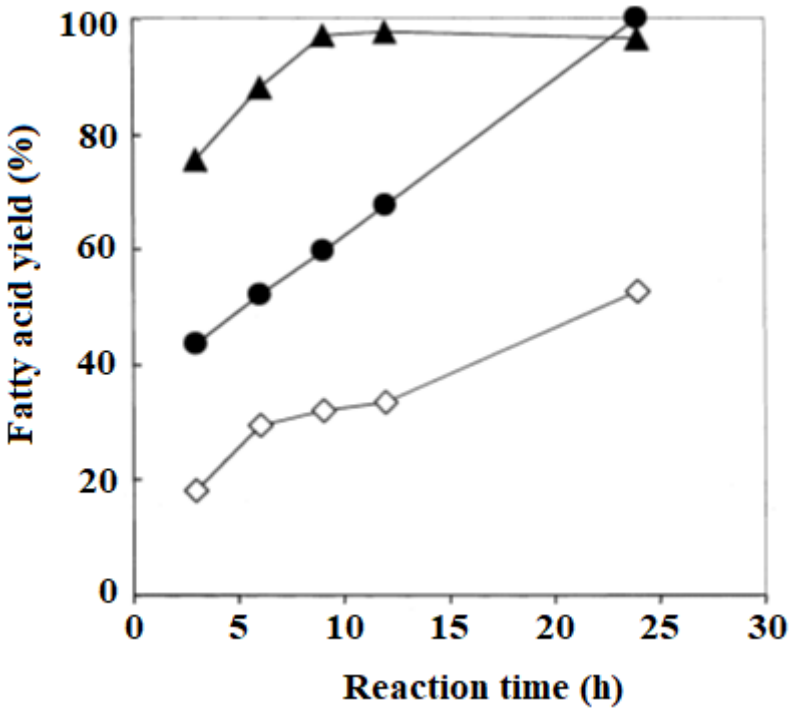

Figure 2.1. Effect of different temperature (70 °C, 80 °C and 95 °C) on fatty acid yield (%). The reaction mix consisting of 40:1 methanol to oil molar ratio and 5% H_2SO_4 acid catalyst. The reaction was carried out for 24 h. This plot is adopted from Crabbe et al., (2001).

Granados et al., (2007) prepared activated CaO catalyst to generate biodiesel from sunflower oil through transesterification. This heterogeneous catalyst was compared with homogeneous KOH catalyst. Several times (eight) the activated CaO catalyst was reused to produce biodiesel; but the separation process of the biodiesel from both heterogeneous and homogeneous catalysts were not clearly described in this experimental study.

CaO solid base catalyst was used to generate biodiesel through refined soybean at 65 °C reaction temperature, 8% CaO catalyst concentration, 12:1 molar ratio of methanol to oil and 3 h reaction time resulted the best 95% biodiesel yield (Liu et al., 2008).

Sinha et al., (2008) reported the production of the biodiesel from rice bran oil through transesterification reaction using KOH and NaOH alkaline catalyst. Although the reaction time is less (1 h), on the other hand, a lengthy (12 h) separation time was required to achieve

the desired purity of product biodiesel. First 6 h was required to separate glycerol from the reaction mixture and the second 6 h was required to remove other impurities i.e. catalyst, unreacted methanol and unreacted oil from biodiesel.

Rapeseed oil was used by Rashid and Anwar, (2008) to produce biodiesel through transesterification while maintaining temperature (35–65 °C) for 2 h. 95-96% biodiesel yield was obtained at the optimal conditions (65 °C temperature, 6:1 methanol/oil molar ratio, 1.0% KOH catalyst concentration, 600 rpm mixing intensity). A comparative study was performed using three other alkaline catalysts viz. NaOH, $NaCH_3O$ and KCH_3O at the same optimal condition. Physico–chemical properties of rapeseed methyl esters (i.e. biodiesel) produce from different homogeneous catalysts are given in Table 2.1.

Table 2.1. Physico–chemical properties of rapeseed methyl esters (i.e. biodiesel) produce from different homogeneous catalysts; adopted from Rashid and Anwar, (2008)

Different catalyst used to produced methyl esters from rapeseed oil	KOH	NaOH	$NaCH_3O$	KCH_3O
Density (25℃) (kg m^{-3})	880	881	880	881
Specific gravity (15/15℃)	0.869	0.871	0.872	0.873
Cloud point (℃)	-3	-3	-2	-3
Pour point (℃)	-9	-8	-7	-7
Flash point (℃)	165	155	151	158
Combustion point (℃)	171	164	158	164
Cetane index	50.4	49.8	49.5	49.2
Kinematic viscosity (mm^2/s)				
15 ℃	7.85	8.07	8.18	8.06
20 ℃	6.98	7.03	7.12	7.25
25 ℃	6.02	6.31	6.26	6.49
30 ℃	5.22	5.48	5.56	5.61
35 ℃	4.70	4.89	4.89	4.92
40 ℃	4.15	4.41	4.49	4.50
Higher heating value (MJ/kg)	44.9	45.0	44.9	44.9
Sulphur (% mass)	0.0095	0.0090	0.0089	0.0089
Water (% mass)	<0.01	<0.01	<0.01	<0.01
Ash (% mass)	0.022	0.041	0.038	0.034
Acid value (mg KOH/g)	0.37	0.48	0.50	0.26

Kaya et al., (2009) reported the production of biodiesel from peanut (*Arachis hypogea L.*) seed oil through transesterification using NaOH base homogeneous catalyst. conversion of 89% was achieved with in 2 h at 60 ℃ temperature in a batch process.

Chakraborty et al., (2010) produced 96.97% FAME content through transtesterfication (for 5 h) using refined soybean oil as a feedstock. Lengthy reaction time and base heterogeneous catalyst was reported for this experimental study.

Nakpong and Wootthikanokkhan (2010) synthesised biodiesel from coconut oil through a two-step process. Esterification of FFA was carried out in the first step using H_2SO_4 acid catalyst and in the second step potassium hydroxide alkaline catalyst was used for transesterification of triglyceride. The methyl ester content was achieved 98.4% w; which was confirmed through GC analysis. The researchers reported that settling process took 2 h after completion of esterification; and after transesterification reaction the mixture was allowed to settle through overnight. Settling process being the integral part of biodiesel purification step, a lengthy settling time is a typical drawback of homogeneous catalytic process.

Kumar et al., (2010) investigated the effect of ultrasonic irradiation on the preparation of biodiesel from coconut oil using KOH base catalyst. Remarkable short reaction time (7 min) was reported in this study to achieve ≥98% biodiesel yield through transesterification. However, relatively higher energy and equipment cost could possibly prohibit the scale-up of such system.

Various EVO are globally consumed as cooking oil and thus usually represent costly feedstocks for diesel production. Extensive use of EVO can lead to food, energy nexus creating uncertainty in sustaining biodiesel production.

2.1.3. Non-edible vegetable oil (NEVO)

Non-edible vegetable oils (NEVO) are not consumed for cooking purpose, so these types of vegetable oils are easily available at relatively cheaper price to produce biodiesel.

NEVO such as Jatropha (*Jatropha Curcas*) was identified as a potential cost-effective sustainable feedstock for biodiesel production by GOI (National biodiesel mission). Poor soils, waste land soil, low rainfall and drought areas are suitable for Jatropha seed plantation. This plant cannot grow in flooding and waterlogged area.

Puhan et al, (2005) studied fuel properties and exhaust emission characteristics of the biodiesel (92% methyl ester conversion) which was derived from the Mahua oil (*Madhuca Indica*) through transesterification using NaOH base catalyst. Emissions of CO, HC of the produced biodiesel from Mahua oil were found lower compared to diesel.

Karmee and Chadha, (2005) prepared biodiesel from crude pongamia pinnata oil through transesterification using both homogeneous and heterogeneous base catalyst. Time required for the homogeneous reaction system was less than heterogeneous reaction system. The maximum conversion 92% was increased to 95% by adding co-solvent tetrahydrofuran in the reaction.

However, as the overall biodiesel production involved two separate reaction steps, it might not be cost-effective. Moreover, the first step involving H_2SO_4 generated considerable quantity of waste streams. An investigation, to avoid the saponification, two-step process was reported for biodiesel preparation from rubber seed oil (containing high FFA) by Ramadhas et al., 2005. Sulphuric acid catalyst was used for esterification and in the next step NaOH alkaline catalyst was employed for transesterification.

Ghadge and Raheman, (2006) obtained 98% mahua biodiesel yield through esterification and transesterification by two-step process. At 60 ℃ temperature the optimum operating conditions of the first step process (esterification reactions) were 0.32 v/v methanol-to-oil ratio, 1.24% v/v H_2SO_4 catalyst and 1.26 h reaction time. In the second step transesterification reaction was carried out and the maintained process conditions of the reaction were 0.25 v/v methanol-to-oil ratio (6:1 molar ratio) and 0.7% w/v KOH, alkaline catalyst.

Tiwari et al., (2007) reported the two-step reaction process to synthesise 99% biodiesel yield from jatropha oil (*Jatropha Curcas*) at 60℃. Acid H_2SO_4 catalyst was used for eseterification in the first step process and KOH an alkaline catalyst was used in the second step process for transesterification. The process parameters were optimised through statistical method response surface methodology (RSM). The process conditions of the esterification reaction were 0.28 v/v methanol-to-oil ratio, 88 min reaction time and 1.43% v/v H_2SO_4 acid catalyst. Methanol-to- oil ratio was 0.16 v/v and 24 min of reaction time for the next step process (transesterification). Notably, use of homogeneous catalyst in both steps, generated enormous waste streams, besides posing problem in product purification and catalyst reusability.

SathyaSelvabala et al., (2010) generated biodiesel from Azadirachta indica (Neem) seed oil through esterification reaction using phosphoric acid modified catalyst. Classical method was used for this study and the reaction temperature was 60℃.

Non-edible Jatropha oil was used to produce biodiesel through two-step process (Deng et al., 2011). In the first step, sulfuric acid was used as homogeneous catalyst to perform acid-esterification in an ultrasonic reactor. Calcined nanosized solid base hydrotalcite catalyst was used in the second step transesterification reaction process. This reaction was also carried out in the ultrasonic reactor. 95.2% FAME yield was achieved within 1.5 h. The authors also

reported the stability of the biodiesel after 1 year storage; the data are resulted in the Table 2.2.

Table 2.2. Stability of Jatropha biodiesel (Deng et al., 2011)

Parameter	**Biodiesel (fresh produced)**	**Biodiesel (stored for 1 year)**
Acid value (mg KOH/g)	0.154	0.36
Viscosity (mm^2/s, 313 K)	3.89	4.05
Density (g/mL, 289 K)	0.886	0.887
Oleic acid	42.61%	38.96%
Palmitoleic acid	0.95%	0.87%
Palmitic acid	13.79%	15.2%
Stearic acid	6.33%	8.37%
Oleic acid	42.61%	38.96%
Linoleic acid	26.34%	25.41%
Linolenic acid	0.06%	---

Needless to mention that the inherent drawbacks of homogeneous process (difficulty in product purification, waste stream generation etc.) could not be overcome.

The NBM recognised jatropha (*jatropha curcas*) as the most suitable inedible oilseed for biodiesel production to achieve a proposed biodiesel blend of 20% with conventional diesel by 2017. The central government recommended that it and several state governments will promote planting of jatropha and other inedible oilseeds by providing financial incentives to various public, private, and cooperative sectors. The former Planning Commission of India (now National Institution for Transforming India (NITI) Commission) had set target to plant 11.2 to 13.4 million hectares of jatropha by the end of April 2012. But the target was unmet

due to a mass of agronomical and economic limitations. To fulfil the gap, several existing biodiesel units changed operations to adopt multiple feedstock technology, which utilizes used cooking oil (UCO), animal fats, other unusable oil fractions, and inedible oils.

2.1.4. Waste derived feedstock

A huge amount of household / restaurant-derived waste oil is generated every day after cooking or frying. Though it is a liquid substance which is usually drained and thus, these wastes create water pollution.

On the other hand, beef tallow, pork lard, chicken fat, goat tallow etc. animal waste fats are regularly generated in slaughter house. These types of wastes are used for animal feeding soap / glycerine manufacturing by fat splitting process and partly become municipality waste. The waste can be managed by preparing biodiesel as an alternative utilization avenue.

Zhang et al., (2003) investigated raw material cost had been reduced by preparing biodiesel from WCO. The study indicated that, while generating biodiesel from the virgin oil using base catalyst, the raw material cost and the overall process was higher in comparison with the biodiesel derived through WCO using acid catalysed process, owing to lower complexity of the later than the alkali-catalysed process.

Waste cooking oil (WCO) contains high amount of FFA. A very high 75.92 ± 0.036 mg KOH/g acid value was reported for a WCO from which biodiesel was derived by Wang et al., (2007). Ferric sulphate solid acid catalyst was used for esterification to derive biodiesel from FFA at 95 ℃ over 4 h reaction duration; while the unreacted triglyceride was utilised for the transesterification in the second step process. For the transesterification taguchi orthogonal experimental design was used to optimize the process factors for evaluating maximum 97.02% FAME yield.

Demirbas, (2009) reported production of biodiesel through transesterification reaction from WCO using KOH alkaline catalyst. Reduction in catalyst efficacy and soap formation were the negative effects in the production of biodiesel using such alkaline/based catalyst. This study was compared with supercritical methanol transesterification method. This method could reduce the pre-treatment costs without the need of any catalyst. Although, 40-107 ℃ temperatures were used in the catalytic transesterification for 2 h but 247- 287 ℃ were used in supercritical methanol transesterification for 30 min. Thus, the supercritical process required much higher temperature and was more energy intensive than its catalytic counterpart.

Ma et al., 1998 reported the production of biodiesel from beef tallow through transesterification using NaOH or NaMeO base catalyst. Beef tallow was melted at 65 °C to conduct the reaction. After completion of the reaction the reaction mixture was neutralized adding acetic acid with biodiesel yield was 97-99% within 20-40 min (reaction time).

da Cunha et al., (2009) reported biodiesel production in a pilot scale through beef tallow using KOH catalyst. The Figure 2.2. shows schematic block flow diagram of the pilot plant for biodiesel production. The reaction temperature of 65 ^{o}C, 1.5 wt.% of KOH, 6:1 molar ratio of methanol to tallow, 400 rpm stirrer speed and 3 h reaction time were the reaction conditions of the plant while preparing the biodiesel. This was followed by 4 h decantation time to separate glycerol from the reaction mixture. The upper methyl ester phase was washed with hot acidified water to remove residual catalyst, glycerol, methanol and soaps.

The biodiesel production capacity of the pilot plant was 800kg/day. Solidification is the major disadvantage concerning beef fat utilisation particularly in the cold climate conditions for biodiesel production. In order to overcome the problem of high pour point of the product biodiesel, it was mixed with Petro-diesel prior to application in diesel engine.

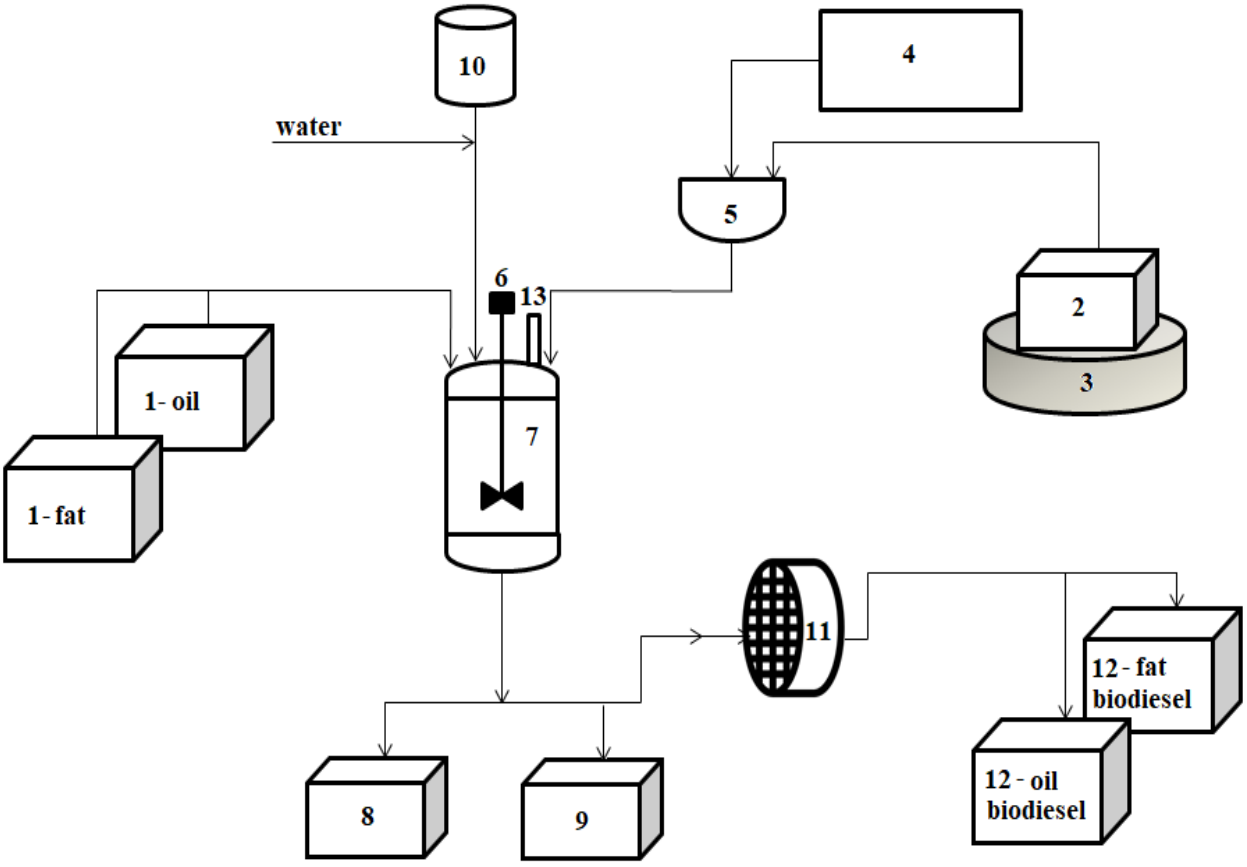

1 - tank of fat and oil
2 - tank of methanol
3 - containment basin
4 - reservoir of KOH
5 - methoxi reactor
6 - mechanic stirrer
7 - main reactor
8 - tank of glycerol
9 - tank of waste water
10 - reservior of phosphoric acid
11 - filter
12 - tank of biodiesel
13 - relief valve

Figure 2.2. Schematic block flow diagram of the pilot plant for biodiesel production (da Cunha et al., 2009).

Mata et al., (2011) performed a study to synthesise biodiesel from three different types of raw materials; viz. beef tallow, pork lard and chicken fat. Alkaline KOH catalyst was used for the transesterification to produce biodiesel. Purification through conventional neutralization (CN), water washing, followed by drying and another purification method using cationic exchange resins (CER); these two methods were used for comparison of purification of produced biodiesel. Cationic exchange resins purification method decreased production costs and time, moreover it demonstrated additional advantage by eliminating water requirement.

The authors also reported that the purified biodiesel (B100) could not be directly used in the diesel engine; however, the biodiesel blended with petro diesel in the form of B20 could be used in car engines. Biodiesel produced from beef tallow, in form of B20 (20% biodiesel and 80% Petro-diesel) resulted best performance compared to the other blends.

Table 2.3. provides the characterization of methyl ester produced from beef tallow, pork lard and chicken fat after two different types of purifications.

Table 2.3. Characterisation of methyl ester produced from beef tallow, pork lard and chicken fat after two different types of purifications (Mata et. al. 2011)

Parameter	Methyl ester from beef tallow		Methyl ester from pork lard		Methyl ester from chicken fat	
	CN	CER	CN	CER	CN	CER
Reaction yield (wt %)	90.8	90.8	91.4	91.4	76.8	76.8
Density at 15 °C (kg/m^3)	870	870	873	871	877	888
Flash point (°C)	172	172	147	147	171	171
Ester content (wt. %)	84.40	81.15	80.74	83.00	73.80	83.68
Acid value (mg of KOH/g of fuel)	0.20	0.21	0.22	0.17	0.55	0.09
Cold Filter Plugging Point (°C)	+10	+10	+5	+4	+3	+11
Kinematic viscosity at 40 °C (mm^2/s)	5.35	5.44	5.08	4.84	6.86	4.83

Chakraborty and Sahu, (2014) reported biodiesel production from waste goat tallow through simultaneous trans/esterification process using H_2SO_4 homogeneous acid catalyst. Within 2.5 h, 96.7% FFA conversion was achieved with the help of infrared radiation assisted reactor. Artificial neural network and response surface methodology these two statistical methods were compared to prove modelling efficiency in predicting FFA conversion to biodiesel.

Chicken and swine waste fats were used as feedstock to derive biodiesel using alkaline KOH catalyst. To overcome the waste management problem, these easily available cost-effective

wastes fats were used to produce biodiesel; 83.5% conversion was achieved in 30 ℃ (Cunha Jr. et al., 2013).

2.1.5. Selection of alcohols for biodiesel production

TG reacts with alcohol through transesterification to produce biodiesel while FFA reacts with alcohol through esterification to produce ester. Different types of alcohols viz. methanol using waste frying soybean oil (Chakraborty and Banerjee, 2010), ethanol (Anastopoulos et. al., 2009), isopropanol and butanol employing used frying oil (Sanli and Canakci, 2008), were used to produce biodiesel. For biodiesel production methanol is mostly preferable because it is cheaply available. On the other hand ethanol is less toxic than methanol, while it is little bit costlier than methanol. Isopropanol and butanol are much costlier than methanol and ethanol.

2.2. Homogeneous Catalyst for biodiesel production

Catalysts mainly enhances the reaction rate, by reducing the activation energy of reaction, thus, helps in reducing reaction time, temperature and energy requirement. Both homogeneous acid and base types' catalysts have been used in biodiesel production. The major demerits in using homogeneous catalysts can be ascribed to their high solubility in reaction mix, creating difficulty in separation of catalyst from the reaction mixture, making biodiesel purification a tedious task. Besides, use of homogeneous catalyst generates enormous amounts of waste stream, creating environmental pollution unless treated properly. Moreover, these catalysts can't be reused, thus, requiring higher amount of catalysts per unit mass of biodiesel production in comparison with their heterogeneous counterparts.

The selection of base or acid catalyst should depend on the type of feedstock. Principally base catalyst should be used for feedstock (refined vegetable oil) with low acid number (<0.5) while acid catalyst should be employed for waste derived feedstock (Waste cooking oil, animal fat, unrefined vegetable oil) having higher acid number (>0.5).

Various homogeneous base catalysts were used for biodiesel production from refined sunflower oil through transesterification reaction; viz: sodium methoxide, potassium methoxide, sodium hydroxide and potassium hydroxide over a reaction duration of 4 h (Vicente et al., 2004) resulting in the highest 99.33 ± 0.36% biodiesel (FAME) yield using sodium methoxide catalyst (Figure 2.3.). The main disadvantages of using base homogeneous catalysts are saponification and dissolution of methyl ester in glycerol; these phenomena eventually result in reduced FAME (fatty acid methyl ester) yield in production of biodiesel.

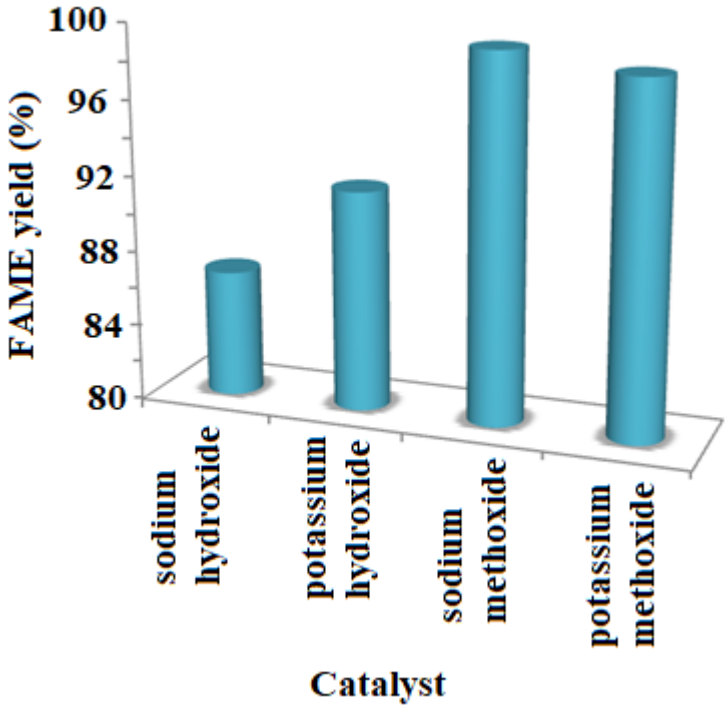

Figure 2.3. Effects of types of base homogeneous catalyst on FAME yield.

Sinha et al., (2008) reported the production of biodiesel through transesterification reaction using KOH and NaOH alkaline catalyst from rice bran oil. Although the reaction time was less (1 h), on the other hand, a lengthy (12 h) separation time was required to achieve the desired purity of product biodiesel. First 6 h was required to separate glycerol from the reaction mixture and the second 6 h was required to remove other impurities i.e. catalyst, unreacted methanol and unreacted oil from biodiesel.

Kaya et al., (2009) investigated on the production of biodiesel from peanut (*Arachis hypogea L.*) seed oil through transesterification using NaOH base homogeneous catalyst. Conversion of 89% was achieved with in 2 h at 60 ℃ temperature in a batch process.

Di Serio et al., (2005) prepared homogeneous Lewis acid catalyst using different types of metals viz. Ca, Ba, Mg, Cd, Mn, Pb, Zn, Co, Ni. Transesterification of soybean oil carried out for 55 min at a considerably high from 150–200 ℃ reaction temperature; thus, rendering an energy intensive process.

In yet another study, Ferdous et al. (2013), generated biodiesel from karanja oil using three-step homogeneous acid catalyzed protocol employing sulphuric acid. At 100 ℃ temperature 98% FFA conversion was achieved within 2 h. Separation process was too much critical in this study; thus, the economy of the production could not be justified.

In another investigation, our research group (Chakraborty and Sahu, 2014) reported biodiesel production from waste goat tallow through simultaneous trans/esterification process using H_2SO_4 homogeneous acid catalyst. Within 2.5 h, 96.7% FFA conversion was achieved with the help of infrared radiation assisted reactor. Two well –known statistical methods viz. artificial neural network (ANN) and response surface methodology (RSM) were employed to predict FFA conversion and the modelling efficiency of these two methods were compared in predicting FFA conversion to biodiesel. Nevertheless, the inherent demerit of homogeneous catalyst i.e. difficulty in catalyst separation from biodiesel phase, generation of waste streams could not be avoided.

2.3. Heterogeneous Catalyst for biodiesel production

Heterogeneous catalysts can be separated conveniently from reaction mixture, thus facilitates product purification and catalyst recovery and reusability, while minimizing waste stream generation.

The conventional homogeneous catalysts are expected to be completely replaced by eco-friendly heterogeneous catalysts in the near future owing to the ease of catalyst recovery and simplifications in biodiesel purification. Thus, the development of heterogeneous catalysts has recently gained tremendous importance in view of the current economic climate e.g. increased competition, stringent pollution regulations (Neto et al., 2007).

In the past, several attempts were made (Park et al., 2008) to prepare solid acid catalysts for transesterification. Solid acid catalyst comprising of SO_4−/TiO_2–SiO_2 was exhibited as capable of performing esterification and transesterification simultaneously to synthesize biodiesel from several low cost feed stocks with high FFAs. However, the acceptable catalytic activity was achieved at the expense of high reaction temperature (200 °C). Similarly, investigations have also been reported on heterogeneous base catalysts viz. CaO, $Sr(NO_3)_2$/ZnO, KI/Al_2O_3, Na/NaOH/Al_2O_3, KF/MgO, ion exchange resins etc. capable of conducting transesterification reaction (Abreu et al., 2003) . Besides, a few research works (Zabeti et al., 2009) have been published on development and application of Al_2O_3/SiO_2 supported CaO base catalysts prepared from reagent grade chemicals for production of biodiesel from low FFA refined vegetable oils. The deployment of reagent grade chemicals invariably increased the cost of above mentioned catalyst.

2.3.1. Catalyst developed from Industrial waste

The wastes which are produced through industrial activities may contain hazardous or non-hazardous material in solid or liquid form. These industrial wastes may be utilized for catalyst preparation.

Fly ash (FA) contains SiO_2, Al_2O_3, Fe_2O_3, Na_2O, CaO, MgO, TiO_2, BaO and K_2O. Metal oxides such as Al_2O_3 is usually used as the support for heterogeneous catalyst. In recent days many technologies have been reported for utilization of FA for development of value added products. The presence of high amount of SiO_2 and Al_2O_3 prompts its potential applicability as a low-cost catalyst support. It offers some desirable properties such as thermal stability and it can also be used as a catalytically active component (Ojha and Pradhan, 2001). Solid heterogeneous catalysts were prepared using FA as a support by several research groups. In Knoevenagel condensation reaction, FA supported calcium oxide base catalyst was employed; while, other FA supported metallic acid and base catalysts were synthesized and characterized for different reactions (Khatri and Rani, 2008). In transesterification of sunflower oil (Kotwal et. al., 2009) and soybean oil (Chakraborty et al., 2010), FA supported metal impregnated based catalysts were used. Nano crystalline solid acid catalyst produced from FA have been utilised successfully for esterification and transesterification reaction (Khatri et.al., 2010). FA can be also used in photocatalysis and as an active component in the reduction of VOC's.

Fly ash supported calcium oxide has been employed as a recyclable solid base catalyst for Knoevenagel condensation reaction (Jain et al., 2010); however, the CaO was derived from reagent grade $CaCO_3$ which might increase the cost of catalyst preparation. In a recent work, (Chakraborty et al., 2010) reported the application of FA supported CaO heterogeneous catalyst prepared .using waste egg shell (as a natural resources for CaO) for

transesterification of soybean oil to yield fuel grade biodiesel; this work demonstrated the application of municipal solid waste materials for preparation of highly efficient, low cost heterogeneous base catalyst.

FA supported many solid base and acid catalysts are produce for different reaction purpose; but still now there is no report found for esterification reaction using FA supported acid catalyst.

2.3.2. Catalyst developed from Natural/ Biological waste

In recent years, solid waste management had drawn attention of global researchers. Bones of animals, fish scales, egg shells etc. are solid wastes which could provide natural hydroxyapatite (NHAp) to prepare low-cost catalysts as these were much cost-effective than chemical HAp (CHAp) (Chakraborty et al., 2014).

The low cost highly effective heterogeneous base catalysts derived from waste resources e.g. waste eggshell (Wei et al., 2009), oyster shell (Nakatani et al., 2009), shrimp shell (Yang et al., 2009), mud crab shell (Boey et al., 2009), waste shells of mollusc (Viriya-empikul et al., 2010) and waste fish scale (Chakraborty et al., 2011) were successfully used for biodiesel production from refined vegetable oil with low FFA content low acid number (<0.5).

Hydroxyapatite (HAp) offers useful properties, viz. ion-exchange ability, acid−base and adsorption attributes besides being nontoxicity and thermally stable; thus demonstrating its suitability for catalytic applications. CHAp supported Cr heterogeneous catalyst was used to produce 5-hydroxymethylfurfural from glucose. Further, ion-exchange preparation method was used to synthesize Chromium-loaded hydroxyapatite catalyst to study the propane cracking. This heterogeneous catalyst played an important role in improving the conversion rate. However, costly chemical reagents were used to prepare the CHAp, making the catalyst intensive.

Chakraborty et al., (2011) reported the production of 97.73% biodiesel yield was derived from soybean oil using calcined fish scale as a heterogeneous base catalyst which is a NHAp catalyst. The biodiesel was obtained at 70 ºC within 5 h.

Chakraborty et al., (2012) prepared Ni-HAp solid acidic catalyst for biodiesel production from waste frying soybean oil. Fish scale a NHAp support was used for the Ni-HAp heterogeneous catalyst preparation. At 60 ºC temperature 59.76% FFA conversion was achieved within 2 h.

Till date, NHAp catalysts have been used primarily biodiesel production. Use of such catalysts for other applications are currently being researched upon and will soon be successfully applied.

It is evident from the cited literatures, that the production of biodiesel over NHAp derived catalyst is much more efficient and provide greater yield along with requirement of milder reaction conditions. Thus the preparation process for unexplored metal impregnated NHAp or FA supported catalysts and their application for cost-effective synthesis of biodiesel/ ester products would be an important and challenging tasks in the present research work.

2.3.3. Amberlyst 15: Commercial Heterogeneous Catalyst for biodiesel preparation

Very useful acidic properties, combined with benign environmental character, reusable and commercial available Amberlyst-15 catalyst was used in transesterification reaction for biodiesel production (Chavan et al., 2006).

In another investigation, Talukder et al. (2009) had vividly described biodiesel production (97% FAME yield) from palm oil using Amberlyst-15 catalyst; however, it required a lengthy 8 h reaction time.

Commercial heterogeneous Amberlyst-15 acid catalyst (possessing regeneration and recyclability characteristics) was used in both esterification and transesterification reactions (Pal et al., 2012) owing to its favourable catalytic properties. Applications of Amberlyst-15 catalyst permitted use of mild operating conditions while rendering highly selective conversions to biodiesel in a facile and environmentally approachable manner. The catalyst could be regenerated and recycled. The physical properties of brown-grey solid Amberlyst-15 are given in Table 2.4.

Table 2.4. Physical properties of brown-grey solid Amberlyst-15 (adopted from Pal et al., 2012)

Ionic form as shipped	hydrogen
Moisture holding capacity	52 to 57% (H^+ form)
Shipping weight	770 g/L
Concentration of active sites	≥ 1.7 eq/L; ≥ 4.7 eq/kg
Particle size	0.600 to 0.850 mm
Maximum operating temperature	120 ºC (250 ºF)
Total pore volume	0.40 mL/g
Average pore diameter	300 Å

Chakraborty and Mondal, (2015) applied Amberlyst-15 catalyst for esterification of glycerol with lauric acid (LA). A very high LA conversion of 99.0% was achieved at optimal conditions viz. 6.2 glycerol to LA molar ratio, 80 °C temperature, 900 rpm stirrer speed and 5 wt.% catalyst concentration. Thus, Amberlyst-15 catalyst was found very effective heterogeneous acid catalyst.

2.4. Diesel additives

Utilization of biodiesel or a single methyl ester as an additive to petro-diesel could help to reduce the dependence on limited fossil fuel resources and mitigate the harmful emissions (CO, HCs) resulted from conventional petro-diesel. Biodiesel as an additive plays an imperative role to circumvent the associated problems with petro-diesel (Chandler et al., 1992). Moreover, high cetane number, low greenhouse gas emission and low exhaust gas temperature (Smith et al., 2010; Ali et al., 2013) make biodiesel/ FAME suitable as a diesel additive (viz. methyl oleate; ester of oleic acid and methanol).

Additives can improve certain fuel properties (such as lower pour point, lower cloud point, increasing flash point, cetane number, lubricity etc.) which facilitate enhanced engine performance can favourable exhausts emissions. The diesel/biodiesel additives should be carefully chosen depending on their different properties viz., flash point, fire point, viscosity, density, calorific value, solubility, cetane number etc. (Silitonga et al., 2013).

Thus, cost-effective green catalyst should be prepared to facilitate sustainable synthesis of fuel additives and biodiesel for economic and eco-friendly utilization.

2.5. Intensification of reaction using Electromagnetic radiation

Chakraborty and Sahu, (2014) reported biodiesel production from waste goat tallow through simultaneous trans/esterification process using H_2SO_4 homogeneous acid catalyst. Within 2.5 h, 96.7% FFA conversion was achieved employing an indigenously fabricated infrared radiation assisted reactor.

In yet another exploratory work, Chakraborty and Mondal, (2015) applied far-infrared (FIR) radiation for augmentation of lauric acid conversion to glyceryl laurate using Amberlyst-15 catalyst. Within only 30 min of reaction time, 99.0% Lauric acid conversion was achieved at optimal conditions; which was much higher than obtained from a conventionally heated reactor under otherwise identical optimal conditions. The results clearly indicated superiority of far-infrared (FIR) radiation in comparison with conventionally heated reactor system.

2.6. Statistical analysis of experimental methods

Classical methods have been traditionally used in experimental scientific investigations. However, now-a-days the experimental studies are being increasingly carried out using statistical "design of experimental" (DOE). Statistical DOE demonstrates the interactions between any two process independent factors while keeping the other factors constant. Moreover, the DOE can also reveal the individual factorial effects governing the process response (dependent) variable (viz. biodiesel yield/ FAME content).

2.6.1. Response Surface Methodology (RSM)

Response surface methodology (RSM) is a collection of mathematical and statistical techniques for empirical model building. By careful selection of particular DOE, the objective becomes optimization of a response (output/ dependent) variable which is influenced by several independent variables. Moreover, RSM provides a statistically significant correlation among the independent and response variables.

Chakraborty et al., (2010) reported transesterification of soybean oil using RSM preidcted optimal process conditions involving several independent process factors viz. CaO loading, catalyst concentration and methanol/oil molar ratio. Fly ash and egg shell derived solid catalyst was prepared in the research work which was employed to achieve 96.97% FAME yield at optimal conditions.

Chakraborty et al., (2011) also investigated the production of biodiesel using calcined waste fish (*Labeo rohita*) scale derived heterogeneous catalyst by applying RSM optimization method. Maximum 97.73% FAME yield was achieved at the RSM predicted optimal parametric conditions viz. methanol/oil molar ratio, 6.27:1, calcination temperature, 997.42 ℃ and catalyst concentration, 1.01 wt.%.

In yet another investigation, Chakraborty and Das (2012) produced biodiesel from waste frying soybean oil using RSM for process optimization purpose. The face cantered central composite design (FCCD) method of RSM considered several process parameters viz. $Ni(NO_3)_2 \cdot 6H_2O$ loading, methanol flow rate and calcination temperature and evaluated the maximum biodiesel yield over the selected parametric range.

2.6.2. Taguchi Orthogonal Design (TOD)

The salient advantage of TOD optimization process lies in the fact that much lower numbers of experimental runs are required for process optimization in comparison with RSM when several process parameters are considered for a particular process. The Taguchi method involves analysis of experiments considering several process parameters with the smallest number of experiments using a design matrix, referred to as the orthogonal array.

Chongkhong et al., (2007) generated biodiesel from palm fatty acid distillate (PFAD) through esterification reaction and the effects of process independent variables and optimal parametric combinations were evaluated using L_9 experimental matrix of TOD. The independent variables considered in this study were temperature, time, H_2SO_4 amount (catalyst) and molar ratio of methanol to PFAD. Additionally, Ganapathy et al., (2009) used TOD optimization method to predict parametric conditions for maximum biodiesel production from Jatropha oil.

In yet another investigation, Chakraborty and RoyChowdhury, (2013) reported optimisation of oleic acid esterification using TOD method. Maximum predicted oleic acid conversion (91.86%) could be achieved within 1 h reaction time, which corroborated well with the experimental observations.

2.6.3. D-Optimal Method

D-optimal design is a model-specific design which can be generated by an iterative search algorithm and it seeks to minimize the covariance of the parameter estimates for a specified model.

Iqbal et al., (2008) applied D-optimal method in MQL-employed finish hard-milling process. The D-optimal method was a relatively newer technique in comparison with RSM and could be used as a 'design of experiment' involving the analysis of variance, and the empirical modelling.

Sarteshnizi et al., (2015) analyzed the effects of using β-glucan and resistant starch by D-optimal mixture design approach; which required only 13 experimental runs to determine the optimal parametric values and the correlation among the process variables.

However, scientific reports on use of D-optimal method for process optimization have been relatively scanty in comparison with other methods of statistical DOE.

References

Abreu, F.R., Alves, M.B., Macêdo, C.C., Zara, L.F. and Suarez, P.A., 2005. New multi-phase catalytic systems based on tin compounds active for vegetable oil transesterificaton reaction. Journal of Molecular Catalysis A: Chemical, 227(1-2), pp.263-267.

Ali, O.M., Mamat, R. and Faizal, C.K.M., 2013. Review of the effects of additives on biodiesel properties, performance, and emission features. Journal of renewable and sustainable energy, 5(1), p.012701.

Anastopoulos, G., Zannikou, Y., Stournas, S. and Kalligeros, S., 2009. Transesterification of vegetable oils with ethanol and characterization of the key fuel properties of ethyl esters. Energies, 2(2), pp.362-376.

Antczak, M.S., Kubiak, A., Antczak, T. and Bielecki, S., 2009. Enzymatic biodiesel synthesis–key factors affecting efficiency of the process. Renewable energy, 34(5), pp.1185-1194.

Boey, P.L., Maniam, G.P. and Hamid, S.A., 2009. Biodiesel production via transesterification of palm olein using waste mud crab (Scylla serrata) shell as a heterogeneous catalyst. Bioresource Technology, 100(24), pp.6362-6368.

Canacki, M. and Gerpen, J.V., 1999. Biodiesel production via acid catalysis. Trans ASAE, 42(5), pp.1203-1210.

Chakraborty, R. and Banerjee, A., 2010. Prediction of fuel properties of biodiesel produced by sequential esterification and transesterification of used frying soybean oil using statistical analysis. Waste and Biomass Valorization, 1(2), pp.201-208.

Chakraborty, R., Bepari, S. and Banerjee, A., 2010. Transesterification of soybean oil catalyzed by fly ash and egg shell derived solid catalysts. Chemical Engineering Journal, 165(3), pp.798-805.

Chakraborty, R., Bepari, S. and Banerjee, A., 2011. Application of calcined waste fish (Labeo rohita) scale as low-cost heterogeneous catalyst for biodiesel synthesis. Bioresource technology, 102(3), pp.3610-3618.

Chakraborty, R. and Das, S.K., 2012. Optimization of biodiesel synthesis from waste frying soybean oil using fish scale-supported Ni catalyst. Industrial & Engineering Chemistry Research, 51(25), pp.8404-8414.

Chakraborty, R. and RoyChowdhury, D., 2013. Fish bone derived natural hydroxyapatite-supported copper acid catalyst: Taguchi optimization of semibatch oleic acid esterification. Chemical engineering journal, 215, pp.491-499.

Chakraborty, R. and Sahu, H., 2014. Intensification of biodiesel production from waste goat tallow using infrared radiation: process evaluation through response surface methodology and artificial neural network. Applied energy, 114, pp.827-836.

Chakraborty, R. and Mandal, E., 2015. Fast and energy efficient glycerol esterification with lauric acid by near and far-infrared irradiation: Taguchi optimization and kinetics evaluation. Journal of the Taiwan Institute of Chemical Engineers, 50, pp.93-99.

Chandler, J.E., Horneck, F.G. and Brown, G.I., 1992. The effect of cold flow additives on low temperature operability of diesel fuels (No. 922186). SAE Technical Paper.

Chattopadhyay, S. and Sen, R., 2013. Fuel properties, engine performance and environmental benefits of biodiesel produced by a green process. Applied energy, 105, pp.319-326.

Chavan, S.P., Subbarao, Y.T., Dantale, S.W. and Sivappa, R., 2001. Transesterification of ketoesters using Amberlyst-15. Synthetic Communications, 31(2), pp.289-294.

Chongkhong, S., Tongurai, C., Chetpattananondh, P. and Bunyakan, C., 2007. Biodiesel production by esterification of palm fatty acid distillate. Biomass and Bioenergy, 31(8), pp.563-568.

Crabbe, E., Nolasco-Hipolito, C., Kobayashi, G., Sonomoto, K. and Ishizaki, A., 2001. Biodiesel production from crude palm oil and evaluation of butanol extraction and fuel properties. Process biochemistry, 37(1), pp.65-71.

da Cunha, M.E., Krause, L.C., Moraes, M.S.A., Faccini, C.S., Jacques, R.A., Almeida, S.R., Rodrigues, M.R.A. and Caramão, E.B., 2009. Beef tallow biodiesel produced in a pilot scale. Fuel Processing Technology, 90(4), pp.570-575.

Demirbas, A., 2009. Biodiesel from waste cooking oil via base-catalytic and supercritical methanol transesterification. Energy Conversion and Management, 50(4), pp.923-927.

Deng, X., Fang, Z., Liu, Y.H. and Yu, C.L., 2011. Production of biodiesel from Jatropha oil catalyzed by nanosized solid basic catalyst. Energy, 36(2), pp.777-784.

Di Serio, M., Tesser, R., Dimiccoli, M., Cammarota, F., Nastasi, M. and Santacesaria, E., 2005. Synthesis of biodiesel via homogeneous Lewis acid catalyst. Journal of Molecular Catalysis A: Chemical, 239(1-2), pp.111-115.

Ferdous, K., Uddin, M.R., Mondal, S.K. and Khan, M.R., Preparation of Biodiesel Using Sulfuric Acid as a Catalyst.

Freedman, B.E.H.P., Pryde, E.H. and Mounts, T.L., 1984. Variables affecting the yields of fatty esters from transesterified vegetable oils. Journal of the American Oil Chemists Society, 61(10), pp.1638-1643.

Ganapathy, T., Murugesan, K.A. and Gakkhar, R.P., 2009. Performance optimization of Jatropha biodiesel engine model using Taguchi approach. Applied Energy, 86(11), pp.2476-2486.

Ghadge, S.V. and Raheman, H., 2006. Process optimization for biodiesel production from mahua (Madhuca indica) oil using response surface methodology. Bioresource technology, 97(3), pp.379-384.

Granados, M.L., Poves, M.Z., Alonso, D.M., Mariscal, R., Galisteo, F.C., Moreno-Tost, R., Santamaría, J. and Fierro, J.L.G., 2007. Biodiesel from sunflower oil by using activated calcium oxide. Applied Catalysis B: Environmental, 73(3-4), pp.317-326.H

Iqbal, A., Ning, H., Khan, I., Liang, L. and Dar, N.U., 2008. Modeling the effects of cutting parameters in MQL-employed finish hard-milling process using D-optimal method. Journal of Materials Processing Technology, 199(1-3), pp.379-390.

Jain, D., Khatri, C. and Rani, A., 2010. Fly ash supported calcium oxide as recyclable solid base catalyst for Knoevenagel condensation reaction. Fuel Processing Technology, 91(9), pp.1015-1021.

Karmee, S.K. and Chadha, A., 2005. Preparation of biodiesel from crude oil of Pongamia pinnata. Bioresource technology, 96(13), pp.1425-1429.

Kaya, C., Hamamci, C., Baysal, A., Akba, O., Erdogan, S. and Saydut, A., 2009. Methyl ester of peanut (Arachis hypogea L.) seed oil as a potential feedstock for biodiesel production. Renewable Energy, 34(5), pp.1257-1260.

Khatri, C. and Rani, A., 2008. Synthesis of a nano-crystalline solid acid catalyst from fly ash and its catalytic performance. Fuel, 87(13-14), pp.2886-2892.

Kotwal, M.S., Niphadkar, P.S., Deshpande, S.S., Bokade, V.V. and Joshi, P.N., 2009. Transesterification of sunflower oil catalyzed by flyash-based solid catalysts. Fuel, 88(9), pp.1773-1778.

Kumar, D., Kumar, G. and Singh, C.P., 2010. Fast, easy ethanolysis of coconut oil for biodiesel production assisted by ultrasonication. Ultrasonics Sonochemistry, 17(3), pp.555-559.

Liu, X., He, H., Wang, Y., Zhu, S. and Piao, X., 2008. Transesterification of soybean oil to biodiesel using CaO as a solid base catalyst. Fuel, 87(2), pp.216-221.

Ma, F., Clements, L.D. and Hanna, M.A., 1998. Biodiesel fuel from animal fat. Ancillary studies on transesterification of beef tallow. Industrial & engineering chemistry research, 37(9), pp.3768-3771.

Mata, T.M., Cardoso, N., Ornelas, M., Neves, S. and Caetano, N.S., 2011. Evaluation of two purification methods of biodiesel from beef tallow, pork lard, and chicken fat. Energy & Fuels, 25(10), pp.4756-4762.

Nakatani, N., Takamori, H., Takeda, K. and Sakugawa, H., 2009. Transesterification of soybean oil using combusted oyster shell waste as a catalyst. Bioresource Technology, 100(3), pp.1510-1513.

Nakpong, P. and Wootthikanokkhan, S., 2010. High free fatty acid coconut oil as a potential feedstock for biodiesel production in Thailand. Renewable Energy, 35(8), pp.1682-1687.

Neto, B.A.D., Alves, M.B., Lapis, A.A., Nachtigall, F.M., Eberlin, M.N., Dupont, J. and Suarez, P.A., 2007. 1-n-Butyl-3-methylimidazolium tetrachloro-indate (BMI· InCl4) as a media for the synthesis of biodiesel from vegetable oils. Journal of Catalysis, 249(2), pp.154-161.

Ojha, K. and Pradhan, N.C., 2001. Treated fly ash: A potential catalyst for catalytic cracking.

Pal, R., Sarkar, T. and Khasnobis, S., 2012. Amberlyst-15 in organic synthesis. ARKIVOC: Online Journal of Organic Chemistry.

Park, Y.M., Lee, D.W., Kim, D.K., Lee, J.S. and Lee, K.Y., 2008. The heterogeneous catalyst system for the continuous conversion of free fatty acids in used vegetable oils for the production of biodiesel. Catalysis Today, 131(1-4), pp.238-243.

Puhan, S., Vedaraman, N., Ram, B.V., Sankarnarayanan, G. and Jeychandran, K., 2005. Mahua oil (Madhuca Indica seed oil) methyl ester as biodiesel-preparation and emission characterstics. Biomass and bioenergy, 28(1), pp.87-93.

Ramadhas, A.S., Jayaraj, S. and Muraleedharan, C., 2005. Biodiesel production from high FFA rubber seed oil. Fuel, 84(4), pp.335-340.

Rashid, U. and Anwar, F., 2008. Production of biodiesel through optimized alkaline-catalyzed transesterification of rapeseed oil. Fuel, 87(3), pp.265-273.

Sanli, H. and Canakci, M., 2008. Effects of different alcohol and catalyst usage on biodiesel production from different vegetable oils. Energy & Fuels, 22(4), pp.2713-2719.

Sarteshnizi, R.A., Hosseini, H., Bondarianzadeh, D. and Colmenero, F.J., 2015. Optimization of prebiotic sausage formulation: Effect of using β-glucan and resistant starch by D-optimal mixture design approach. LWT-Food Science and Technology, 62(1), pp.704-710.

SathyaSelvabala, V., Varathachary, T.K., Selvaraj, D.K., Ponnusamy, V. and Subramanian, S., 2010. Removal of free fatty acid in Azadirachta indica (Neem) seed oil using phosphoric acid modified mordenite for biodiesel production. Bioresource technology, 101(15), pp.5897-5902.

Smith, P.C., Ngothai, Y., Nguyen, Q.D. and O'Neill, B.K., 2010. Improving the low-temperature properties of biodiesel: Methods and consequences. Renewable Energy, 35(6), pp.1145-1151.

Silitonga, A.S., Masjuki, H.H., Mahlia, T.M.I., Ong, H.C., Chong, W.T. and Boosroh, M.H., 2013. Overview properties of biodiesel diesel blends from edible and non-edible feedstock. Renewable and Sustainable Energy Reviews, 22, pp.346-360.

Sinha, S., Agarwal, A.K. and Garg, S., 2008. Biodiesel development from rice bran oil: Transesterification process optimization and fuel characterization. Energy conversion and management, 49(5), pp.1248-1257.

Talukder, M.R., Wu, J.C., Lau, S.K., Cui, L.C., Shimin, G. and Lim, A., 2008. Comparison of Novozym 435 and Amberlyst 15 as heterogeneous catalyst for production of biodiesel from palm fatty acid distillate. Energy & Fuels, 23(1), pp.1-4.

Tiwari, A.K., Kumar, A. and Raheman, H., 2007. Biodiesel production from jatropha oil (Jatropha curcas) with high free fatty acids: an optimized process. Biomass and bioenergy, 31(8), pp.569-575.

Vicente, G., Martınez, M. and Aracil, J., 2004. Integrated biodiesel production: a comparison of different homogeneous catalysts systems. Bioresource technology, 92(3), pp.297-305.

Viriya-Empikul, N., Krasae, P., Puttasawat, B., Yoosuk, B., Chollacoop, N. and Faungnawakij, K., 2010. Waste shells of mollusk and egg as biodiesel production catalysts. Bioresource technology, 101(10), pp.3765-3767.

Wang, Y., Ou, S., Liu, P. and Zhang, Z., 2007. Preparation of biodiesel from waste cooking oil via two-step catalyzed process. Energy conversion and management, 48(1), pp.184-188.

Wei, Z., Xu, C. and Li, B., 2009. Application of waste eggshell as low-cost solid catalyst for biodiesel production. Bioresource technology, 100(11), pp.2883-2885.

Yang, L., Zhang, A. and Zheng, X., 2009. Shrimp shell catalyst for biodiesel production. Energy & Fuels, 23(8), pp.3859-3865.

Zabeti, M., Daud, W.M.A.W. and Aroua, M.K., 2009. Optimization of the activity of CaO/Al2O3 catalyst for biodiesel production using response surface methodology. Applied Catalysis A: General, 366(1), pp.154-159.

Zhang, Y., Dube, M.A., McLean, D.D.L. and Kates, M., 2003. Biodiesel production from waste cooking oil: 1. Process design and technological assessment. Bioresource technology, 89(1), pp.1-16.

CHAPTER: 3

AIMS AND OBJECTIVES

3. AIMS AND OBJECTIVES

Form the foregoing literature review it is evident that although the significant amount of research activities have been conducted for production of biodiesel, yet there exits certain avenues for future advancements in the overall technological and environment aspects for the better sustainability of biodiesel production and utilization.

Following are the few salient points concerning the research gaps that need to be addressed for overcoming the existing demerits concerning biodiesel production and utilization.

1. The conventional homogeneous catalyst(s) should be replaced by heterogeneous catalyst(s). Homogeneous catalytic process results toxic and hazardous waste streams. Hence, intensive research should be conducted on heterogeneous catalytic process for production of biodiesel and diesel additives.
2. Sustainable production of biodiesel requires use of inexpensive inedible vegetable oil feedstock; accordingly, study should be conducted on use of low cost waste cooking oil.
3. Commercially available catalysts are expensive and hence, there is an utmost need to develop cost-effective solid acid catalyst for economically & environmentally sustainable production of biodiesel and fuel additives.
4. As heterogeneous catalytic process for synthesis of fuel additives and biodiesel are usually time consuming and energy intensive; thus, novel intensification protocol for energy-efficient production should be investigated.
5. Scanty reports are available on engine performance of biodiesel derived from waste frying oil. Accordingly, pertinent studies are required to determine the CI engine performance and the corresponding emission profile (CO_2, CO, O_2, HC & NO_x).

In view of the above mentioned research requirements the present research works envisage to accomplish the following objectives.

I. In order to prepare cost-effective metal impregnated supported catalyst, the carrier shall be selected among various natural/industrial waste materials. The natural waste materials will be resource for calcium-hydroxyapatite avoiding the use of costly reagent based chemically synthesised HAp. Similarly industrial waste resources will be utilized as a cost-effective material to harness SiO_2, Al_2O_3 for application of catalyst carrier materials. Suitable catalyst preparations protocols shall be applied to reduce the cost of catalyst while making the catalyst reusable and environ friendly.

II. As pointed out in the literature review NBM (GoI) had failed to met the target utilization of *jatropha curcas*, accordingly alternative inedible feedstock i.e. waste cooking oil (WCO) (vegetable oil) shall be employed for sustainable production of biodiesel while achieving the desired fuel properties confirming to commercial specifications.

    Further the production process of biodiesel through simultaneous esterification-transesterification reaction will be optimized for maximization of FAME yield of experiment with the help of standard statistical software.

III. Yet another objective of the present research will be synthesized fuel additives through esterification reaction employing the prepared cost-effective catalyst for possible improvements in fuel properties of the diesel/biodiesel fuel. The additive (ester) will be prepared using low-cost alcohol such as methanol and common fatty acid (oleic acid) and the optimal process conditions will be evaluated for maximum FA conversion using suitable design of experiment.

IV. Application of energy efficient electro-magnetic radiation will be an exploratory work in order to enhance and accelerate the yield of biodiesel and fatty acid conversion for

FFA methyl ester production. A comparative assessment between conventional heated reactor and the novel energy efficient far-infrared radiation assisted reactor for production of biodiesel and fuel additives will be made for identification of any possible advantage of the infrared radiated system.

V. The product biodiesel obtained from WCO by application of solid acid heterogeneous catalyst will be blended at different ratios with petro-diesel and evaluated in standard CI engine performance. Moreover the engine exhaust emission will be analysed to identify the percentage reduction of harmful gasses like CO and HC. Additionally possible reduction of engine exhaust temperature due to different blends of biodiesel and petro-diesel will be evaluated to ascertain mitigation of global warming.

CHAPTER: 4

EXPERIMENTAL SECTION

4. EXPERIMENTAL SECTION

4.1. Catalyst preparation

4.1.1. Apparatus

Following pieces of apparatus were required in the present research works for preparation of different catalysts through wet-impregnation method:

1. Jaw crusher
2. Mixture grinder
3. Ball mill
4. Screen Analyses Set-up (Sieve Shaker)
5. Digital balance
6. Glass stirrer; Beaker; Funnel; Measuring cylinder
7. A three-neck flask fitted with centrally mounted mechanical stirrer the other two-necks being fitted with reflux condensers while the whole assembly was mounted on a conventional heating mantle.
8. Hot air oven (up to 110 °C)
9. Muffle furnace (up to 1000 °C)
10. Desiccators

4.1.2. Procedure of catalyst preparation

In the present study, both industrial (viz. fly ash (FA)) and municipal (slaughterhouse animal bone) solid waste materials were used as support to prepare metal impregnated heterogeneous solid acid catalyst(s). Collected waste material was subjected to necessary pre-treatment method. Measured amount of catalyst precursor compound was dissolved in measured amount of water to prepare aqueous solution. On the other hand, water was added to the support (pre-processed finely ground samples) to prepare a slurry. Subsequently, the slurry of the support was taken in to the three-neck flask using funnel. Afterwards, the catalyst precursor solution was added to the three-neck flask apparatus; during this process of hydrothermal treatment the mechanical stirrer was set at specific rotational speed for continuous agitation under thermal energy supplied by the heating mantle. The three-neck flask was equipped with two total reflux condensers (Figure 4.1.) to maintain required amount of water in the three-neck flask in order to facilitate proper hydrothermal treatment. This treatment was carried out for required time at a controlled temperature. Certain amount of ammonium hydroxide was added to the mix to maintain pH for precipitation of precursor from aqueous solution onto the support. The mixt was kept for required time for aging. After aging, the supernatant aqueous phase was separated from the settled mix and the latter was heated in a hot air oven at a pre-set temperature over a certain time to remove water and ammonia to obtain the dried catalyst mass which was subsequently ground to using mixer-grinder followed by ball mill to produce fine solid particles of pre-calcined catalyst. The fine particles were calcined in muffle furnace (in presence of air) at pre-set temperature over certain duration. The calcined catalyst powder was kept in the desiccator; afterwards it was passed processed in the sieve- shaker (for screen analyses) to obtain the required particle size of the metal(s) impregnated solid acid heterogeneous catalyst(s).

The specific details of the pertinent catalyst preparation protocols are described in section 4.4. and 4.6.

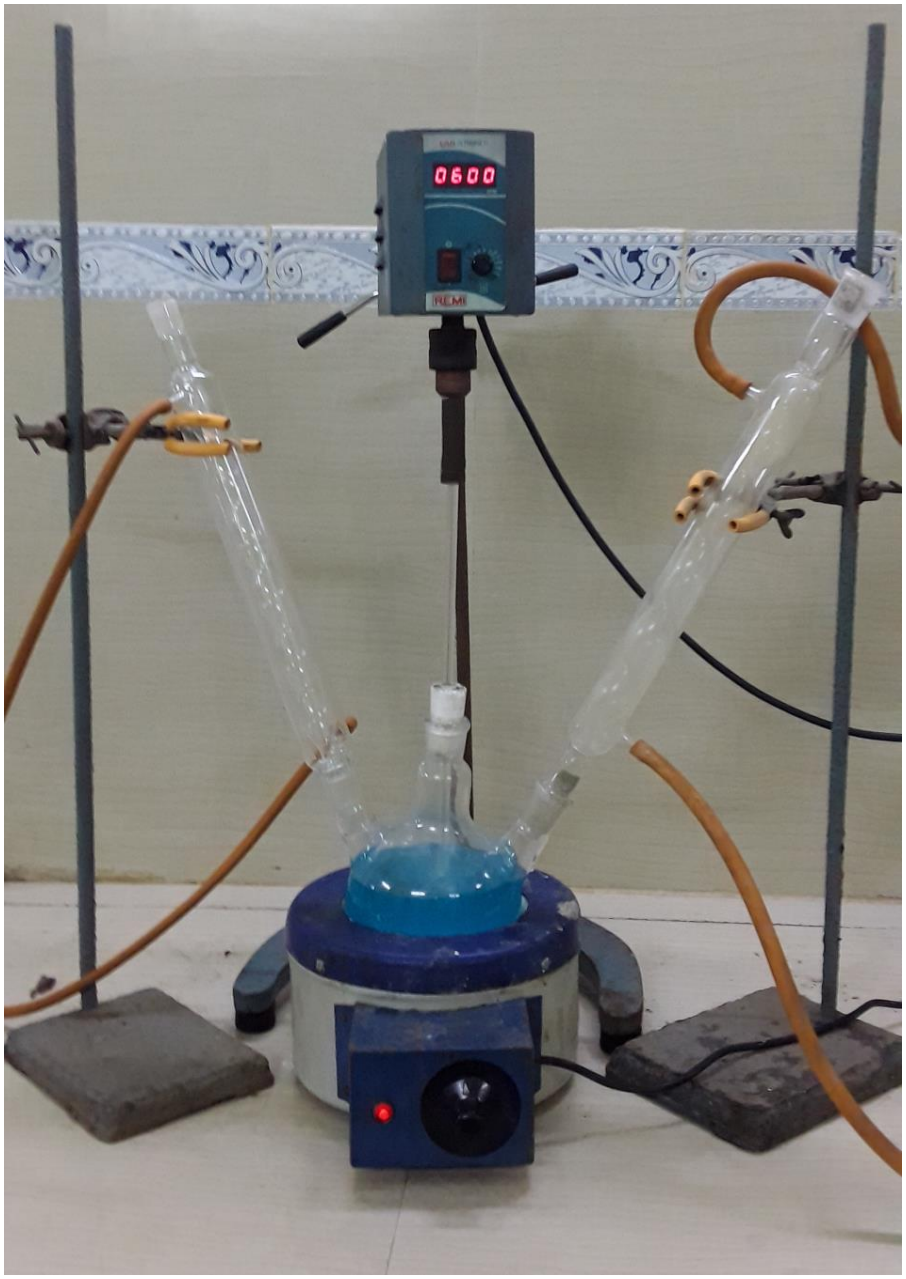

Figure 4.1. Photograph of the catalyst preparation set-up.

4.1.3. Catalyst characterisation methods

4.1.3.1. XRD analysis

In 1912 X-ray diffraction (XRD analysis) method was discovered by Max von Laue. Crystalline phase of a solid material is determined through the XRD analysis. Crystal structures and atomic spacing study of the solid materials are the principal objectives of XRD analysis. The interactions of the incident rays with the sample produces constructive interference (and a diffracted ray) which satisfy Bragg's Law ($n\lambda=2d \sin \theta$). This law relates the wavelength of electromagnetic radiation to the diffraction angle and the lattice spacing in a crystalline sample.

The XRD pattern (Rigaku Miniflex Co., Japan) of solid acid heterogeneous catalyst (prepared in the present research activity) was detected using a Cu Kα source equipped with an Inel CPS 120 hemispherical detector (Figure 4.2.). Analysis was performed at 2θ ranging from 0° to 80° at a scanning speed of 1° min^{-1}.

Figure 4.2. Photograph of the XRD instrument (Rigaku Miniflex Co., Japan).

4.1.3.2. BET and BJH analysis

The first article about the BET (Brunner – Emmett –Teller) theory was published in 1938 by Stephen Brunauer, Paul Hugh Emmett, and Edward Teller. The low-temperature adsorption of the nitrogen gas molecules on the surface of the solid materials (catalyst) is the basic principle of this theory; which quantifies the specific surface area of the catalyst and also classifies the adsorption isotherms of multilayer.

BJH (Barret, Joyner, Halenda) method is mainly used to determine the pore size and pore volume distribution of the catalyst by applying nitrogen gas desorption data.

Quantachrome make NOVA 4000e (Figure 4.3.) instrument was used to measure the specific surface area and pore volume-pore size distribution (adsorption and desorption isotherms) of the prepared catalyst according to BET and BJH methods.

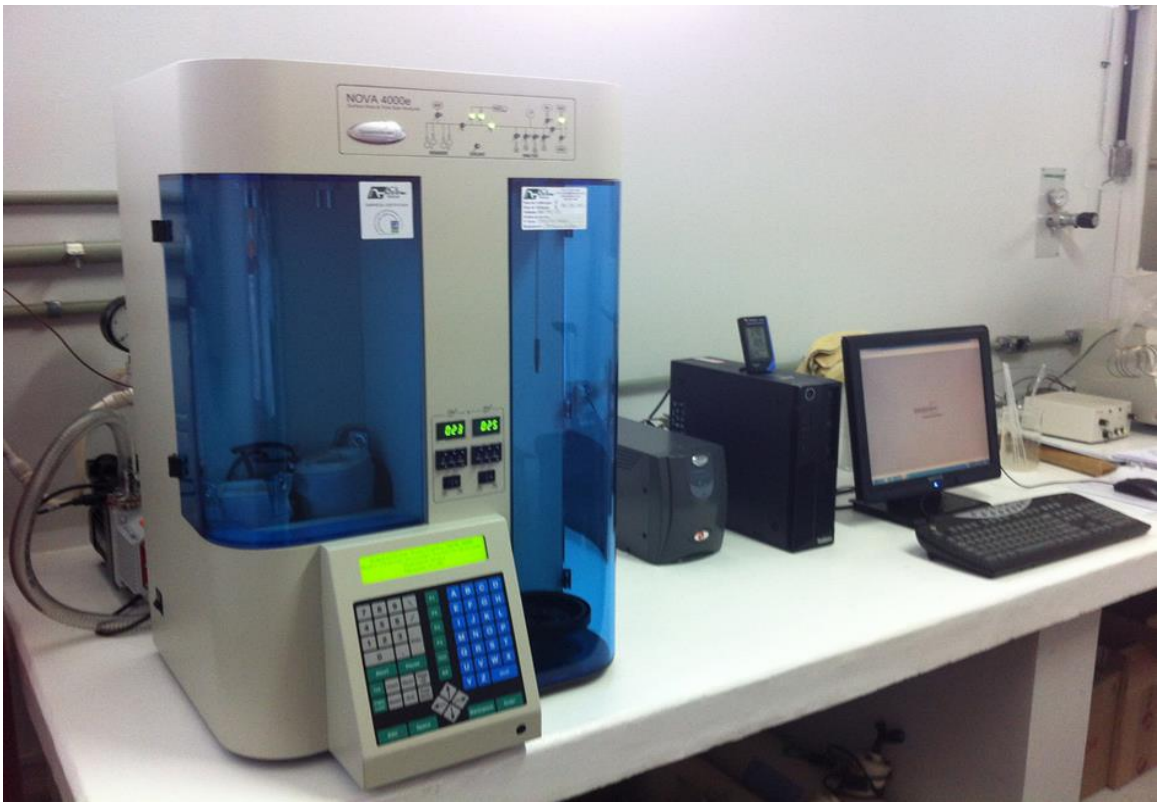

Figure 4.3. Photograph of the surface area and pore size/pore volume analyser (NOVA 4000e).

4.1.3.3. SEM and EDX analyses

The surface morphology of the prepared catalyst was determined using scanning electron microscope (SEM) at 15kV (JEOL Ltd., JSM-6360) (Figure 4.4). Using this same instrument Energy-dispersive X-ray (EDX) analysis was also performed.

SEM produces the magnified image of the surface of the solid material revealing the shape and size of the morphological structure. EDX analytical technique is used for the elemental analysis of the material. Existing elements and the corresponding weight % and atomic % of the solid catalysts are assessed through this method.

Figure 4.4. Photograph of the SEM and EDX analyser.

4.1.3.4. XPS analysis

X-ray photoelectron spectroscopy (XPS) is a surface-sensitive quantitative spectroscopic technique that measures the elemental composition at the parts per thousand range, along with the empirical formula, chemical state and electronic state of the elements that exist within a material. XPS requires high vacuum (P ~ 10^{-8} mbar) or ultra-high vacuum (UHV; P < 10^{-9} mbar) conditions, although a current area of development is ambient-pressure XPS, in which samples are analysed at pressures of a few tens of mbar.

PHI 5000 Versaprobe II scanning XPS microprobe instrument (manufactured by UL-VAC PHI, USA) was used to measure the binding energy of the prepared metal impregnated supported solid catalyst. For monochromatic scanning, Al Kα X-ray source and 180° hemispherical electron analyser, model PHI 10-371 (Figure 4.5.) was deployed.

Figure 4.5. Photograph of the XPS instrument.

4.1.3.5. FTIR analysis

FTIR analysis is a very useful analytical spectroscopic technique for investigation of the surface chemistry of the materials. FTIR spectra of test materials were detected through matching of peaks at a few wavenumbers by comparing with known spectra of chemical species. The theory behind the FTIR analysis underlies that the materials absorb infrared radiation of definite frequencies which are compatible to the structures and the corresponding stretching vibrations of the functional groups in terms of absorbance (Beer's law) at specific wave numbers render its identification. In a typical protocol, the sample powder was mixed with alkyl halide (KBr) and the absorbance was recorded with respect to the KBr window.

In the present research investigations, the FTIR (Fourier Transform Infrared) spectra of the prepared catalyst(s)/support materials were detected with a FTIR, SHIMADZU (Alpha), over a wavenumber ranging from 400 to 4000cm^{-1}.

Figure 4.6. Photograph of the FTIR analyser.

4.1.3.6. TGA analysis

Thermo gravimetric Analysis (TGA) evaluates the magnitude and rate of change in weight of the test sample as a function of temperature or time under a controlled atmosphere at a given heating rate. The testing procedure can characterize the thermal behavior of the test sample which exhibits weight loss or gain owing to dehydration, decomposition, oxidation or other chemical or physical transformations. The testing protocol, thus, in turn, can also determine the compositional change of the test sample due to the application of thermal energy which helps in predicting the thermal stability of the test material (support/ catalyst).

In the present research, the TGA analysis of the support/ catalyst was performed using Perkin–Elmer TGA analyser (Pyris Diamond TG/DTA) over the temperature range from 30 °C to 500 °C. **A** measured amount of the test sample was taken in a vessel which was covered by a quartz tube under constant air flow. The weight of the sample was recorded using the TGA balance as a function of temperature of the sample. The whole assembly was placed in a furnace. The experiment was executed by raising temperature at a rate of 10°C/min and the corresponding change in the weight of sample is logged automatically with time.

Figure 4.7. Photograph of the TGA analyser.

4.1.3.7. TPD analysis

TPD or temperature-programmed desorption is a characterisation technique for determination and assessment of active sites present on the catalyst surface. Specifically, ammonia (NH_3) TPD technique was applied for detection of acidic sites. In a particular NH_3-TPD analysis, the sample of specified amount was preliminarily subjected to degassing at desirable temperature and subsequently cooled at room temperature, while dry ammonia gas (20% NH_3 balance He (UHP)) passed over the sample. He gas was used for wiping the physically adsorbed ammonia. Afterwards, the test sample was gradually heated from room temperature to a prerequisite temperature at a particular heating rate and the desorbed ammonia was measured using a thermal conductivity (TC) detector connected to the sample tube. The strength of acidic sites can be estimated through the amount of NH_3 consumed using the peak area.

In the present research, the TPD analyses (at NH_3 flow rate of 30 mL STP/min) of catalyst samples were performed employing Micromeritics instrument (Figure 4.8.).

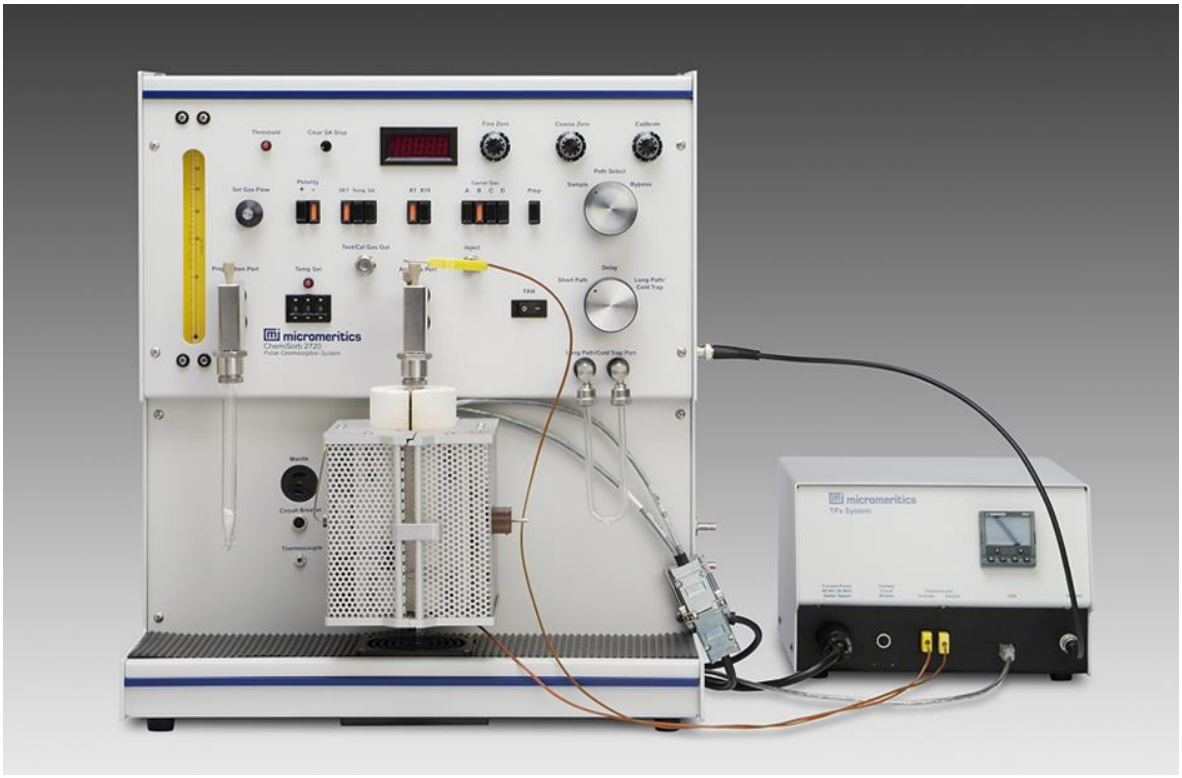

Figure 4.8. Photograph of the TPD instrument.

4.1.3.8. Titration analysis

The acidity of the prepared catalyst was also determined using the method of titration as described by Singh and Fernando (2008).

4.2. Design of experiments

4.2.1. Response Surface Methodology

Response surface methodology (RSM) involves combined mathematical and statistical techniques important for modeling and analysis of problems where the response variable is influenced by operating variables with an objective to optimise the response function over the selected range of the process variables.

The Face-centered central composite design (FCCD) is a standard procedure under RSM that helps in assessing the polynomial relationships between the process independent variables and the dependent (response) variable. The FCCD also reveals the individual effects of process variables on the response variable. Moreover, FCCD can evaluate the interactive effects among operating/process variables in governing the process response. Design Expert 8.0 (State Ease, Inc., Minneapolis, MN, USA) is a well-known software for execution of experimental design through RSM.

A FCCD comprises of lj factorial points (usually coded as ±1), increased by 2j axial points {(±, 0, 0, ..., 0), (0, ±, 0, ..., 0), (0, 0, ±, ..., 0), (0, 0, ..., ±)} and ^{n}c are the centre points (0, 0, 0, ..., 0). Where j is the number of controllable process variables, l is the number of levels for each process parameter.

The relation among independent and dependent (response) variables of the process under investigation can be enumerated by the following empirical equation:

$$Y = \beta_0 + \sum_{i=1}^{j} \beta_i X_i + \sum_{i=1}^{j} \beta_{ii} X_i^{\,2} + \sum_{i=1}^{j-1} \sum_{i=1}^{j=2} \beta_{ij} X_i X_j \; + e = \check{}0 \qquad (4.1.)$$

Where Y is the response variable and X is the input variable. β_0 is constant coefficient, β_i is the coefficient showing linear effects, β_{ii} represents quadratic effects and β_{ij} demonstrates interactive effects of the independent variables on the response variable. Furthermore, the

polynomial functions of response(s) and the degree of influence of input variables were assessed by ANOVA technique.

In the present investigation, the "Face-centered central composite design (FCCD)" has been used in the analyses and optimisation of methyl oleate (MO) production under an energy-efficient application of far-infrared radiation in presence of the prepared FA supported Fe-Ni-solid acid catalyst.

4.2.2. Taguchi Orthogonal Design

Taguchi Orthogonal Design, a robust method of 'design of experiment', has been implemented in recent times to optimize process involving several interactive factors/variables. Taguchi orthogonal array ['MINITAB-16': Minitab Inc. USA for Windows7] provides a set of experimental runs involving process factors and response variable in order to evaluate the effect of all process factors on the response variable. Furthermore, it also provides a set of optimum process factors for maximisation of process response by analysing the signal to noise ratio (S/N) and analysis of variance (ANOVA). Here, signal (S) symbolizes the arithmetic mean of replicated three experimental values of the response variable while noise (N) represents the corresponding standard deviation for each trial. The S/N ratio was calculated using "larger the better" criterion for each trial by Equation 4.2.

$$S/N = -10\log\left(\frac{1}{n}\sum_{i=1}^{n}\frac{1}{\gamma_{MG,i}^{2}}\right) \qquad (4.2.)$$

In the present investigation, the "Taguchi Orthogonal Design" has been used in the analyses and optimisation of biodiesel production from used frying mustard oil employing commercially available Amberlyst 15 catalyst.

4.2.3. D-Optimal Method

D-optimal method is another form of experimental design provided by a specific algorithm. D-optimal method matrices are usually not orthogonal and factorial effect estimates are correlated. D-optimal designs are optimizations based on a chosen optimality criterion with corresponding fitting of the best model. The optimality criterion used in generating D-optimal designs is one of maximizing |X'X|, the determinant of the information matrix X'X.

This optimality criterion results in minimizing the generalized variance of the parameter estimates for a pre-specified model. The computer algorithm chooses the optimal set of design runs from a candidate set of possible design treatment runs. This candidate set of treatment runs usually consists of all possible combinations of various factorial levels over the selected parametric range of the desired experiment.

The reasons for using D-optimal designs instead of standard classical designs:

- Standard factorial or fractional factorial designs require too many runs for the amount of resources or time allowed for the experiment.
- The design space is constrained (the process space contains factor settings that are not feasible or are impossible to run).

Design Expert 8.0.4 (State Ease, Inc., Minneapolis, MN, USA) software was used to generate D-optimal experimental design for the biodiesel production through concurrent esterification-transesterification reaction in the present study.

4.3. Biodiesel and Diesel additives preparation

4.3.1. Apparatus

Following pieces of apparatus were required in the present research works for preparation of diesel additives and biodiesel from different resources:

1. A three-neck flask fitted with centrally mounted mechanical stirrer the other two-necks being fitted with reflux condensers.
2. Glass stirrer; Beaker; Funnel; Measuring cylinder; Burette; Conical flask
3. Vacuum filter
4. Far infrared radiated heating system
5. Centrifuge
6. Rotary evaporator
7. Heating mantle
8. Digital balance

4.3.2. General procedure of biodiesel production

The collected waste cooking oil (WCO) was initially filtered to separate suspended impurities and subsequently washed with water to remove the soluble impurities. Afterwards, a specified amount of pre-treated WCO was poured into a three-neck flask (equipped with total reflux condenser and fitted with mechanical stirrer and required heating system) to prepare biodiesel. Solid acidic heterogeneous catalyst (required amount) was added to the flask and was stirred at controlled speed for mixing. Then a measured volume of methanol was added into the reaction mixture through the funnel into the flask; while the pre-set reaction temperature was maintained by supplying necessary thermal energy employing an energy-efficient far infrared (FIR) radiation system (Figure 4.9.). Simultaneously, esterification and transesterification reactions could be carried out for certain time to generate biodiesel from WCO/ used frying mustard oil.

Afterwards the solid heterogeneous acid catalyst was separated from the reaction mixture using vacuum filtration. After separation of the solid catalyst, centrifugation process was carried out to separate glycerol (by product) from the fatty acid methyl ester (FAME)/ biodiesel layer. The existence of biodiesel was found in the top layer and the by-product (of transesterification reaction) glycerol was separated as bottom layer. Water [by-product of the esterification reaction between free fatty acid i.e. FFA (present in WCO) and methanol] and excess methanol were also present in the top layer with the product biodiesel. Using rotary evaporator water and excess methanol was removed from the biodiesel and it was stored in glass containers for subsequent evaluation of fuel properties, engine performance and emission assessments.

In order to evaluate the supremacy of the far infrared (FIR) radiation system over the conventional heating system, experiments were also carried-out deploying conventional

heating system (Figure 4.10.) at otherwise identical process conditions. The results obtained under the influence of the two different heating systems were compared in terms of biodiesel yield, reaction time requirement and energy consumption.

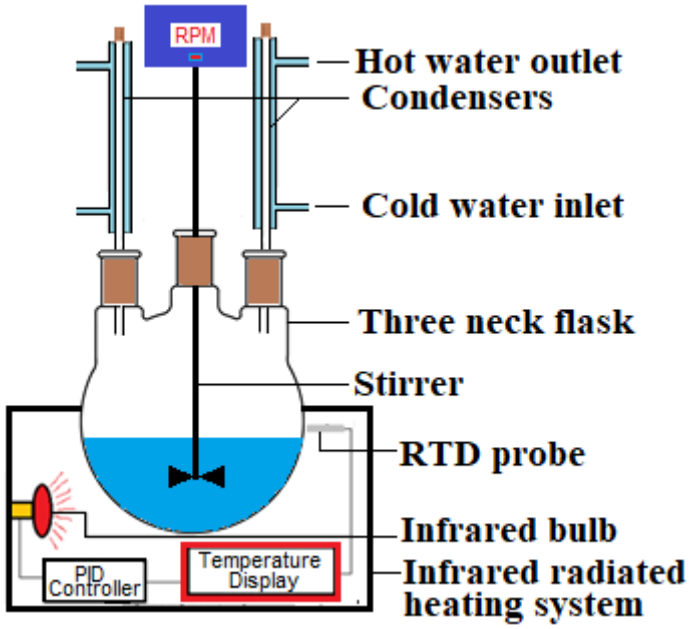

Figure 4.9. Schematic of experimental setup using far infrared (FIR) radiated heating system.

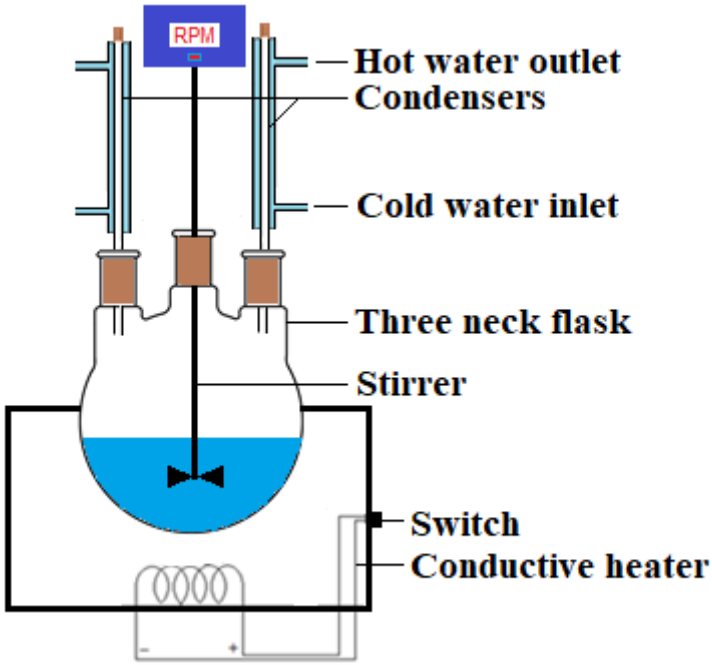

Figure 4.10. Schematic of experimental setup using conventional heating system.

4.3.3. GCMS analysis of biodiesel

The composition of the product biodiesel was determined using GC–MS (model: TRACE GC ULTRA; Thermo- Fisher Scientific Ltd.) (Figure 4.11.) with POLARIS Q Mass Selective Detector. TR-WAX capillary column (30m × 0.25mm × 0.25µm) was used; using He as the carrier gas (50 mL/min). The initial oven temperature was 50 ℃ for 1 min and was subsequently increased to 260 ℃ at the rate of 10 ℃ min^{-1}. A hold time of 30 min was used to determine the methyl esters. Electron ionisation of mass spectroscopy was 70 eV (electron Volts) while maintaining the mass ranges 50–900 in full scan mode. FAMEs were identified and quantified with internal standard calibration suitable for methyl esters between C14 and C24 according to EN Method 14103.

Figure 4.11. Photograph of GC-MS analyser.

4.4. Fly ash supported Ni—Fe solid acid catalyst for efficient production of diesel additive: intensification through far-infrared radiation

4.4.1. Materials

- Hexahydrate nickel nitrate
- Methanol (>99% purity) (M)
- Oleic acid (OA)
- Ammonium hydroxide
- Silica gel
- Molecular sieve
- Ferric sulphate monohydrate
- Fly ash (FA), which was collected from Kolaghat Thermal Power Plant (Figure 4.12.), West Bengal, India.

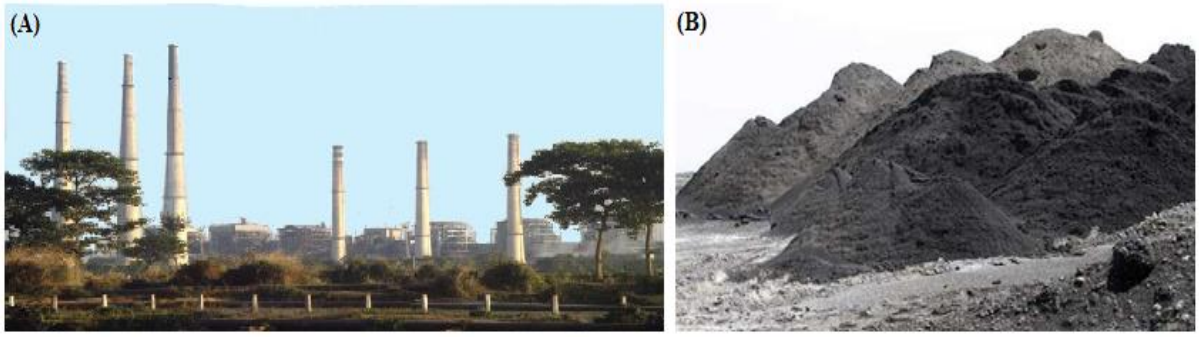

Figure 4.12. (A) Photography of Kolaghat Thermal Power Plant, West Bengal, India and (B) Fly ash of the power plant.

4.4.2. Catalyst preparation method

Initially, FA was calcined at 900 °C in a muffle furnace for 2 h to remove carbonaceous impurities. Aqueous solutions of $Ni(NO_3)_2 \cdot 6H_2O$ and $Fe_2(SO_4)_3 \cdot H_2O$ were separately prepared and finally added to a measured amount of calcined-FA in three weight ratios: $Ni(NO_3)_2 \cdot 6H_2O$:$Fe_2(SO_4)_3 \cdot H_2O$:FA of 1:5:2 (NI-5), 1:10:2 (NI-10) and 1:15:2 (NI-15). The mixture was vigorously agitated as per wet-impregnation protocol at 60 °C, for 2 h under total reflux in a three-necked flask. Subsequently, ammonium hydroxide solution was added to maintain pH at 10 for completion of precipitation. It was aged for 48 h and consequently dried for 12 h, at 105 °C in hot air oven. The dried mass was grinded to fine powder (150 mesh). Finally, at 700 °C, the dried mass was calcined for 4 h to obtain the Ni—Fe/FA catalyst.

4.4.3. Design of experiment

Statistical analysis of experimental design was performed using Design Expert 8.0 software. Face centred central composite design (FCCD) was used with three factors viz. M to OA molar ratio (Q_{MR}), $Fe_2(SO_4)_3 \cdot H_2O$ loading (Q_L) and catalyst concentration (Q_C) (Table 4.1.).

Table 4.1. Experimental Ranges and Levels of the Process Factors used in FCCD

Factors	Name	Units	-1 level	0 level	+1 Level
Q_{MR}	Methanol/OA molar ratio	-	5.00	10.00	15.00
Q_L	$Fe_2(SO_4)_3.H_2O$ loading	wt%	5.00	10.00	15.00
Q_C	Catalyst concentration	wt% of OA	2.00	3.00	4.00

Experimental runs were performed based on 15 different combinations of the coded variables (Table 4.2.). Coded variables are $q_{MR} = \frac{Q_{MR} - 10}{5}$, $q_L = \frac{Q_L - 10}{5}$ and $q_C = \frac{Q_C - 3}{1}$.

Table 4.2. Face-centred central composite Design (FCCD) layout for esterification of OA using Ni-Fe/FA catalyst

Run	Factor (q_{MR})	Factor (q_L)	Factor (q_C)	Response (γ_{OA})
	Methanol/oleic acid molar ratio	**$Fe_2(SO_4)_3.H_2O$ loading (wt%)**	**Catalyst concentration (wt% of OA)**	**OA conversion (%)**
1	0.00	0.00	-1.00	91.09 ± 0.20
2	-1.00	1.00	-1.00	97.24 ± 0.15
3	-1.00	-1.00	1.00	87.77 ± 0.17
4	-1.00	-1.00	-1.00	90.11 ± 0.10
5	0.00	-1.00	0.00	88.78 ± 0.20
6	1.00	-1.00	-1.00	86.50 ± 0.15
7	1.00	-1.00	1.00	87.55 ± 0.14
8	-1.00	1.00	1.00	94.90 ± 0.21
9	1.00	0.00	0.00	92.02 ± 0.15
10	0.00	1.00	0.00	97.21 ± 0.20
11	0.00	0.00	1.00	92.34 ± 0.16
12	0.00	0.00	0.00	92.77 ± 0.18
13	1.00	1.00	1.00	98.37 ± 0.19
14	-1.00	0.00	0.00	92.09 ± 0.15
15	1.00	1.00	-1.00	97.49 ± 0.10
16	0.00	0.00	0.00	92.53 ± 0.20

4.4.4. Reaction procedure

Esterification of OA was primarily performed in a conventionally heated reactor (CHR) (500-mL three-necked flask, equipped with two reflux condensers and a PID temperature controller provided with a 300 W conductive heating mantle) at a controlled stirrer speed of 600 rpm. Initially fixed amount of OA (10 mL, 9.1 g) and measured amount of catalyst were stirred for few minutes at 60 °C to make OA-catalyst slurry. Afterwards, required quantity of M was added to the reactor, and the reaction took place for 1 h. Experiments were conducted according to parametric values (Table 4.1.) and OA conversions were measured as the response values in accordance with the FCCD matrix (Table 4.2.) to evaluate optimal factorial combination for maximizing OA conversion. At the end of the reaction, the mixture was vacuum filtrated to separate the solid catalyst. After filtration, hot distilled water was added to the filtrate to dissolve the excess M. To separate the ester phase from the aqueous phase, the mix was centrifuged for 10 min at about 5000 rpm, to obtain MO (methyl oleate) as the top layer.

$$OA + M \rightarrow MO \text{ (methyl ester)} + H_2O \text{ (by product)}$$

After assessing the optimal factorial values corresponding to maximum OA conversion (from Table 4.2.) in CHR; an attempt was made to enhance and accelerate the OA conversion by incorporating 40 wt.% of silica gel (SG) or molecular sieve (MS) desiccants for adsorption of the by-product water. Moreover, at optimal values of the process factors, in presence of desiccants (SG or MS), efficacy of a far-infrared radiated reactor (FIRRR) system (50 Hz, 100 W, 220 V, frequency 3 THz–300 GHz, wavelength 100 μm–1 mm, energy 12.4 meV–1.24 meV) on OA conversion was also investigated.

4.4.5. Conversion analysis

Through the titration process (Tesser et al., 2009) the concentration of unreacted OA (Equation 4.1.) in the product MO was analysed. From the acid value, the OA conversion (Equation 4.2.) was evaluated (% conversion of the OA) and the details are given below:

$$C_{OA} = \frac{56.11 \times N \times V}{m} \qquad (4.3.)$$

$$\gamma_{OA} = \left[\frac{AV_{OA} - C_{OA}}{AV_{OA}} \times 100 \right] \qquad (4.4.)$$

Where, C_{OA} is the Concentration of oleic acid;

N is the Normality of potassium hydroxide solution;

V is the Volume of potassium hydroxide consumed from burette;

AV_{OA} is the Acid value of oleic acid = 200;

m is the Weight of ester layer;

γ_{OA} is the % of OA conversion.

4.5. Optimization of fast and energy-efficient biodiesel production under infrared radiated from waste mustard oil catalysed by Amberlyst 15: Engine performance and emission quality assessments

4.5.1. Materials

- Waste mustard oil (WMO) was collected from local restaurants
- Amberlyst 15
- Methanol
- Petro-diesel (Indian Oil Corporation)

4.5.2. Design of experiment

Taguchi Orthogonal Design (TOD) was used to assess and optimize the effects of three process factors viz. methanol to WMO molar ratio (λ_{MO}), catalyst concentration (λ_{CC}) and stirrer speed (λ_{SS}) (Table 4.3.) on biodiesel (FAME) yield using MINITAB-16 software (Minitab Inc. USA for Windows 7).

Table 4.3. Experimental process factors and levels for production of biodiesel from WMO under FIR radiation

Process Factors	λ_{MO}	λ_{CC} (wt%)	λ_{SS} (rpm)
Lower Level (LL)	4:1	2	600
Middle Level (ML)	6:1	4	800
Upper Level (UL)	8:1	6	1000

Using TOD, different experimental runs (Table 4.4.) were conducted to evaluate the optimal factorial values for maximum FAME Yield from WMO. Signal to noise ratio (S/N) for each

run was calculated using Equation 4.5. In present study higher FAME yield (Y_{FAME}) was preferred i.e. "Larger is better" criteria was employed.

$$S/N = -10\log\left(\frac{1}{n}\sum_{x=1}^{n} 1/K_x^2\right) \quad (4.5.)$$

$$S/N_{EST} = \overline{S/N} + \sum_{a=1}^{i}\left(S/N_a - \overline{S/N}\right) \quad (4.6.)$$

Where, K_x: Y_{FAME} corresponding to run x; x:number of replication; n:number of experiments conducted using a particular combination of process factors as shown in Table 4.4. $\overline{S/N}$: mean of the S/N ratio; S/N_a: S/N ratio corresponding to the optimal process factors; i & a:the number of the process factors that significantly affected the optimal conditions of Y_{FAME}.

Table 4.4. TOD layout of different factorial combinations and corresponding mean of biodiesel (FAME) Yield (Y_{FAME}) from WMO under FIR radiation and corresponding values of signal-to-noise ratio (S/N)

Run no.	λ_{MO}	λ_{CC} (wt% of WMO)	λ_{SS} (rpm)	Y_{FAME} (%)	S/N (db)
1.	LL	LL	LL	89.71	39.00
2.	LL	ML	ML	94.25	39.43
3.	LL	UL	UL	96.61	39.65
4.	ML	LL	ML	92.10	39.23
5.	ML	ML	UL	95.98	39.59
6.	ML	UL	LL	96.23	39.61
7.	UL	LL	UL	92.99	39.31
8.	UL	ML	LL	94.73	39.47
9.	UL	UL	ML	96.75	39.66

4.5.3. Experimental procedure

The collected WMO was vacuum-filtered to remove any solid-impurities. Using far infrared radiation (FIR) (100 W; wavelength: 2.700–30 μm) the WMO was converted to biodiesel in a 1 L three-necked flask equipped with two reflux condensers and a PID type temperature controller (to maintain temperature at 60 °C). At the outset of the conversion, the catalyst was mixed with WMO to prepare slurry in the reactor. Subsequently, methanol was added to the reactor to produce biodiesel and the reaction was conducted for 30 min and the catalyst was separated using vacuum filtration. The top reaction layer (containing biodiesel) was separated by centrifugation at 5000 rpm for 15 min. As the separated biodiesel layer contained methanol and water; rotary evaporation was done for biodiesel purification. To assess the superiority of infrared radiation protocol over conventionally heated reactor, experiment was conducted at the derived optimal condition (through TOD) with a similar reactor provided with conventional heating system (400 W, laboratory scale heating mantle).

After each batch experiment, the recovered Amberlyst 15 catalyst was washed with methanol and afterwards dried in hot air oven at 110 °C for 2 h for its regeneration and subsequently reused in another batch till it could retain the desired catalytic activity.

4.5.4. Yield analysis of biodiesel

The FAME content of the product biodiesel from WMO was calculated through Equation 4.5. (Chakraborty and Das, 2012).

$$Y_{FAME} = \left(W_b / W_O \right) \mathrm{P}_{FAME} \times 100 \qquad (4.5.)$$

Where, P_{FAME} = purity of FAME;

W_b = weight (g) of biodiesel;

W_O = weight (g) of WMO;

Y_{FAME} = FAME yield of the product biodiesel.

The composition of biodiesel produced from WMO (through both FIR heating system and conventional heating system) was determined using GC–MS.

4.5.5. Engine performance test and exhaust emission analyses

The engine performance test was conducted in a standard diesel engine (Figure 4.13.). The engine specifications are highlighted in Table 4.5. The measurement range of gas analyser emission parameters were: CO: 0–15%; HC: 0–20,000 ppm; CO_2: 0–20%; O2: 0–25%; NO_X: 0– 000 ppm. The exhaust emission detected by the EPM 1601.

Table 4.5. Specification of the diesel engine

Type	4-Stroke, Single Cylinder Diesel Engine (Water Cooled), Compression Ignition
Make	Kirloskar AV-1
Related Power	3.7 KW, 1500 RPM.
Bore and Stroke	80mm*110mm
Compression Ratio	16.5 : 1 and variable from 13 to 20 (Approx.)
Cylinder Capacity	553 cc.
Dynamometer	Eddy current Dynamometer
Starting	Hand cranking
Orifice Diameter	20mm.
Radius of Torque arm	0.150 meter

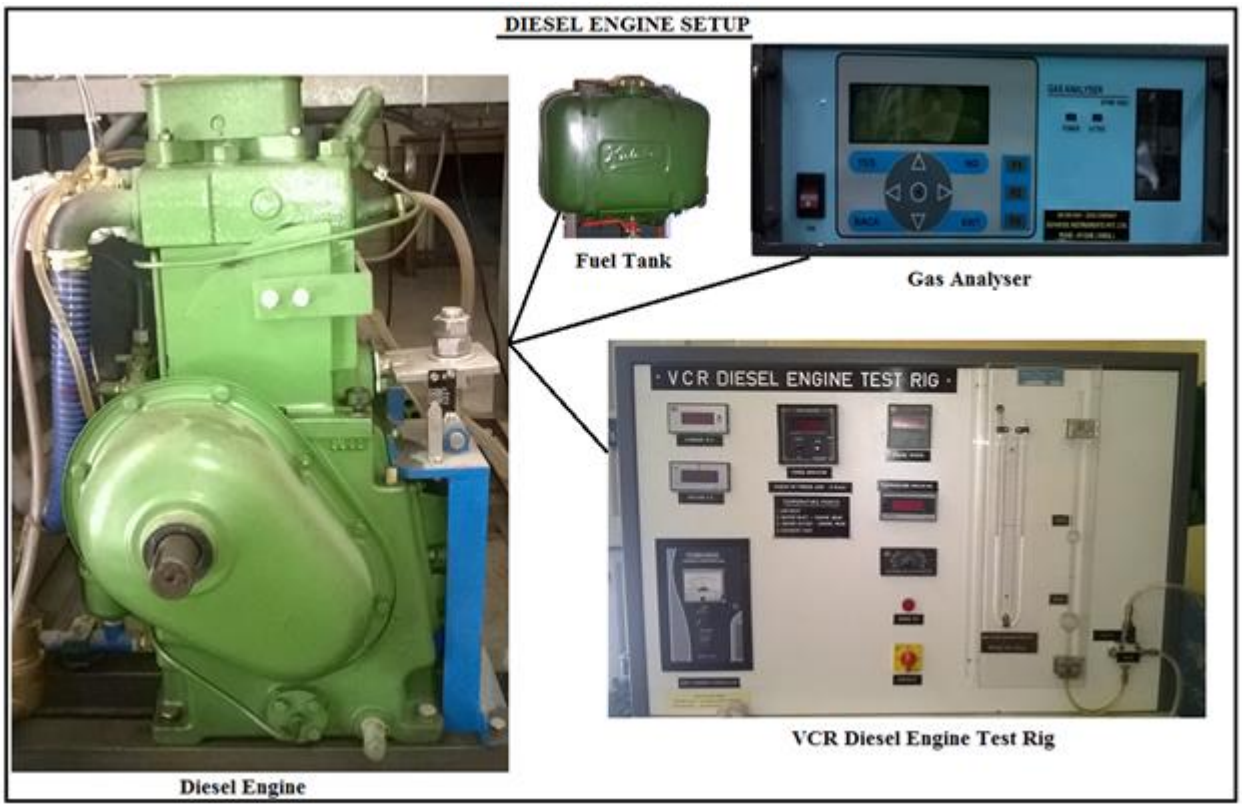

Figure 4.13. Diesel engine setup for Engine Performance Test and Exhaust Emission analyses.

4.6. Optimal efficient biodiesel synthesis from used oil employing low-cost ram bone supported Cr catalyst: engine performance and exhaust assessment

4.6.1. Materials

- Waste ram bone (WRB) (Figure 4.14.) was collected from the local butcher shop of Jadavpur, West Bengal, India.
- Chromium III nitrate (nonahydrate)
- Methanol (≥ 99.8% purity),
- Ethanol (≥ 99.9% purity),
- Ammonium hydroxide
- Used fried mustard oil (UFMO) was collected from a canteen of Jadavpur University.

Figure 4.14. (A) Photograph of (A) raw ram bone and (B) bone powder.

4.6.2. Preparation of ram bone supported Cr catalyst

Collected WRB was washed with hot water repeatedly and rigorously to remove fatty and fleshy materials. Left over minute particles of fats present in the inner layers of the bones were washed with ethanol. Afterwards, WRB was dried for 24 h at 105 ± 1°C in a hot air oven. The dried WRB was crushed in a grinding mill to make ram bone derived biological hydroxyapatite (BiHAp) fine powder (64-53 µm). 10 wt.% of aqueous chromium III nitrate (nonahydrate) was impregnated on BiHAp through wet-impregnation method at 50 °C hydrothermal treatment temperature for 2 h in a 1 L three-neck flask with total reflux condition. In order to facilitate precipitation, NH_4OH aq. solution (25%) was added drop wise while maintaining the pH at 10. The mixture was aged for 24 h and subsequent drying was carried out for 12 h at 105 ± 1 °C to remove water. Afterwards, the dried mass was calcined in air (using muffle furnace) at three different temperatures i.e. 200 °C, 300 °C and 400 °C for 4 h to prepare three different BiHAp supported-chromium heterogeneous catalysts designated respectively as CH2, CH3 and CH4. The final prepared catalysts were again ground to maintain the particle size (64-53 µm).

4.6.3. Design of Experiment

In the present study, D-optimal experimental design was executed to evaluate the factorial effects on FAME yield through Design Expert 8.0.4 Software. Three process factors viz. calcination temperature (N_{CT}), catalyst concentration (N_{CC}) and methanol/UFMO molar ratio (N_{MR}); at three different levels (Table 4.6.) were used for the optimization of FAME yield.

Table 4.6. Experimental process factors and levels used in the experimental design

Factors	Name	Units	-1 Level	0 level	+1 Level
N_{CT}	Calcination temperature	°C	200	300	400
N_{CC}	Catalyst concentration	wt.% of UFMO	2.00	3.00	4.00
N_{MR}	Methanol/UFMO molar ratio	-	4.00	6.00	8.00

The coded variables are $n_{CT} = \frac{N_{CT} - 300}{100}, n_{MR} = \frac{N_{MR} - 6}{2}$ and $n_{CC} = \frac{N_{CC} - 3}{1}$. "D" optimality condition for maximum FAME yield was chosen corresponding to maximum polynomial coefficients. In order to find the best design points, a set of candidates was chosen employing point exchange search. The set of candidate points chosen for the experiments were vertices, centers of edges and overall centroid with total 21 points. Experiments were carried out using different combinations (Table 4.7.) of the process factors in coded form.

Table 4.7. D-optimal layout depicting different factorial combinations of concurrent transesterification-esterification of UFMO

Run	Factor (n_{CT})	Factor (n_{CC})	Factor (n_{MR})	Response (ψ_{FAME})
	Calcination temperature	**Catalyst concentration**	**Methanol/UFMO molar ratio**	**FAME Yield (%)**
1	-1.00	1.00	1.00	96.85
2	-1.00	1.00	-1.00	95.62
3	-1.00	0.00	-1.00	94.20
4	0.00	0.00	0.00	88.79
5	-1.00	-1.00	-1.00	92.58
6	-1.00	-1.00	1.00	94.99
7	1.00	-1.00	1.00	85.71
8	1.00	-1.00	1.00	85.54
9	1.00	1.00	-1.00	89.42
10	1.00	-1.00	-1.00	81.51
11	1.00	1.00	1.00	93.73
12	1.00	1.00	0.00	90.11
13	0.00	1.00	-1.00	91.89

4.6.4. Reactor setup and biodiesel production

Using laboratory-scale vacuum filtration, collected UFMO was filtered three times consecutively to separate the suspended solid matters. Subsequently, the filtrate (UFMO) was washed with hot water for several times to remove the dissolved salt impurities. Water phase and oil phase were separated employing a high speed centrifuge at 5000 rpm, for 10min (Chakraborty and Das, 2012). Separated upper layer of UFMO (acid value: 5.3 mg KOH/ g UFMO) was collected for the concurrent transesterification-esterification (CTE) reaction.

The biodiesel production was carried out in a three-neck flask (1 L) equipped with two water-cooled condensers to maintain total reflux condition at 60 °C, in presence of the far infrared

radiated heating system (FIRRHS) (50Hz, 100W, 220 V, frequency 3THz–300GHz, wavelength 100μm–1mm, energy 12.4meV–1.24meV) for 30 min. At the out-set, catalyst-UFMO slurry was made; next, methanol was added in to the reactor under agitation (700 rpm). After the stipulated reaction time (30 min, determined from preliminary runs), solid catalyst was separated through vacuum filtration process. Due to CTE reactions, water and glycerol were produced as by-products. The reaction mixture was centrifuged (5000 rpm, 10 min) to separate it into the top (biodiesel) and bottom (water and glycerol) layers. For comparative assessment, experiments were also conducted using a conventionally heated (400 W heating mantle) reactor at the predicted optimal factorial combinations.

4.6.5. Analysis of the product biodiesel

Equation (4.7.) is used to calculate the FAME content (ψ_{FAME}) of the produced biodiesel from UFMO:

$$\psi_{FAME} = \left(W_B / W_{UFMO} \right) \mathrm{P}_{FAME} \times 100 \qquad (4.7.)$$

Where, P_{FAME} = purity of FAME;

W_B = weight (g) of biodiesel;

W_{UFMO} = weight (g) of UFMO.

The composition of biodiesel produced from UFMO (through both FIR heating system and conventional heating system) was determined using GC–MS.

4.6.5. Engine performance test and exhaust emission analyses

The engine performance test was conducted using the standard DE (details of the engine is given in section 4.5.5) available at chemical engineering department of Jadavpur university.

References

Chakraborty, R. and Das, S.K., 2012. Optimization of biodiesel synthesis from waste frying soybean oil using fish scale-supported Ni catalyst. Industrial & Engineering Chemistry Research, 51(25), pp.8404-8414.

Singh, A.K. and Fernando, S.D., 2008. Transesterification of soybean oil using heterogeneous catalysts. Energy & Fuels, 22(3), pp.2067-2069.

Tesser, R., Casale, L., Verde, D., Di Serio, M. and Santacesaria, E., 2009. Kinetics of free fatty acids esterification: batch and loop reactor modeling. Chemical Engineering Journal, 154(1-3), pp.25-33.

CHAPTER: 5

RESULTS AND DISCUSSIONS

5. RESULTS AND DISCUSSIONS

5.1. Fly ash supported Ni—Fe solid acid catalyst for efficient production of diesel additive: intensification through far-infrared radiation

5.1.1. Design of experiment

In the present research work, to estimate the optimal process factors for maximum conversion of Oleic acid (OA) to Methyl oleate (MO) in esterification reaction, the RSM model based on FCCD has been established with three factors viz. Q_{MR}, Q_L and Q_C.

The experimental outcomes exhibiting OA conversion (γ_{OA}) as a function of process factors are formulated according to FCCD (Table 4.2.).

From the statistical 'Model Fit Summary' (Table 5.1.), 2FI model has been the best fitted model to signify the parametric effects on compared to the linear and quadratic models. Here, 2FI model exhibits superior statistical criteria than the linear or quadratic models in terms of the standard deviation, R^2, predicted-R^2 and adjusted-R^2. The Equation 5.1. represents the 2FI model equation that correlates γ_{OA} and process factors in coded form. On the other hand Eqnuation 5.2. that represents in the terms of actual factors.

Table 5.1. Model summary statistics of linear, 2FI and quadratic model formulated for predicting OA conversion to methyl oleate using different Ni-Fe/FA catalysts

source	Prob > F	Stander deviation	R^2	Adjusted R^2	Predicted R^2	Press value
linear	<0.0001	1.17	0.9239	0.9049	0.8292	36.66
2FI	0.0031	0.64	0.9826	0.9709	0.9528	10.13
quadratic	0.2451	0.57	0.9909	0.9771	0.9300	15.01

Analysis of variance (ANOVA) portraying the F-Test is shown in Table 5.2. The F- Test recommends that a two-factor interaction (2FI) model with a p-value (probability of error value) of <0.0001 is significant to predict γ_{OA}.

$$\gamma_{OA} = 92.42 - 0.018q_{MR} + 4.45q_L - 0.15q_C + 0.94q_{MR}q_C + 0.83q_{MR}q_C - 0.021q_Lq_C$$
$$(R^2 = 0.9826) \qquad (-1 < q_{MR}, q_L, q_C < +1) \qquad (5.1.)$$

$$\gamma_{OA} = 92.42250 - 0.018000Q_{MR} + 4.45000Q_L - 0.15000Q_C + 0.94375Q_{MR}Q_C + 0.8265Q_{MR}Q_C - 0.02125Q_LQ_C \qquad (5.2.)$$

Table 5.2. ANOVA results of OA Conversion Corresponding to Equation 5.1.

Source	**Sum of Squares**	**df**	**Mean Square**	**F Value**	**p-Value Probability p>F**
model	210.84	6	35.14	84.54	<0.0001
q_{MR}	0.00324	1	0.00324	0.00795	0.9316
q_L	198.03	1	198.03	476.43	<0.0001
q_C	0.22	1	0.22	0.54	0.4806
q_{MR} q_L	7.13	1	7.13	17.14	0.0025
q_{MR} q_C	5.46	1	5.46	13.14	0.0055
q_L q_C	0.003613	1	0.003613	0.008691	0.9278
residual	3.74	9	0.42		
lack of fit	3.71	8	0.46	16.11	0.1905
pure error	0.029	1	0.029		
corrected total	214.58	15			

5.1.2. Influence of individual parametric effect on OA conversion

The ANOVA (Table 5.2) revealed that q_L (coded form of $Fe_2(SO_4)_3.H_2O$ loading over flyash) was the most significant model term ($p \prec 0.05$) and had maximum effect on γ_{OA}; while, q_{MR} (coded form of methanol/oil molar ratio) and q_C (coded form of catalyst concentration) were statistically insignificant tem and has relatively lower effect on γ_{OA}. These interpretations corroborate well with the model equation (Equation 5.1.). The increase in q_L resulted greater acidity of the catalyst thus, increasing the conversion of OA to MO.

5.1.3. Optimal process conditions

The optimal process conditions viz. M/OA molar ratio (Q_{MR}) of 15:1, NI-15 $Fe_2(SO_4)_3.H_2O$ loading (Q_L) and 4 wt.% of catalyst concentration (Q_C) were determined through RSM. Maximum predicted OA conversion was 98.43% which was computed at the optimal process conditions of the reaction. MO production was accomplished in triplicate at the predicted optimum conditions rendering an experimental 98.37 ± 0.01 % OA conversion. It demonstrates approximately 0.06% differences between predicted and experimental OA conversion.

Kusmiyati, 2010 reported that using homogeneous H_2SO_4 catalyst 97.71% OA conversion was achieved, while in the present work the optimum OA conversion was 98.37%; which is greater than the previous study. Besides, the maximum conversion of OA achieved in the present study is remarkably higher than that reported (93.0%) (Chakraborty and RoyChowdhury, 2013) while using biological-hydroxyapatite supported Fe catalyst. Thus, the developed catalyst prepared in present study represents an efficient acid catalyst for performing esterification reaction.

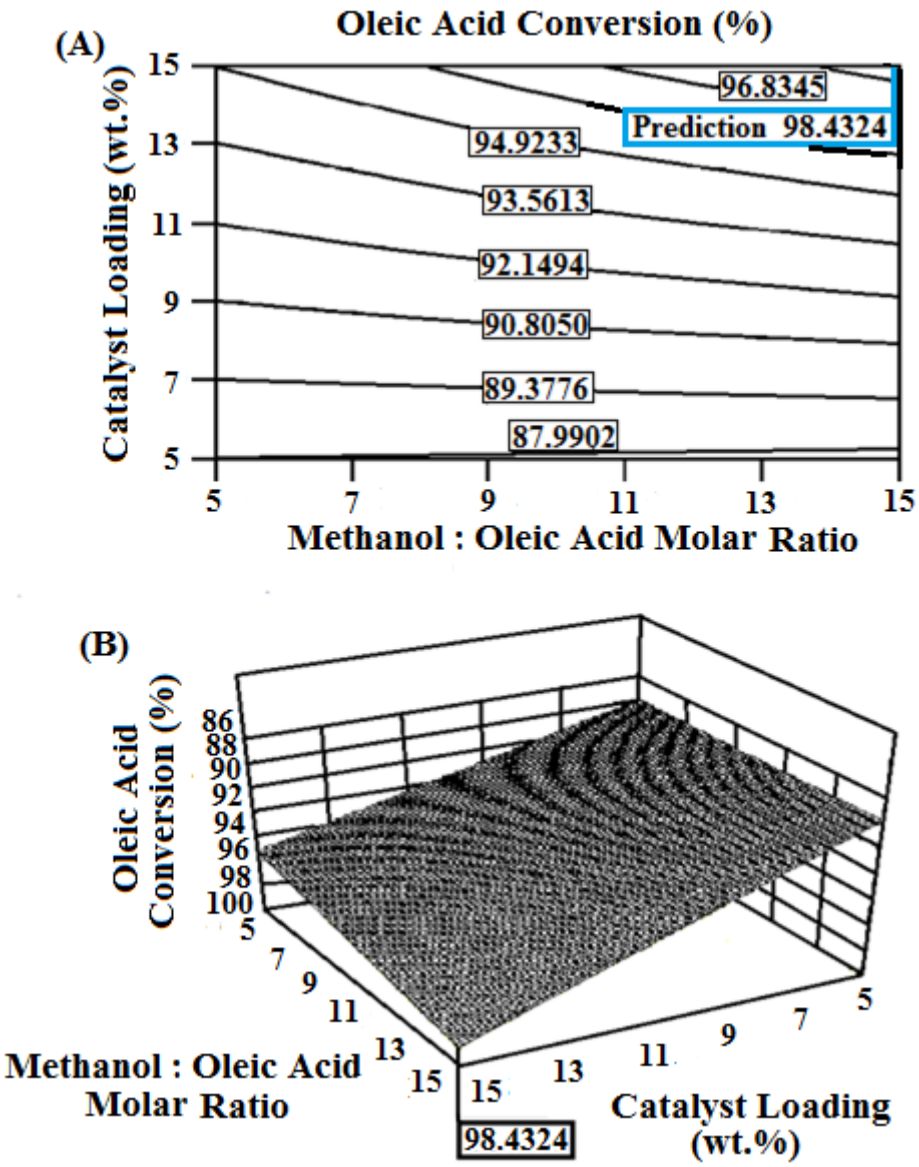

Figure 5.1. Catalyst loading vs. methanol/OA molar ratio at optimal catalyst concentration for predicted C (A) Contour plot and (B) 3-D plot.

Careful observations of the contour and 3-D plots (Figure 5.1.A and B) indicate that γ_{OA} increases monotonically with increase in Q_L. At lower Q_L, Q_{MR} has positive effect, while a moderately weaker effect of Q_{MR} on γ_{OA} is observed at higher Q_{MR} corresponding to higher Q_L keeping Q_C at optimal level. Excess of M (high Q_{MR}) provides negative effect on γ_{OA} at a given acidity of the catalyst (i.e., fixed Q_L) as second order esterification mechanism thus reducing reaction rate. Besides, high Q_{MR}, M molecule may obstruct the surface chemical adsorption of OA on the Ni-Fe/FA catalyst and thus, rendering reduced conversion of OA. At both the lowest and highest M/OA molar ratios, an increase in catalyst concentration could improve the OA conversion due to presence of augmented catalyst active sites for the esterification reaction.

5.1.4. Characterisation of Ni-Fe/FA catalyst

5.1.4.1. Determination of Acidity

Titration method (Singh and Fernando, 2008 and Chakraborty et al., 2014) was used for the acidity analysis of different Ni-Fe/FA catalyst samples i.e. NI-5, NI-10 and NI-15.With increase in the ferric sulphate loading, the acidity was found to increase gradually from 2.4 to 5.5 mmol KOH/g catalyst corresponding to NI-5 to NI-15.

5.1.4.2. XRD analysis

The intense difractrogram enunciates the presence of Fe_2O_3 (card no. 33-0664) crystalline phase at scanning angles 2θ = 24.29°, 33.26°, 35.78°, 43.52°, 49.61°, 54.17°, 57.47°, 62.51°, 72.20°, 71.78°, 72.20°. The Figure 5.2. (a-c) shows that the intensity of Fe_2O_3 peaks gradually increases from NI-5 to NI-15 due to increase in ferric sulphate loading. In presence of less intense peaks of Al_2SiO_5 (card no. 11-0046) (2θ = 28.16°, 30.38°, 37.88°, 48.35°,

55.79°, 64.13°) (Figure 5.2. a-c) in NI-15 compared to NI-5 attributes to the fact that Al_2SiO_5 renders basic characteristics to the catalyst sample. In other words, decrease in Al_2SiO_5 crystalline phase increases the acidity of NI-15; thus, rendering higher yield of MO. Figure 5.2. also represents the presence of Ni_2O_3 (card no. 14-0481) and NiS (card no. 02-1273) crystalline phases detected at 27.65°, 39.35°, 44.99°, 51.86°, 66.59° and at 29.96°, 34.22°, 53.03°, 78.32° respectively; which corroborate the fact that gradual increase in intensity of Ni_2O_3 and NiS peaks from NI-5 to NI-15 indicated highest acidity of the NI-15 catalyst sample.

With increase in ferric sulphate loading from 5% to 15% (Figure 5.2.a-c); the crystallite size of the corresponding catalyst was found to increase gradually. Using Bragg's law and Scherrer' sequation, lattice parameter and crystallite size of the the specific peaks of Fe_2O_3, Ni_2O_3 and NiS (Table 5.3.) crystalline phases were evaluated in concurrence with the XRD analysis (Chakraborty et al., 2014).

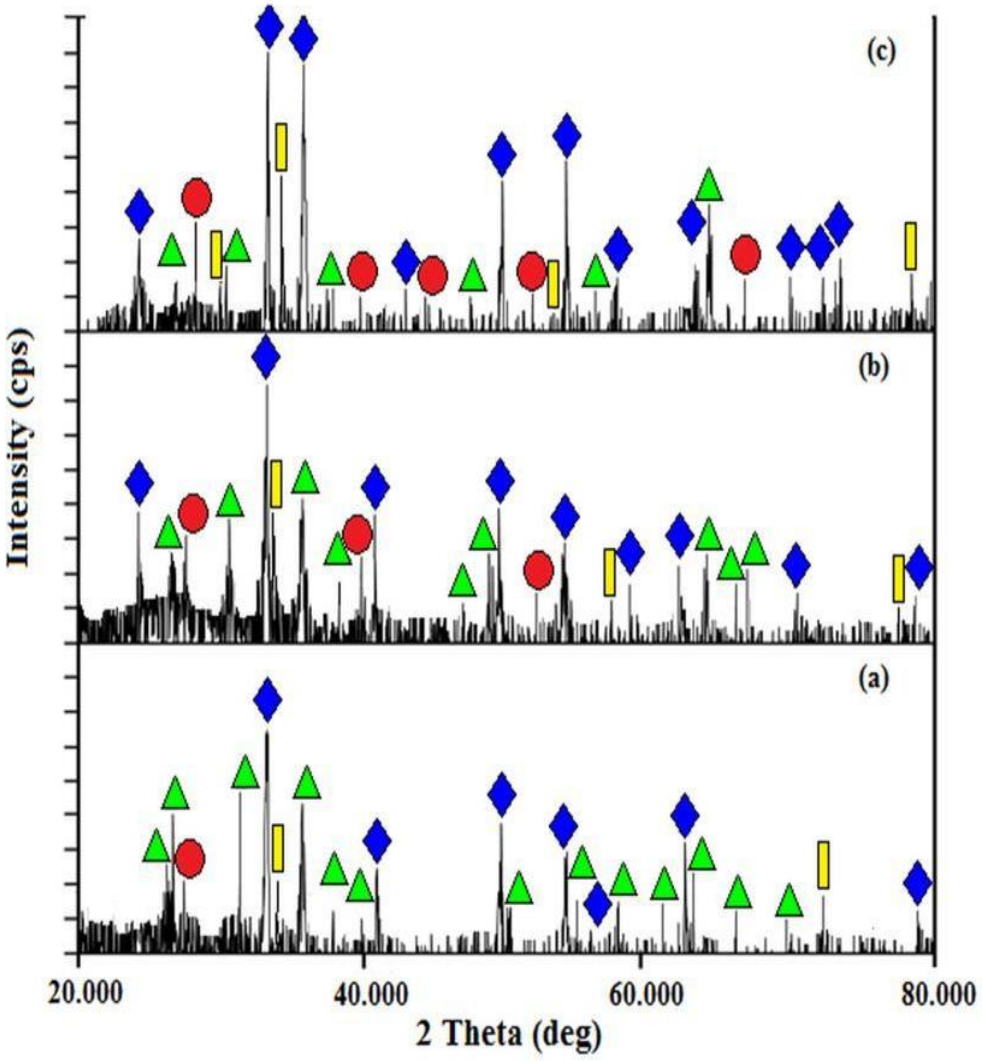

Figure 5.2. XRD patterns of fly ash supported Ni-Fe catalyst prepared at different iron loading ratio (a)NI-5, (b)NI-10 and (c)NI-15 [Characteristic peaks due to Fe_2O_3 ( ), Al_2SiO_5 ( ), Ni_2O_3 ( ) and NiS ( )]

Table 5.3. Crystallite size and Lattice parameter of Fe_2O_3, Ni_2O_3 and NiS determined through XRD analysis

		Fe_2O_3	
Figure no.	2θ(˚)	**Crystallite size (nm)**	**Lattice parameter (nm)**
5(c)	33.26	2.61	0.4779
5(b)	33.37	2.35	0.5305
5(a)	33.23	2.14	0.5836
		Ni_2O_3	
5(c)	27.65	3.92	0.3833
5(b)	28.25	3.36	0.4371
5(a)	27.68	3.23	0.5629
		NiS	
5(c)	34.22	2.52	0.4645
5(b)	33.26	2.14	0.5831
5(a)	33.23	2.09	0.5912

5.1.4.3. FTIR analyses of FA and NI-15 catalyst

FTIR analyses of the calcined-FA (Figure 5.3.a) and the generated NI-15 (Figure 5.3.b) solid acid catalyst detect the peaks at 537.99, 554, 570.01, 602.02, 646.44 and 1108.92 cm^{-1} of the octahedral and tetrahedral sites of Fe-O deformation (Mahmoudi et al., 2009; Fan et al., 2008; Li et al., 2009). The peak located at 2000 cm^{-1}represents the DMD (Double-metal) Fe-Ni vibration (Sreeprasanth et al., 2006) and stretching vibration at 463.29 and 479.64 cm^{-1} denote Ni-O (Biju and Khadar, 2003; Chakraborty and Das, 2012). Asymmetric stretching vibration at 996.87 cm^{-1} of X-O (X=Si, Al) bonds (Li et al., 2009; El-Naggar et al., 2008) and peaks at 1098.25 cm^{-1} representing Si-O-Si detected for FA corroborate well with previous discoveries (Jain et al., 2011; Liping et al., 2008). The peak at 1643.83 cm^{-1} is ascribed to the

vibration of O-H stretching (δ_{O-H}) present in FA (Jain and Rani, 2011) and weak band of OH^- ions is located around 2343.66 cm^{-1} (Mekala and Goli, 2014).

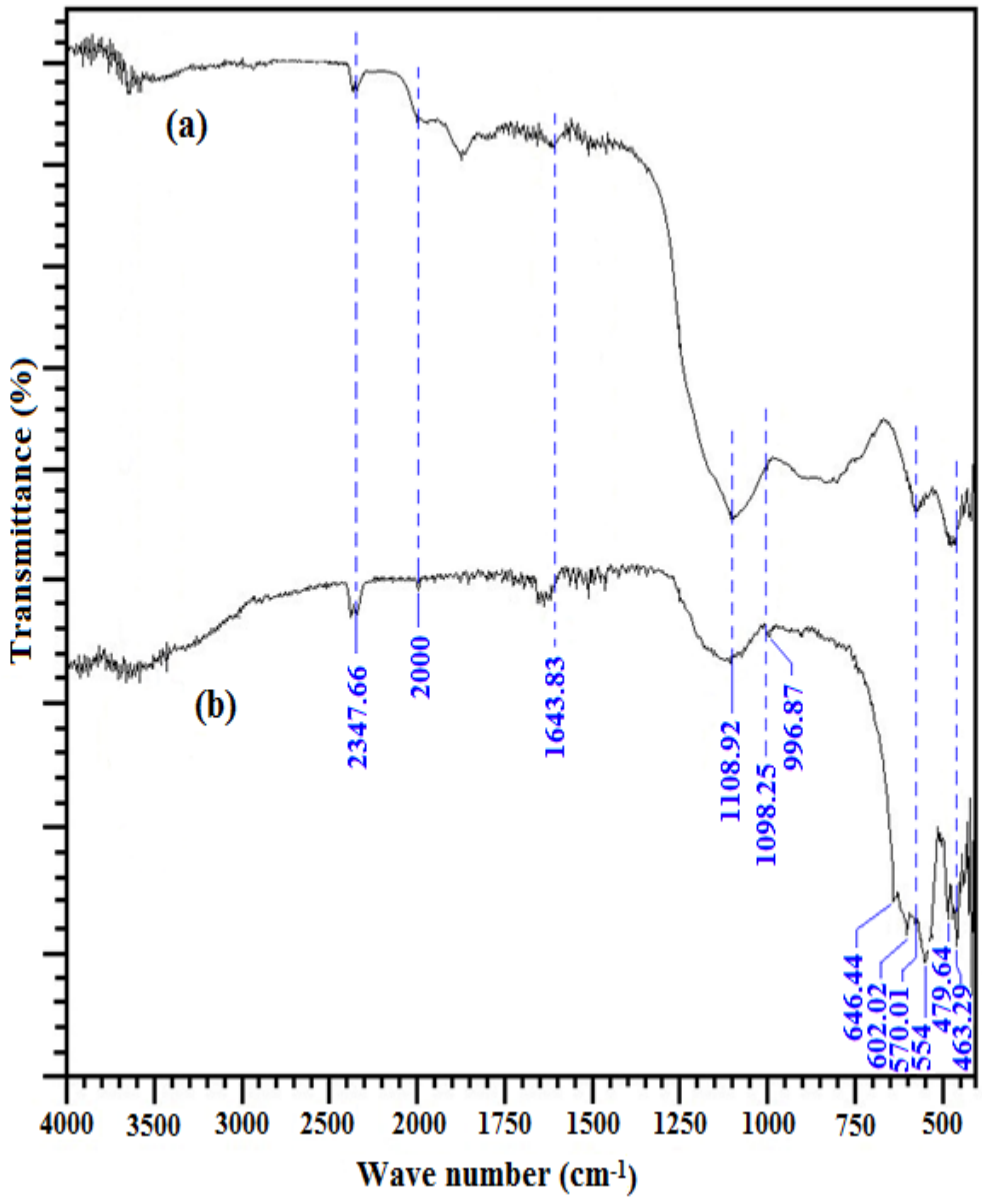

Figure 5.3. FTIR analyses of: (a) calcined FA and (b) NI-15 catalyst.

5.1.4.4. BET and BJH analyses

The BET specific surface area of the NI-15 optimal catalyst has been determined as 27.64m^2/g indicating a substantial increase in BET area compared to that of the FA support (0.60m^2/g). The BET plot of the NI-15 catalyst characterizes type II isotherm (IUPAC) (Figure 5.4.A) implying unrestricted monolayer-multilayer adsorption (Sing et al., 1985).

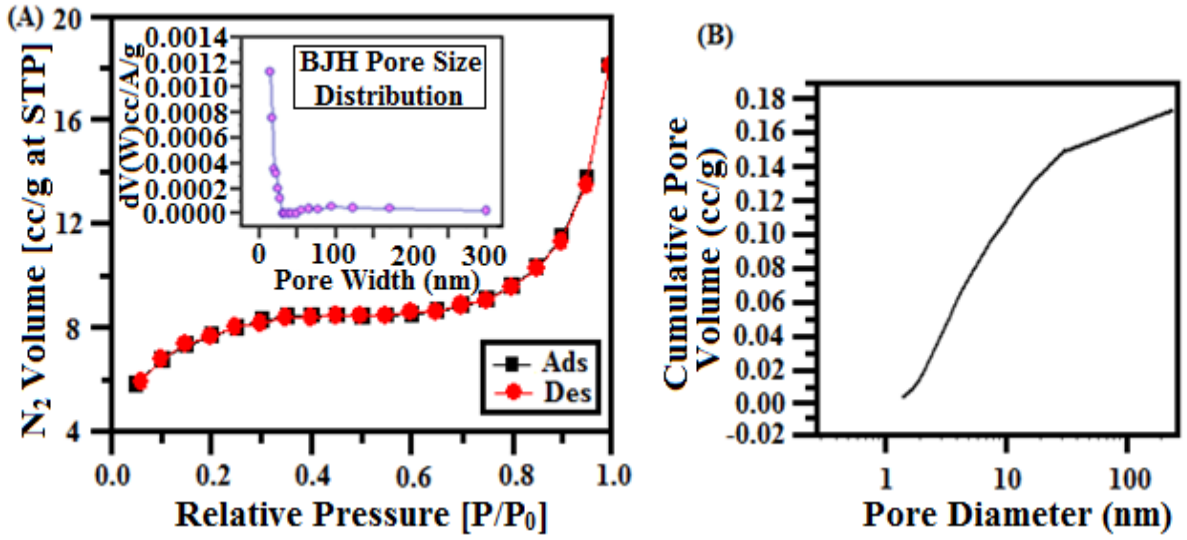

Figure 5.4. (A) BET and BJH (inset) plot and (B) Penetration curve of NI-15 catalyst.

The catalyst pore volume of 0.0233cc/g (0.005cc/g for FA) and a modal pore diameter of 1.5nm (1.8nm for FA) were determined using BJH method (inset of Figure 5.4.A). The penetration curve of the NI-15 catalyst sample (Figure 5.4.B) indicates presence of 11.21% micropores, 77.27% mesopores and 11.52% macropores in the NI-15 catalyst. Thus, together 88.79% of pore volume was contributed by meso and macro-pores rendering high conversion (98.37%) of OA to MO.

5.1.4.5. SEM and EDX analyses

The morphology of the unevenly porous and granular NI-15 uncalcined catalyst sample has been exhibited through SEM image (Figure 5.5.A). Upon calcination, the catalyst particles became agglomerated and flattened (Figure 5.5.B) with non-uniform pores distributed over catalyst surfaces. Existing elements in Ni 15 catalyst and their optimal corresponding weight % and atomic % are demonstrated in the EDX analyses for the optimal catalyst i.e. NI-15 (Table 5.4.).

Table 5.4. EDX analyses of NI-15 catalyst

Elements present in NI-15	Weight%	Atomic%
O	46.29	68.83
Al	1.43	1.26
Si	2.37	2.01
S	21.26	15.77
Fe	25.40	10.82
Ni	3.25	1.32

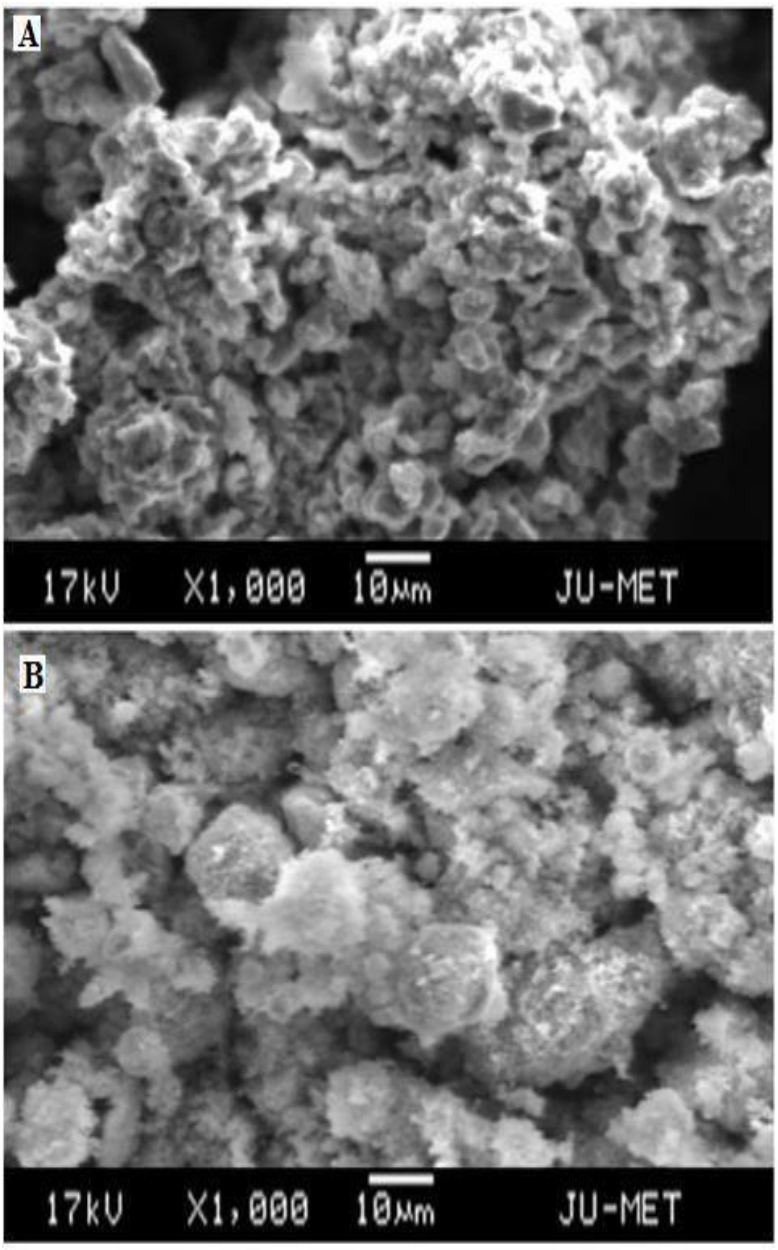

Figure 5.5. SEM images of the NI-15 catalyst: (A) before calcination and (B) after calcination at 700 °C.

5.1.4.6. XPS analysis of NI-15 catalyst

The XPS diagram of the NI-15 catalyst that exhibited the optimal catalytic performance for synthesis of MO is displayed in Figure 5.6.A-B. The XPS analysis of NI-15 catalyst (Figure 5.6.A) identifies the binding energies pertaining to Fe_2O_3 through the characteristic XPS

bands at 710.3 eV corresponding to Fe^{3+} $2p_{3/2}$ and at 724.1eV in relation to Fe^{3+} $2p_{1/2}$ (Yu et al., 2008) The peak pertaining to lower binding energy is attributed to Fe $2p_{3/2}$ spin, while that at higher binding energy can be ascribed to Fe $2p_{1/2}$. In concurrence with these observations, it might be inferred that Fe^{3+}species existing in the prepared NI-15 catalyst rendered appreciable acidity (5.5 mol KOH/g) vis-à-vis significant catalytic activity.

In Figure 5.6.B, the 854.8 eV XPS peak represents a mixed Ni^{2+}/Ni^{3+} phase of Ni compounds which is in accordance well with the observations of Grosvenor et al., 2006 and Jain and Rani, 2011. It may be renowned that the absolute binding energy values were allowed to vary by ±0.1 eV to allow for error associated with charge referencing to adventitious C 1s.

From the experimental result of MO synthesis (Table 4.2.) it may be inferred that an increase in Fe precursor i.e. $Fe_2(SO_4)_3.H_2O$ loading could improve the catalytic performance. This signifies that Fe^{3+} detected in XPS analysis was the major active site (acting as Lewis acid) in the OA conversion to yield MO.

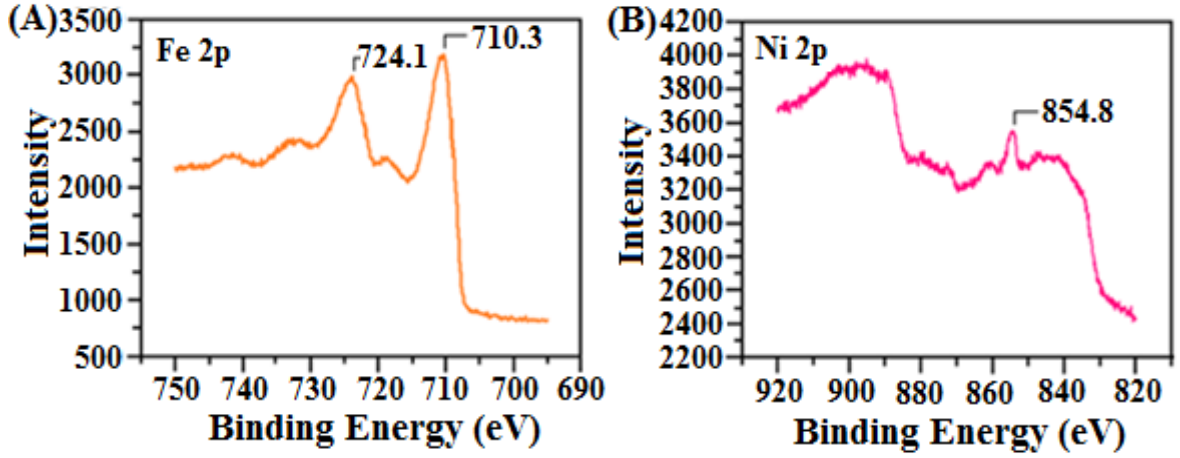

Figure 5.6. XPS spectra of (A) Fe 2p and (B) Ni 2p of NI-15 catalyst.

5.1.5. Effect of desiccant and heating protocol on esterification

Silica gel (SG) and molecular sieve (MS) both adsorbent were used in this esterification reaction. In the forward reaction of the esterification water is formed as by-product. While using the adsorbent in the reaction it adsorbs the water from the reaction and stops the backward reaction. Thus, it improves OA conversion for enhancing MO yield at the derived optimal reaction conditions. In absence of any desiccant, 98.37% MO conversion was achieved in 1 h using conventionally heated reactor (CHR). Application of 40 wt.% each of SG and MS separately helped to gain 99.1% and 99.2% conversions (Figure 5.7.A) respectively at otherwise identical conditions. From Figure 5.7 A-B, it is evident that MS rendered better performance for both CHR and far-infrared radiated reactor (FIRRR) systems in comparison with SG. Notably, at optimal condition, changing the reactor system from CHR (97.36%) to FIRRR (99.20%) in presence of MS (Table 5.5.), resulted significant enhancement in OA conversion within only 10 min. Table 5.5. presents some interesting experimental results establishing that FIRRR system incorporating MS desiccants could provide the highest conversion in minimum time and hence, rendered best performance while consuming lower energy (since FIRRR had a power rating of 100 W ; i.e. 1/3rd power of the CHR).

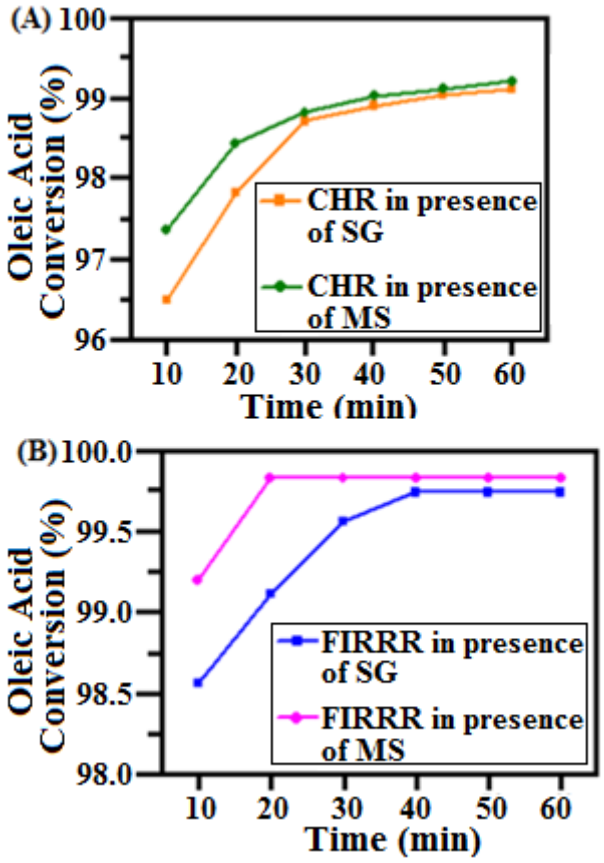

Figure 5.7. Effect of heating system on OA conversion: (A) conductive heated reactor (CHR), (B) far-infrared radiated reactor (FIRRR).

Table 5.5. Effect of different types of desiccants (SG and MS) used in CHR and FIRRR on OA esterification

Reaction Time (min)	OA Conversion(%) using CHR		OA Conversion(%) using FIRRR	
	In presence of SG	In presence of MS	In presence of SG	In presence of MS
10	96.49	97.36	98.56	99.20
20	97.83	98.43	99.11	99.83
30	98.71	98.82	99.56	99.83
40	98.90	99.02	99.74	99.83
50	99.04	99.11	99.74	99.83
60	99.10	99.20	99.74	99.83

5.1.6. FTIR analyses of optimally produced MO

Infrared spectra of optimally produced MO are shown in Figure 5.8. The peaks at 1285, 1381.05 and 1413.06cm^{-1} show the presence of CH_3 group which are in concurrence well with the findings of Che Man and Setiowaty, 1999. Vibrations of methylene (—CH_2) group are identified at 1466.42, 2855.77 and 2925.31 cm^{-1}. The intense peaks of ester carbonyl group(C=O vibrations) at 1711.84 cm^{-1} and that of C—O vibrations around 1124.93 and 1247.65 cm^{-1} are evident (Grosvenor and Biesinger, 2006). A weak band at 3005.53 cm^{-1} signify insignificant presence of unsaturated OA (cis-double bond stretching) in the ester product (Rohman and Che Man 2010).

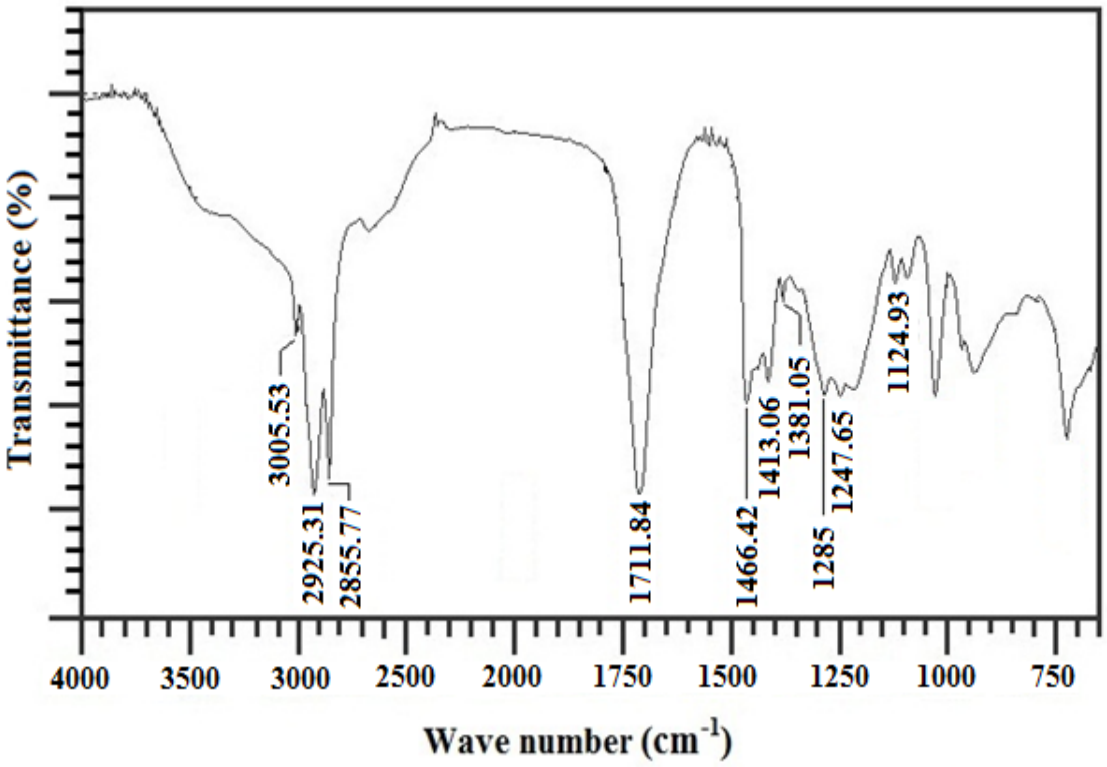

Figure 5.8. FTIR analyses of product methyl Oleate.

5.1.7. Properties of B10 fuel derived from product MO

The product MO achived at optimal condition (using FIRRR) was blended with commercial petro-diesel. To prepare B10 diesel fuel; 1:9 (MO: petro-diesel) volumetric ratio were mixed. B10 was tested to evaluate the pertinent fuel properties (Table 5.6.). The results indicate that fuel properties of B10 satisfied ASTM D7467-10 specifications. It may be mentioned here that MO represents a biodiesel molecule.

Table 5.6. Properties of B10 fuel (10% methyl oleate and 90% petro-diesel)

Properties	**Specification**	**Result**
standard number	**B6-B20 (ASTM D7467-10)**	**B10 (ASTM D7467-10)**
Specific gravity (g/ml)	0.88	0.85
Flash point (K)	52 (min)	105
Cetane number	40 (min)	50
Cloud point (K)	Report[a]	-1
Pour point (K)	-3	-13
Kinematic viscosity (40°C,mm²/s)	1.9-4.1	2.41

[a] Cloud point is dependent on several factors, viz. place and time of year, and is not specified in ASTM D7467-10.

5.1.8. Catalyst reusability

The reusability of the NI-15 catalyst was tested by carrying out the esterification reactions using the recycled catalyst several times at the optimal process conditions. At optimal conditions, 1 h esterification resulted same conversion for eight successive batches. However, OA conversion was found to decrease from 98.37% to 97.76% in ninth run. The decrease in conversion in the nineth batch might be ascribed to negligible leaching of the active metal

species into the reaction medium. Form the ICP analyses the leaching of the metal was confirmed. The NI-15 catalyst could be regenerated by methanol washing followed by air drying in the hot air oven for 2 h at 105 ℃. Afterwards, the dried sample was calcined at 700 ℃ for 4 h and the regenerated catalyst could render approximately 97.5% OA conversion for additional five batches.

5.2. Optimization of fast and energy-efficient biodiesel production under infrared radiated from waste mustard oil catalysed by Amberlyst 15: Engine performance and emission quality assessments

5.2.1. Statistical analysis of parametric effects

As shown in Table 5.9.; the results of ANOVA (corresponding to Table 4.4.) revealed that the factors catalyst concentration (λ_{CC}) and stirrer speed (λ_{SS}) were significant (p-value<0.05; 95% confidence level) in affecting biodiesel generation, from waste mustard oil under infrared radiation in presence of Amberlyst 15 solid acid catalyst.

According to the "F" and "p" criteria methanol/oil molar ratio (λ_{MO}) is statistically insignificant and has least effect on biodiesel production from WMO amongst other factors. The most significant factor according to F value is "catalyst concentration" followed by stirrer speed is represented in Table 5.9.

The main effect plot for mean of FAME yields exhibits in the Figure 5.9.a. The increment in all three factors viz. (λ_{MO}, λ_{CC} and λ_{SS}) resulted in enhanced FAME yield which is shown in Figure 5.9.a. From the main effect plot (Figure 5.9.b) for S/N ratio, it can be easily predicted that the increase in factorial values resulted in the augmented biodiesel yield (Y_{FAME}). However, an increase in λ_{MO} beyond 6 could not further enhance FAME yield.

Table 5.7. Analysis of variance (ANOVA) of the different process factors (Table 4.4.) affecting the biodiesel production

Process Factor	DF	Sum of squares	Mean square	F value	p-value
λ_{MO}	2	3.247	1.624	3.37	0.139
λ_{CC}	1	36.457	36.457	75.63	0.001
λ_{SS}	1	4.018	4.018	8.34	0.045
Error	4	1.928	0.482		
Total	8	45.651			

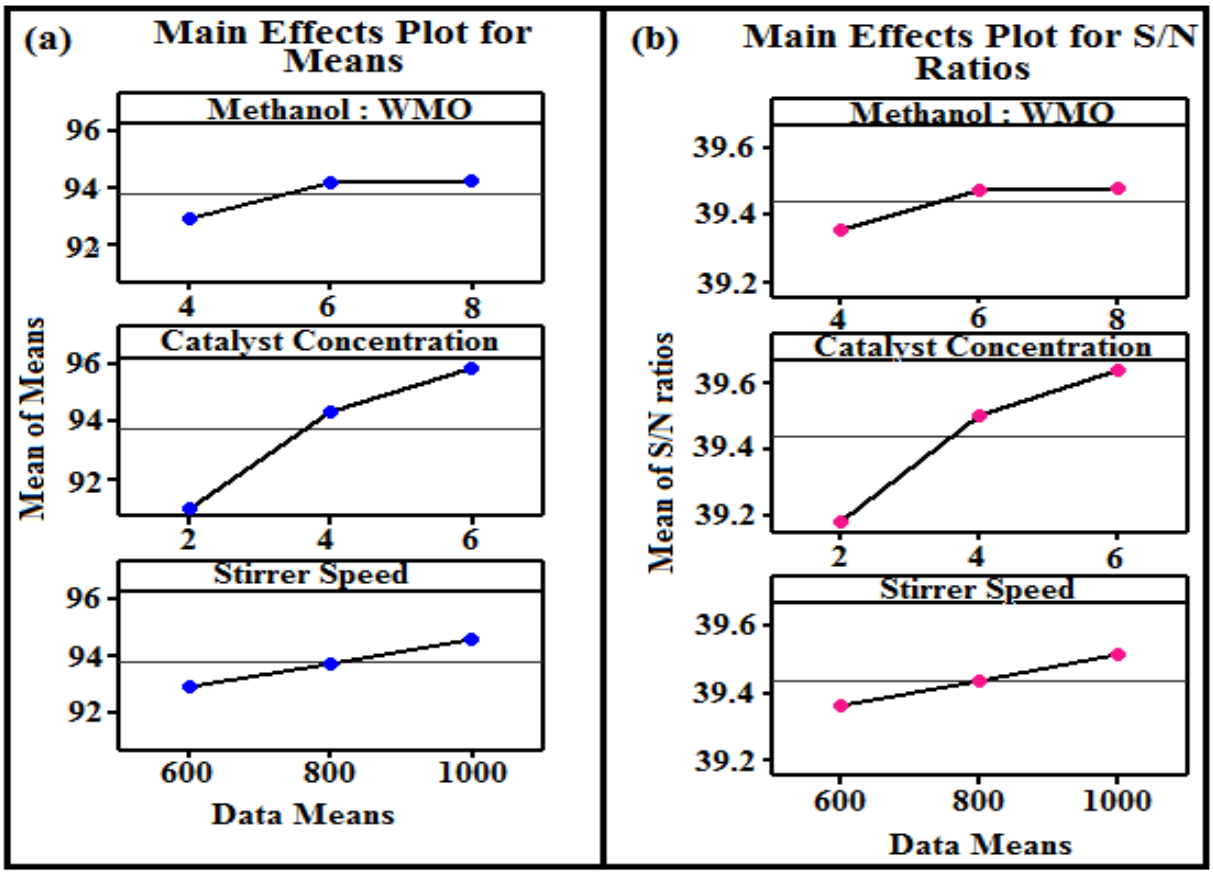

Figure 5.9. Factorial effects on FAME yield expressed as mean and S/N ratio.

5.2.2. Determination of Optimal process conditions and parametric interactions

In Table 5.8., delta value and S/N ratio of each factor are presented. The highest S/N ratio in each factor was desirable to maximise Y_{FAME} (Rahman et al., 2013 and Ismail et al., 2013). Accordingly, λ_{MO} (6:1), λ_{CC} (6 wt.%) and λ_{SS} (1000 rpm) were derived as the optimal factorial values through use of Taguchi Orthogonal Design employing Minitab 17 software.

Table 5.8. S/N ratios at different levels of the process factors and corresponding delta values

Level	λ_{MO} Methanol/ WMO molar ratio	λ_{SS} (rpm) Stirrer Speed	λ_{CC} (wt% of WMO) Catalyst Concentration
1	39.36	39.36	39.18
2	39.48*	39.44	39.50
3	39.48	39.52*	39.64*
Delta	0.12	0.15	0.46
Rank	3	2	1

The Figure 5.10. shows the interaction effects between any two process factors in affecting FAME yield have been analysed keeping the other factor at the optimal level. From the interactions between λ_{MO} and λ_{CC}, it can be inferred that 6:1 λ_{MO} along with maximum λ_{CC} would result maximum FAME yield when λ_{SS} is fixed at optimal level. Again, the interactions between λ_{MO} and λ_{SS} show that at maximum λ_{MO}, an increment in λ_{SS} favours a higher Y_{FAME} up to 800 rpm; however, for 6:1 of λ_{MO}, the maximum FAME yield was observed at 1000 rpm; which is consistent with derived optimal conditions. The interaction between λ_{CC} and λ_{SS} demonstrates that, λ_{CC} has profound positive effect on Y_{FAME} at any λ_{SS}; accordingly the reaction appears to be surface kinetics controlled. At maximum λ_{CC}, an

increase in λ_{SS} from 800 to 1000 rpm, could not appreciably promote enhancement of FAME yield; which further reinforces that the reaction was not significantly mass transfer limited at highest λ_{CC}. Interestingly, at lowest λ_{CC}, λ_{SS} demonstrated a strong effect on Y_{FAME}, indicating the predominance of non-catalytic reaction mechanism.

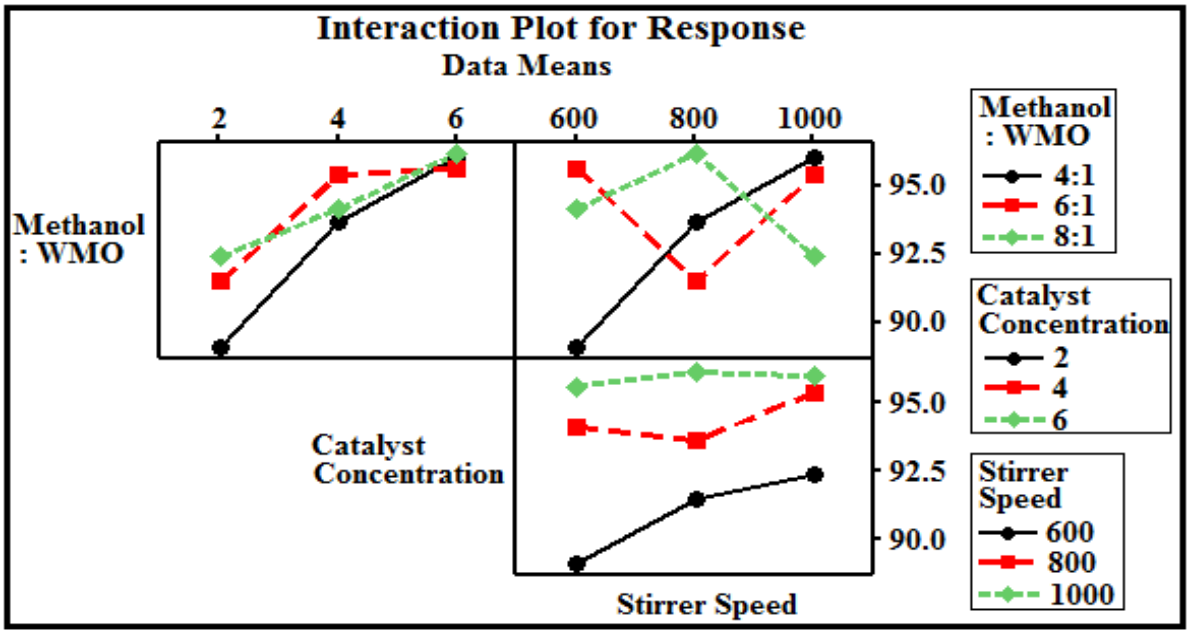

Figure 5.10. Interaction among process factors in governing biodiesel yield..

A maximum FAME yield of 97.13% was resulted at the predicted optimal process conditions i.e. 6:1 methanol to WMO molar ratio, 6 wt.% catalyst concentration and 1000 rpm stirrer speed using FIR radiated reactor and the corresponding biodiesel composition analysis which is denoted in Figure 5.11.a On the other hand, a remarkably low 43.82% FAME yield was obtained when the FIR radiation was replaced with a conventional conductive heating system, at the identical optimal process conditions, (Figure 5.11.b). The significantly higher FAME yield under FIR radiation clearly advocates its remarkable superiority over conventional heating method; notably, a much lower energy requirement ($1/4^{th}$ of the conventional system) of FIR radiation makes it a highly energy-efficient system. The infrared radiation provides both stretching and bending molecular vibrations besides being able to

penetrate intensely through the reaction mixture for supplying necessary thermal energy; these attributes makes FIR radiation superior than conventional heating I promoting biodiesel production.

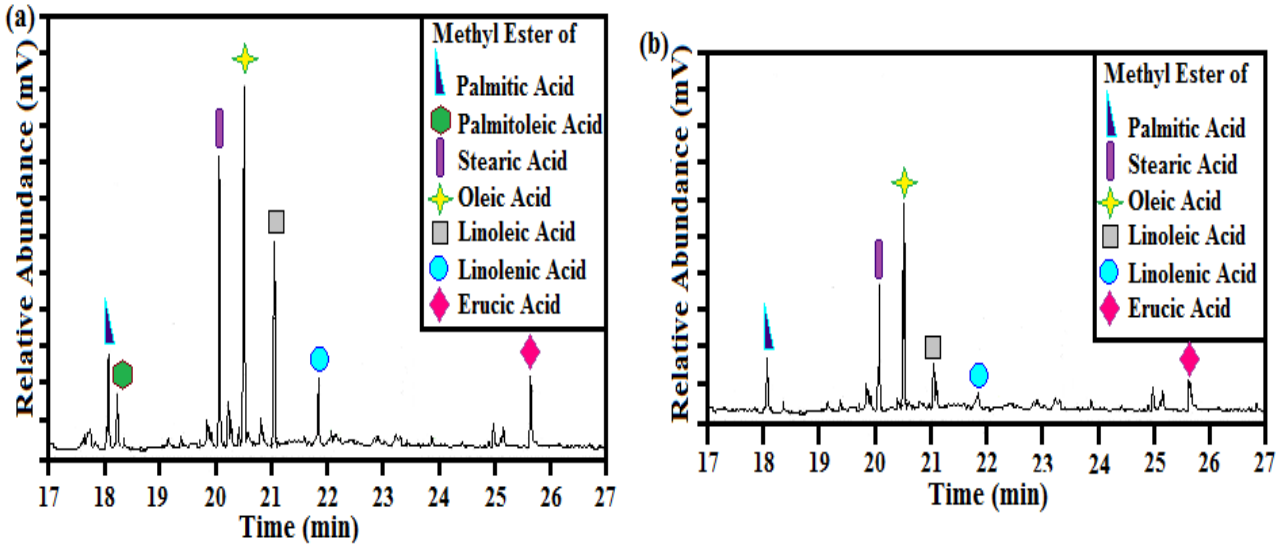

Figure 5.11. GC-MS of product biodiesel obtained from (a) FIR radiated. reactor, (b) Conventionally heated reactor.

5.2.3. Biodiesel Properties

Product biodiesel was blended in different proportions with commercial diesel (B10, B20 and B100). To prepare B10; biodiesel and commercial diesel ware mixed up into 1:9 volumetric ratio. The same process was also carried out for the B20 and B100. The various fuel properties were determined for the B10, B20 and B100; and all the important fuel properties that conformed to ASTM specifications as shown in Table 5.9.

Table 5.9. Fuel properties of B10, B20 and B100

Properties	Specification B6 − B20 (ASTM D7467-10)	B10	B20	Specification B100 (ASTM 6751-11a)	B100
Flash point (°C)	52 (min)	110	117	93 (min)	132
Cetane number	40 (min)	48	53	47 (min)	63
Cloud point (°C)	report[a]	-1	1	-3 to 12	2
Pour point (°C)	-3	-10	-15	-18	-22
Acid value (mg KOH/g)	0.3 (max)	0.19	0.23	0.5 (max)	0.47
Density	810 – 818	815	816	860 – 900	885
Kinematic viscosity (40°C,mm²/s)	1.9 – 4.1	3.32	3.55	1.9 – 6.0	5.19

[a] Cloud point depends on place and time of year, and is not specified in ASTM D7467-10.

5.2.4. Engine performance test

Engine performance was carried out at different proportions of diesel / biodiesel blends i.e. B0 (100% petro-diesel), B10 (i.e.10 vol.% biodiesel, 90 vol.% of petro-diesel), B20 (20% biodiesel , 80% petro-diesel) and B100 (pure biodiesel).

From Figure 5.12.a, it is evident that engine run with B0 (pure petro-diesel) exhibits the highest brake thermal efficiency as compared to any biodiesel blends. A reduction of 7.78% brake thermal efficiency (BTE) was observed for the B10 blend at the highest recorded load of 8 N. This same extent of reduction in BTE was recorded for the B20 blend. Similar declining trend was exhibited for fuels with higher biodiesel blends. It can, therefore be inferred that brake thermal efficiencies comparable with pure petro-diesel are exhibited at low biodiesel blends; best results being observed for the B10 blend. The results of brake thermal efficiency corroborate well with literature reported data (Sun et al., 2010 and Palash

et al., 2014). The Brake Specific Fuel Consumption (BSFC) patterns are exhibited in Figure 5b. B10 and B20 exhibited higher BSFC in comparison with pure diesel (B0); however, the profiles tend towards convergence at higher engine load. Pure biodiesel (B100) demonstrated a similar profile, but exhibited somewhat lower BSFC figure 5.11 at higher engine load compared to B0. The results of BSFC for B0, B10 and B20 are in good agreement with other report (Palash et al., 2014).

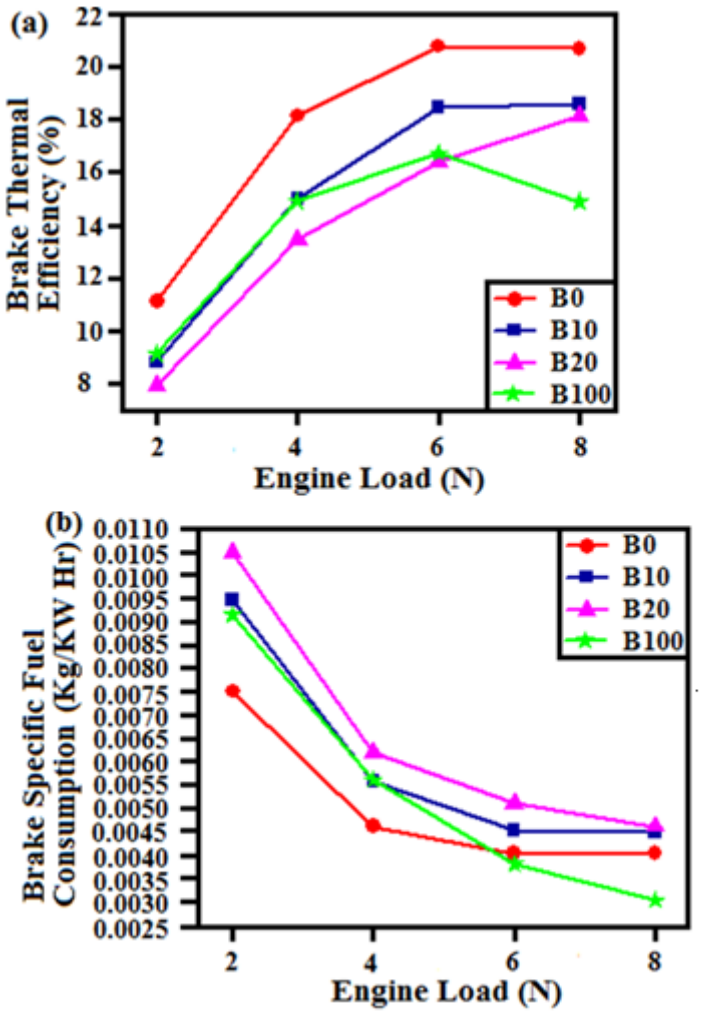

Figure 5.12. (a) Brake thermal efficiency and (b) Brake specific fuel consumption as functions of Engine load.

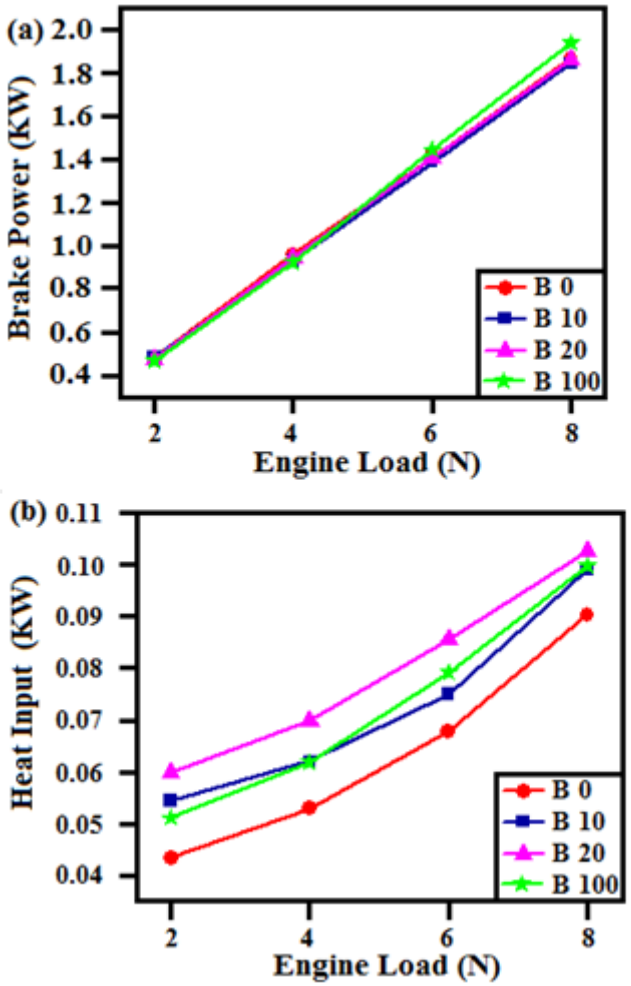

Figure 5.13. (a) Brake power and (b) Heat input as functions of Engine load.

Figure 5.13.a demonstrates variation in brake power as a function of the engine load for various fuel blends. A remarkably uniform relationship was observed, with convergent profiles for all blends. A negligibly small deviation (higher slope) from normal trends was seen for B100 at higher loadings, but the deviation was too small to be numerically substantial (3.7% absolute error). The result signifies that blends of biodiesel produced from WMO through application of FIR radiation holds promise as a potential and novel fuel that can render somewhat equivalent brake power as that of petro-diesel. Figure 5.13.b depicts the heat input or the heat requirement for the Compression Ignition (CI) engine. The heat input

requirements were typically higher for biodiesel blended fuels, in comparison with B0 (pure petro-diesel).

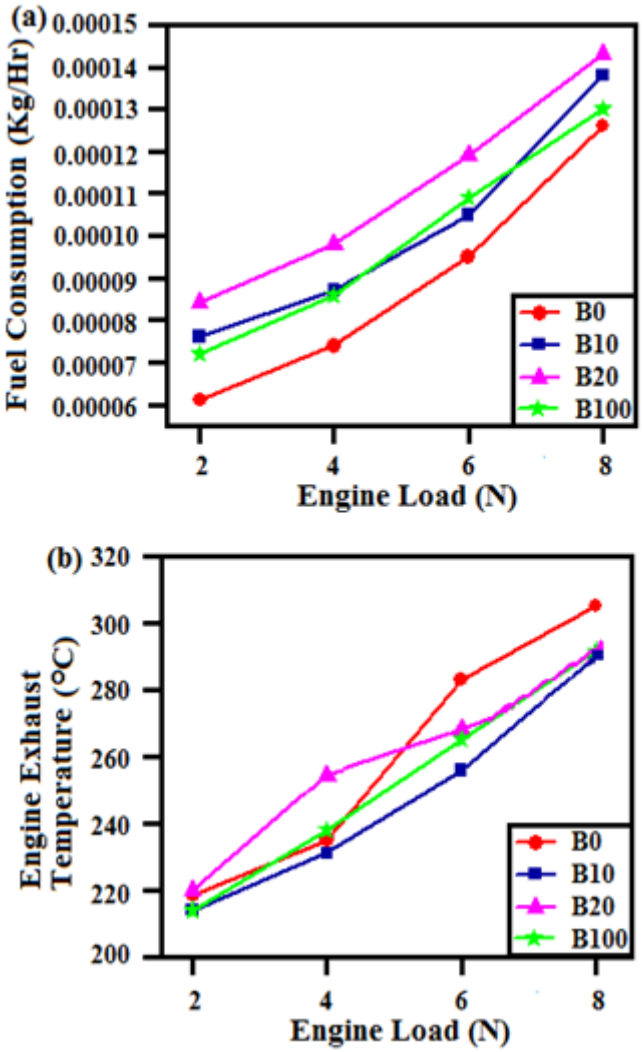

Figure 5.14. (a) Fuel consumption (b) Engine exhaust temperature as functions of Engine load.

Figure 5.14.a elucidates that compared to petro-diesel, the fuel consumption is greater for higher blends of biodiesel; however, at higher engine loads, the fuel consumption for blended fuels is not much different from petro-diesel (B0). Thus, biodiesel produced from WMO can, at higher engine loadings, partially substitute petro-diesel in terms of fuel consumption. Moreover, considering the fact that the present biodiesel was prepared from WMO, a slightly higher value of heat input is justified when considering from the aspect of waste valorisation.

This is certainly considered as a promising feature in view of lessening dependence on petro-diesel.

Figure 5.14.b depicts variation in engine exhaust temperature with change in engine load. Compared to B0, the engine exhaust temperature was lower for all tested fuel blends; particularly at higher engine loadings. The lower exhaust temperature confirms a more efficient and controlled combustion occurring with more biodiesel content in the blended fuel which agrees reasonably with other studies (Antolın et al. 2002 and Palash et al., 2014). This phenomenon can be attributed to lower extent of incomplete combustion with higher biodiesel blends and this result was further reinforced by lower CO and HC emissions for B100 in the exhaust as confirmed through emission test results (Figure 5.15. and Figure 5.16.). The overall effect of additional biodiesel blending, result in declination of the exhaust gas temperature which demonstrated significant reduction in the global warming on account of biodiesel blended fuel combustion.

5.2.5. Emission quality Tests

The gas analyser (section 4.5.5) was used to measure the engine exhaust emission quality for pure and blended fuels. Fig. 8a indicates that, compared to petro-diesel; the CO content in engine exhausts successively reduces with increasing biodiesel content in the blended fuel. This signifies less incomplete combustion for biodiesel-blended fuel. Maximum reduction (75%) in the CO emission was observed for B100 at an initial load of 2 N. Notably, the CO emission reduction decreased to 70.58% at higher engine loads of 8N. CO emission results are consistent with previous observation for biodiesels (Sun et al., 2010 and Palash et al., 2014).

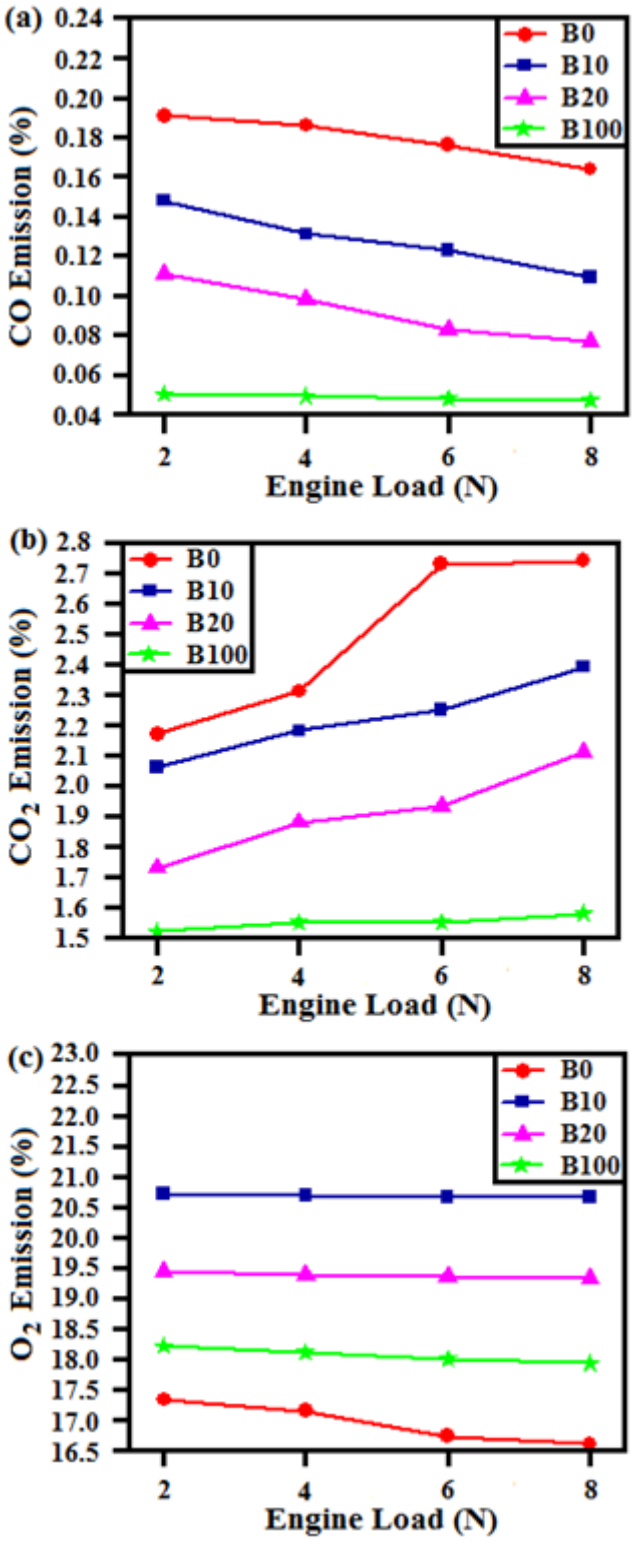

Figure 5.15. (a) CO emission, (b) CO_2 emission and (c) O_2 emission as functions of Engine load.

Figure 5.15.b shows the CO_2 emissions for the considered fuels. For petro-diesel, the carbon dioxide emissions gradually increased with engine loads up to 6N, indicating a more complete combustion at higher loads. Notably, the produced biodiesel demonstrated an almost uniform combustion emission and exhaust data, which indicated uniform combustion right from lower loads. Such uniformity in combustion is desirable and serves as a guideline for identifying a cleaner, environmentally-benign fuel.

Lower exhaust oxygen emissions are indicative of a more efficient combustion dynamics and hence, a more eco-friendly attribute. Figure 5.15.c depicts that for petro-diesel (B0), at higher loadings from 6N to 8N, the oxygen emissions progressively decreased, indicating a more complete combustion. With low biodiesel blends, the emissions are higher compared to B0; however, for B100, the emissions are lesser and tend to approach towards the profile of B0. O_2 emission recorded in present study falls within the range of reported results (Antolın et al., 2002, Sun et al., 2010 and Palash et al., 2014).

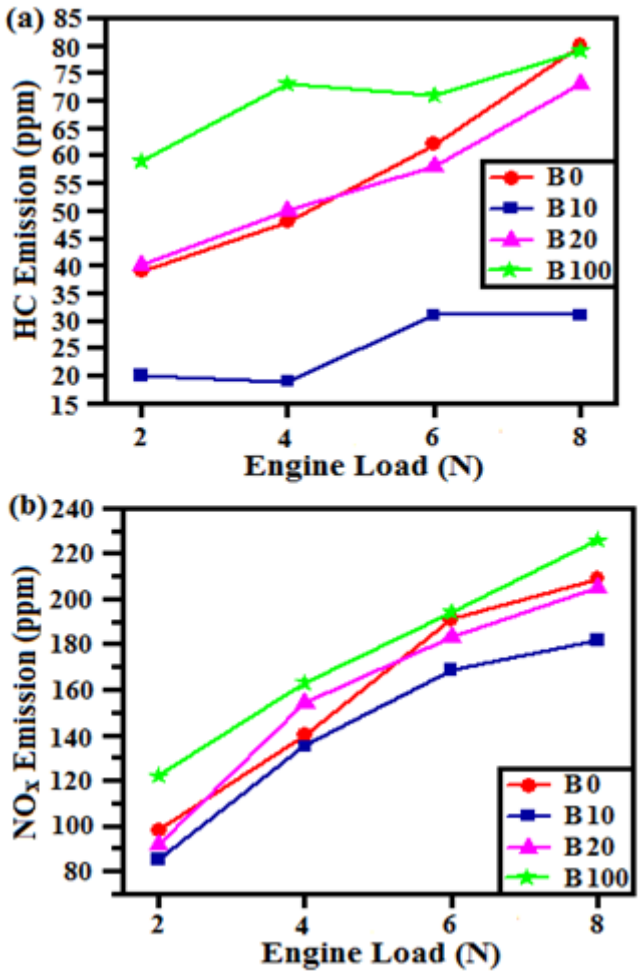

Figure 5.16. (a) HC emissions, (b) NO_x emissions as functions of Engine load.

As displayed in Figure 5.16.a with increase in engine loading, the HC emission increased almost consistently for different fuels. The maximum value (79 ppm) arises for both B0 and B100 at highest engine load of 8 N. B10 exhibited a lower HC emission than B0. However, with increase in biodiesel content in blends, the HC emissions gradually increased and approached the values of B0 for B100. Thus, B10 was found to be the suitable fuel rendering eco-friendly emission profiles. Notably, the HC emission values in the present study is below the range of literature reported values for B10 (60-80 ppm) and B20 (80-120 ppm) (Palash et al. 2014).

The dependence of NOx (Figure 5.16.b) emissions on engine load indicates similar pattern as that of HC emission. Petro-diesel shows a NOx emission of 98 ppm at 2 N, which gradually increases to a maximum value of 209 ppm at 8 N engine load. Similar relations between NOx emission and engine load were observed for blended fuels and B100 also. As expected, B100 or biodiesel shows a maximum NOx emission compared to other fuels. However, NO_X emission reported for the present case is below the range of B10 (100-200 ppm) and B20 (200-300 ppm) (Antolın et al., 2002, Sun et al., 2010 and Palash et al., 2014) reported previously. Notably, B10 was found to be the most suitable fuel with respect to lowest NOx emission profiles among all fuels studied.

Emission quality measurements clearly indicate that the biodiesel-diesel blends at suitable blending ratio can facilitate lower emissions amounts of toxic, hazardous gases and is hence, environmentally more benign compared to petro-diesel alone.

5.3 Optimal efficient biodiesel synthesis from used oil employing low-cost ram bone supported Cr catalyst: engine functioning and exhaust assessment

5.3.1. Statistical design of experiment

In this work for production of biodiesel from used frying mustard oil (UFMO) using the prepared Cr impregnated BiHAp (ram bone derived) supported catalyst, the maximum FAME yield had been evaluated through D-optimal design. The three processes factors viz. Calcination temperature (N_{CT}), Catalyst concentration (N_{CC}) and Methanol/UFMO molar ratio (N_{MR}) were optimized by this statistical design of experiment. The D-optimal experimental design layout and corresponding FAME Yield (ψ_{FAME}) are presented in Table 4.7. Table 5.10. presents the 'Model Fit Summary', enumerating that the quadratic one was the best model for correlating factorial effects on FAME Yield in comparison with liner and 2FI models. The quadratic model (Equation 5.3.) promoted lowest standard deviation, highest values of R^2, predicted-R^2 and adjusted-R^2 hence, it was selected as the best model to predict the FAME yield over the range of process factors.

Moreover, ANOVA (Table 5.11.) implied that the quadratic model with a significant p-value (95% confidence level) of 0.0003 could adequately predict ψ_{FAME}. Significant model terms (<0.05) were n_{CT}, n_{CC}, n_{MR}, $n_{CT}\, n_{CC}$, $n_{CT}\, n_{MR}$, $n_{CC}\, n_{MR}$ and $(n_{MR})^2$ that correlated ψ_{FAME} with process factors in coded form (Equation 5.3.).

Table 5.10. Model fit summary of linear, 2FI, and quadratic models for prediction of FAME yield using Cr-BiHAp catalyst

source	Prob> F	Standard deviation	R^2	Adjusted R^2	Predicted R^2	Press value
linear	<0.0001	1.68	0.8980	0.8640	0.7555	60.68
2FI	0.0393	1.07	0.9722	0.9445	0.8595	34.86
quadratic	0.0158	0.32	0.9988	0.9950	0.9571	10.65

Table 5.11. ANOVA results pertaining to Equation 5.3.

Source	Sum of Squares	df	Mean Square	F Value	p-Value Probability p>F
Model	247.86	9	27.54	268.11	0.0003
n_{CT}	119.27	1	119.27	1161.16	<0.0001
n_{CC}	65.62	1	65.62	638.82	0.0001
n_{MR}	20.42	1	20.24	198.83	0.0008
$n_{CT}\ n_{CC}$	17.40	1	17.40	169.42	0.0010
$n_{CT}\ n_{MR}$	3.15	1	3.15	30.63	0.0116
$n_{CC}\ n_{MR}$	0.13	1	0.13	1.29	0.3380
$(n_{CT})^2$	0.69	1	0.69	6.71	0.0810
$(n_{CC})^2$	0.001295	1	0.001295	0.013	0.9177
$(n_{MR})^2$	2.44	1	2.44	23.79	0.0165
Residual	0.31	3	0.10		
Lack of Fit	0.29	2	0.15	10.16	0.2165
Pure Error	0.014	1	0.014		
Corrected Total	248.17	12			

$$\psi_{FAME} = 88.87 - 3.73\, n_{CT} + 2.65\, n_{CC} + 1.48\, n_{MR} + 1.41\, n_{CT}\ n_{CC} + 0.60\, n_{CT}\ n_{MR} - 0.12\, n_{CC}\ n_{MR} + 1.60\, (n_{MR})^2 \quad (R^2 = 0.9988) \quad (-1 < n_{CT}, n_{CC}, n_{MR} < +1) \qquad (5.3.)$$

5.3.2. Influence of individual factorial effect on FAME yield

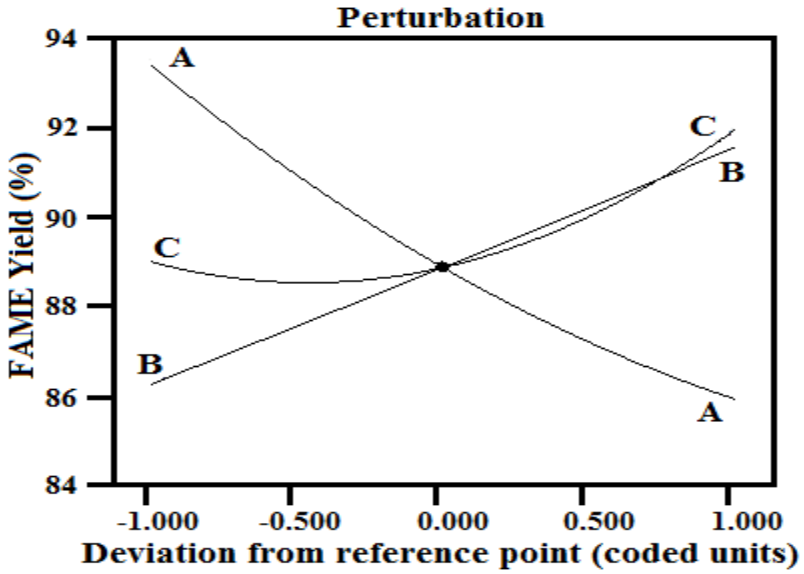

Figure 5.17. Influence of main (individual) factorial effects on FAME yield: (A) calcination temperature; (B) catalyst concentration; (C) methanol/UFMO molar ratio.

The perturbation plot is depicted in Figure 5.17. which analyse the individual factorial effect on biodiesel yield keeping other factors at optimal levels. The optimal levels of the CTE were 200°C calcination temperature, 4 wt.% catalyst concentration and 8 methanol/UFMO molar ratio evaluated through D-optimal method (Table 2: run 1). Highest values of both B and C at lowest value of A, resulted centre maximum FAME yield. At the optimal process condition, the maximum predicted FAME yield was 97.02% (determined through D-optimal method); while 96.85±0.01% FAME yield (maximum) was accomplished experimentally. Thus, about 0.17% difference was found between the experimental and predicted FAME yield, indicating high prediction accuracy of the D-optimal method.

5.3.3. Interactions among process parameters

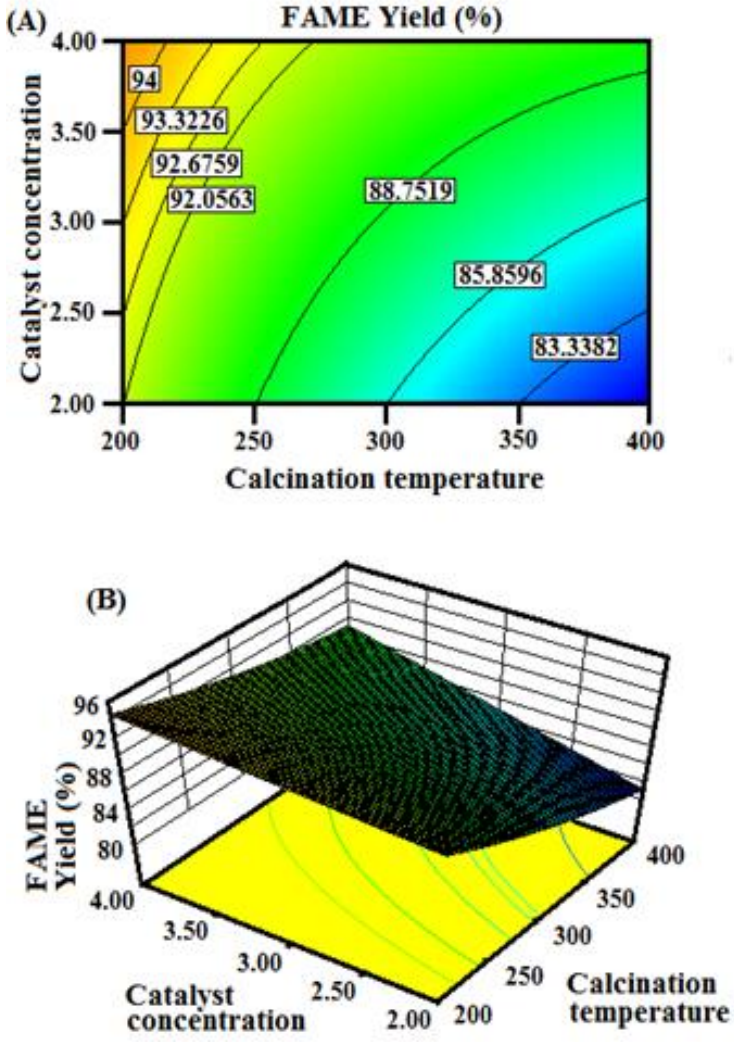

Figure 5.18. (A) Contour plot and (B) 3D plot exhibiting interactions between catalyst concentration and calcination temperature in governing FAME yield.

Figure 5.18. indicates that over the entire range of calcination temperature, an increase in catalyst concentration can render higher FAME yield. However, this dependence of FAME yield on catalyst concentration is more pronounced at lower catalyst temperature. The negative effect of higher calcination temperature could be observed over the entire range of

catalyst concentration. This observation could be attributed to the fact that more tri calcium phosphate (TCP) phases were generated from BiHAp at higher calcination temperature, which reduced Lewis acidity of Cr-BiHAp catalyst. Similar effects of calcination temperature were observed on FAME yield (Figure 5.19.) at all values of methanol to UFMO molar ratio.

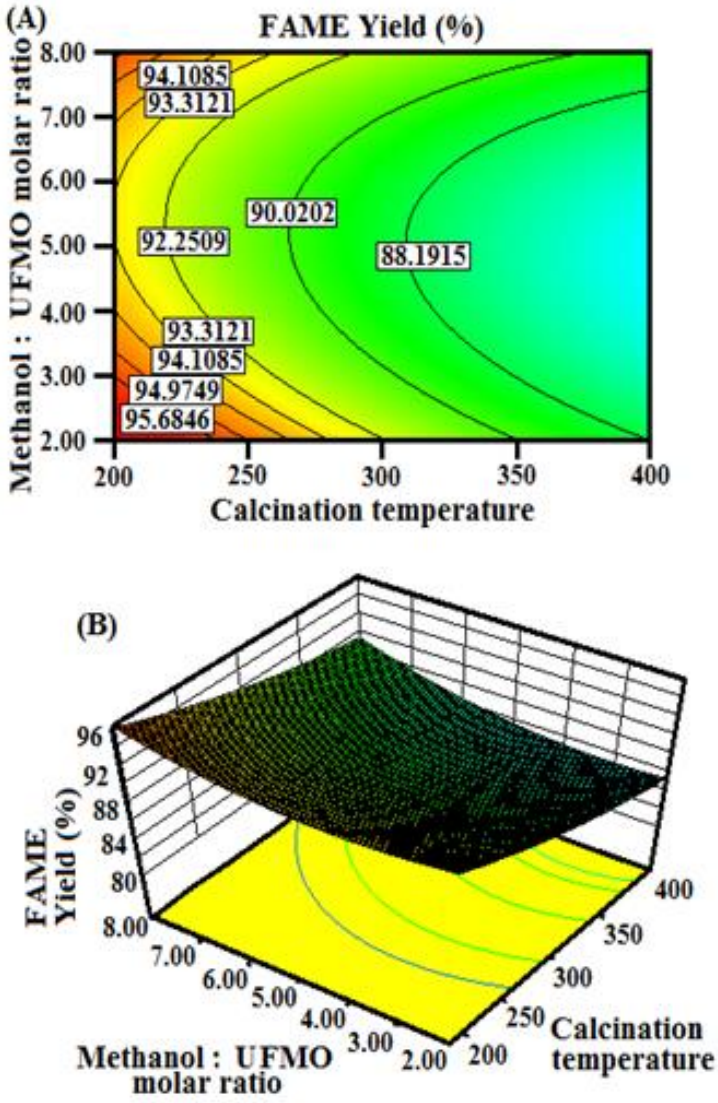

Figure 5.19. (A) Contour plot and (B) 3D plot exhibiting interactions between methanol/UFMO molar ratio and calcination temperature in regulating FAME yield.

GC-MS analysis (Figure 5.20.A) of optimally produced biodiesel from UFMO employing the FIRRHS shows 96.85% FAME yield. Whereas, the conventional conductive heating system provided significantly lower 40.22% FAME yield which is plotted in the Figure 5.20.B. The significantly higher FAME yield under FIRRHS clearly advocates its remarkable superiority over conventional heating method. Notably, a much lower energy requirement (1/4th of the conventional heating system) in FIRRHS could evidence its high energy-efficiency.

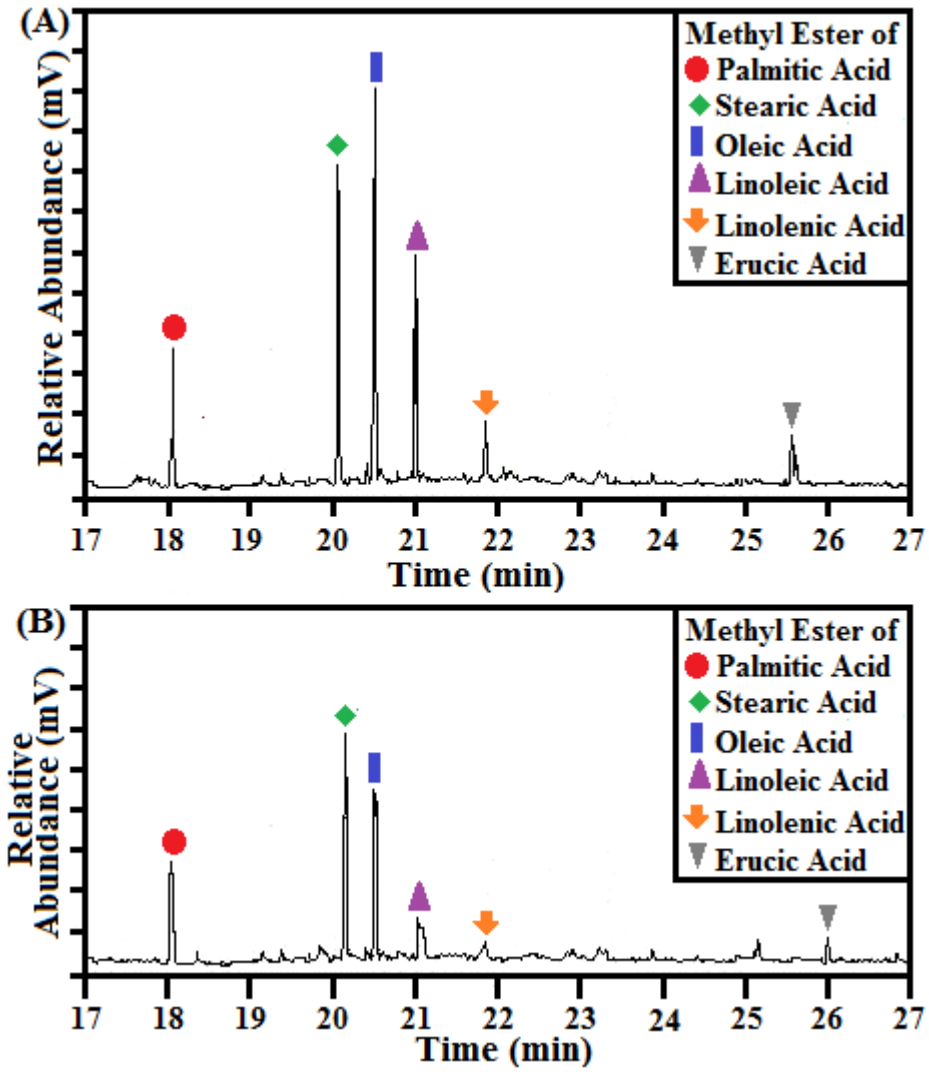

Figure 5.20. GC-MS of product biodiesel obtained from reactor equipped with: (A) FIRRHS (B) Conventional heating system.

5.3.4. Characterization of Cr-HAp catalyst

5.3.4.1. TGA analyses

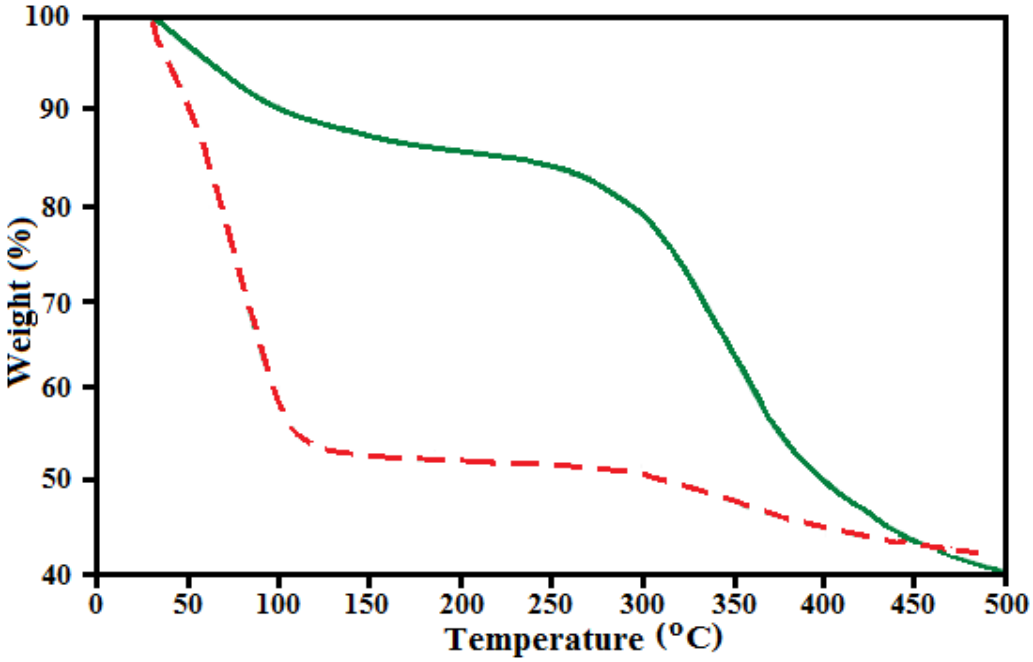

Figure 5.21. TGA analyses from 0 to 500 °C: green line ——— raw BiHAp (ram bone derived hydroxyapatite); red line – – CH2 optimal catalyst.

Figure 5.21. exhibits thermogravimetric analyses of both BiHAp and optimal catalyst (CH2). Solid line indicates occurrence of 15% weight loss of the BiHAp within 100 °C due to evaporation of absorbed water. Additional 7.5% weight reduction took place between 100 and 200 °C owing to desorption of organic substances (Sing et al., 1985). Disintegration of lattice water caused further 27.5% weight loss over the range 300 – 500 °C. Notably, dashed line shows the weight loss of uncalcined CH2 catalyst (Figure 5.21.). A 45.5% weight loss occurred over 30-120 °C temperature due to desorption of water. An additional 3% weight reduction happened on further heating from 120 to 300 °C because of desorption of lattice

water. Decomposition of chromium III nitrate followed by evaporation of gaseous species caused 8.5% additional weight loss between 300 and 500 °C. Remarkably, a very small weight loss occurred between 400 to 500 °C; which indicated an appreciable thermal stability of the CH2 catalyst prepared at 400 °C calcination temperature.

5.3.4.2. XRD analysis

X-ray diffraction patterns of Cr-BiHAp catalysts prepared at different calcination temperatures (200 - 400 °C) are displayed in Figure 5.22 (A-C). Cr_2O_3 (JCPDS card no. 20-1105) and $Cr_3(PO_4)_2$ (JCPDS card no. 40-6829) crystalline phases are represented by peaks at angles 2θ = 50.540, 64.010 and 77.270 and 2θ = 25.820, 28.160, 39.800, 43.730, 49.430, 51.560 and 70.070° respectively. BiHAp (Ghobadian et al., 2009) was partially transformed into Ca_{10} $(PO_4)_6O$ (Figure 5.22.) due to increase in calcination temperature and the representative crystalline phases were identified at 2θ = 34.04, 53.15° (card no. 08-7727). Whereas, hydroxyapatite (HAp) crystalline phases were recorded at 2θ of 31.82, 46.70, 61.46 and 75.38° (card no. 01-086-0740). A decrease in calcination temperature resulted in more prominent peaks of Cr_2O_3 and $Cr_3(PO_4)_2$ crystalline phases while depicting lower peak intensity of $Ca_{10}(PO_4)_6O$. However, the catalyst developed at lower calcination temperature interpreting higher acidity. This could be ascribed to the weaker acidic property of Ca_{10} $(PO_4)_6O$ in comparison with HAp (Smith et al., 2013).

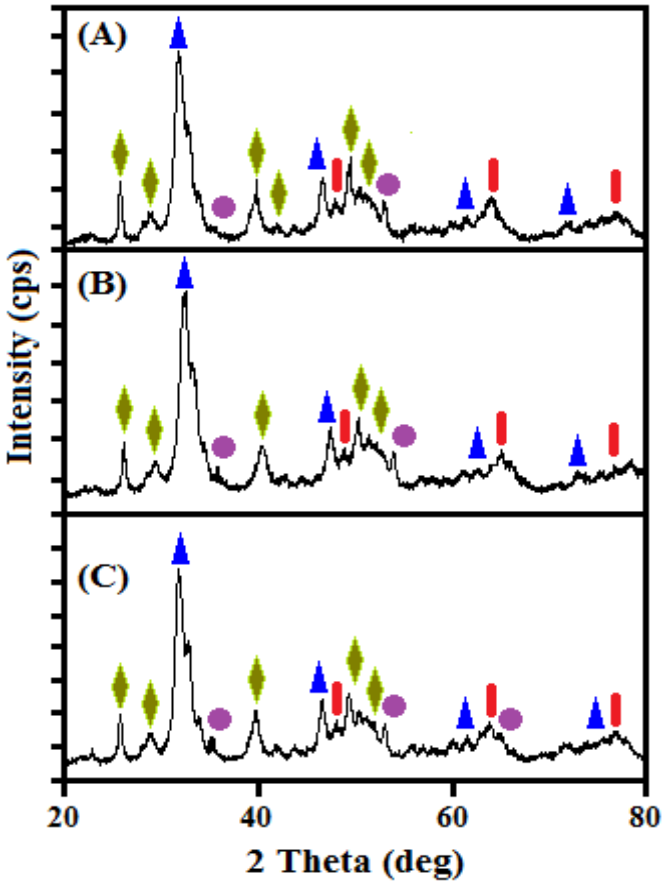

Figure 5.22. XRD patterns of Cr-BiHAp catalysts prepared at different calcination temperatures: (A) CH2, (B) CH3 and (C) CH4 [Characteristic peaks due to $Cr_3(PO_4)_2$ (♦), Cr_2O_3 (▮), HAp (▲) and $Ca_{10}(PO_4)_6O$ (●)].

5.3.4.3. TPD analyses

Temperature programmed desorption of ammonia (NH_3-TPD) analyses were studied to evaluate the surface acidic properties of the three prepared catalyst samples viz. CH2, CH3, CH4; wherein an increase in peak intensity indicated enhanced acidity. The augmentation in peak height from CH4 to CH2 (Figure 5.23.C-A) implied the enhancement of total acidity from 0.65 to 0.78 mmol/g (Fuks et al., 2010 and Prasad et al.,2011) corresponding to the

reduction in calcination temperature from 400 °C to 200 °C. This could be ascribed to the fact that with increase in calcination temperature, BiHAp was partly converted to TCP (tri-calcium phosphate), thus, diminishing catalyst acidity (Chakraborty and RoyChowdhury, 2014)

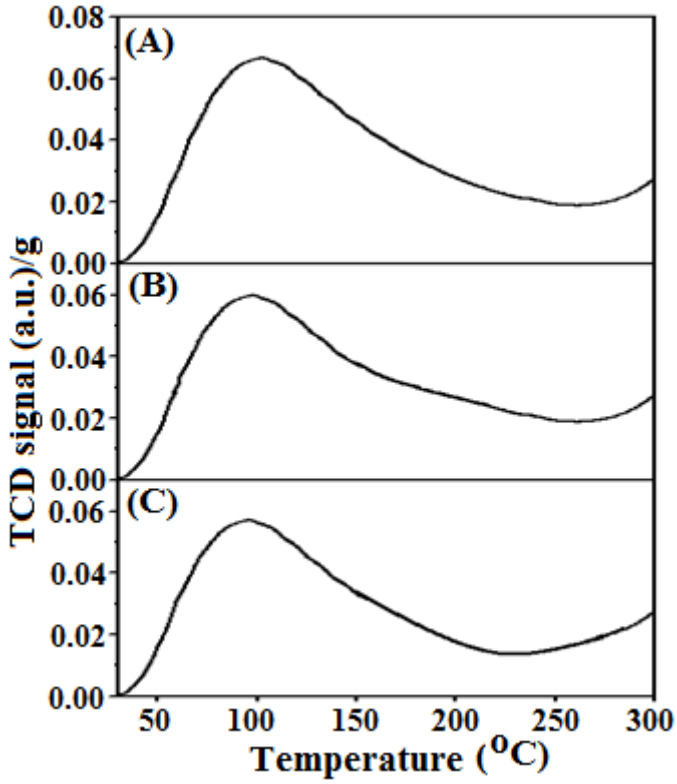

Figure 5.23. NH_3-TPD analyses: (A) CH2, (B) CH3 and (C) CH4.

5.3.4.4. BET and BJH analyses

The BET plot shows 98.45 m2/g specific surface area of the optimal CH2 catalyst. Type II isotherm (IUPAC) suggesting unlimited monolayer-multilayer adsorption (Chattopadhyay and Sen, 2013) represented in the Figure 5.24.A. The pore volume (0.0586 cc/g) and modal pore diameter (19.3nm; mesoporous) of the optimal catalyst were determined through the BJH method (inset of Figure 5.24.A). Fig. 8B represents the penetration curve of CH2 catalyst quantifying 28.47% micropores and 71.53% mesopores. The predominance of

mesopores in the catalyst framework facilitated its high activity in biodiesel production. Since, the mesoporous catalyst could admit voluminous fatty acid and triglyceride molecules to diffuse through its pores; thus, aiding the UFMO conversion to biodiesel.

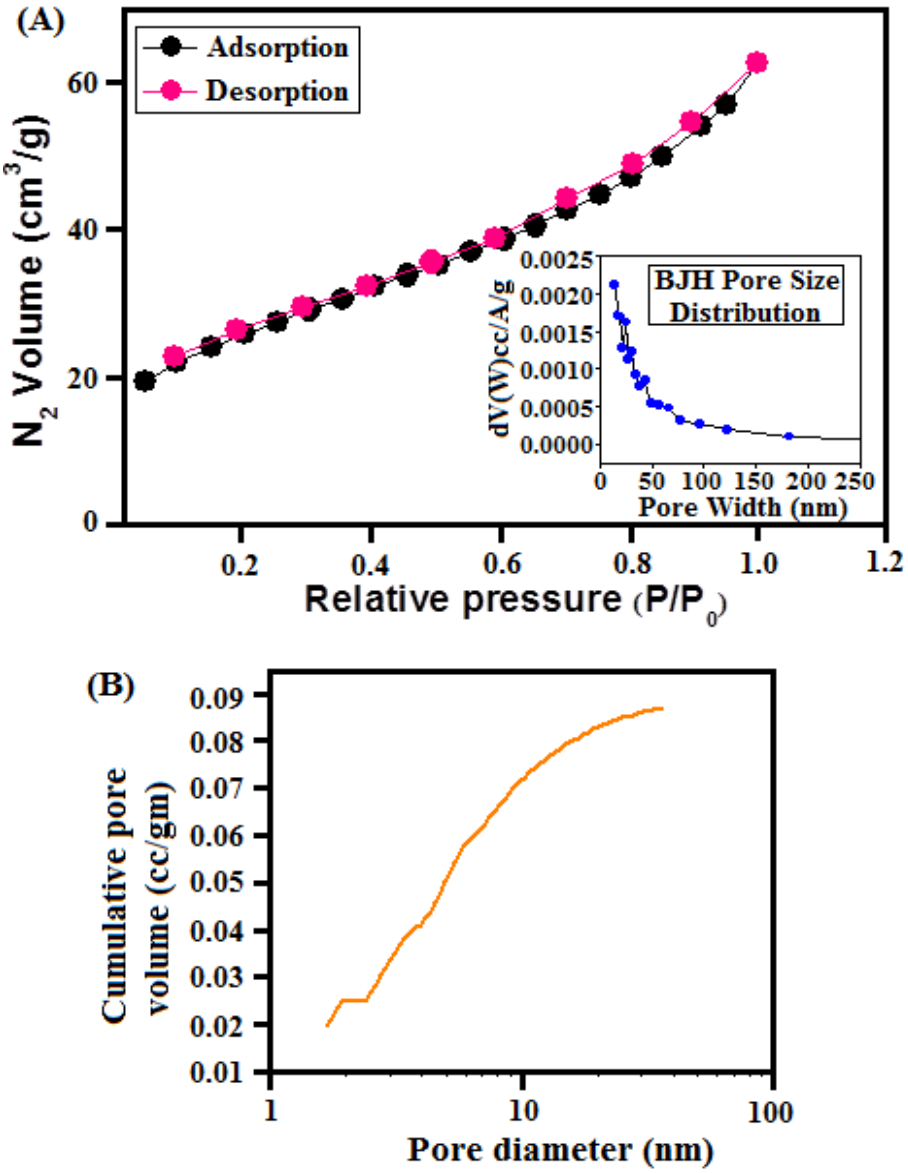

Figure 5.24. (A) BET and BJH (inset) plots and (B) penetration curve of optimal CH2 catalyst.

5.3.4.5. FTIR analyses

FTIR analyses of three Cr-HAp catalysts (CH4, CH3, CH2) are depicted in Figure 5.25. Cr-O vibration band was detected at 458 cm^{-1} and $Cr(PO_3)_3$ peaks could be located at 563 and 604 cm^{-1} (Prasad et al., 2012). Besides, vibration spectra corresponding to carbonate (of ram bone) were detected at 1402 and 1629 cm^{-1} (Ghobadian et al., 2009 and Sanli et al., 2015). Stretching and bending bands at 961 and 1031 cm^{-1} represented P-O (Chakraborty et al., 2011) bond. C-H band was recorded at 2915 cm^{-1} while stretching vibration at 3411 cm^{-1} (Ghobadian et al., 2009) represented the absorbed hydrate peaks. Thus, the FTIR analyses of the optimal Cr-BiHAP catalyst could detect the representative chemical species present in the prepared catalyst.

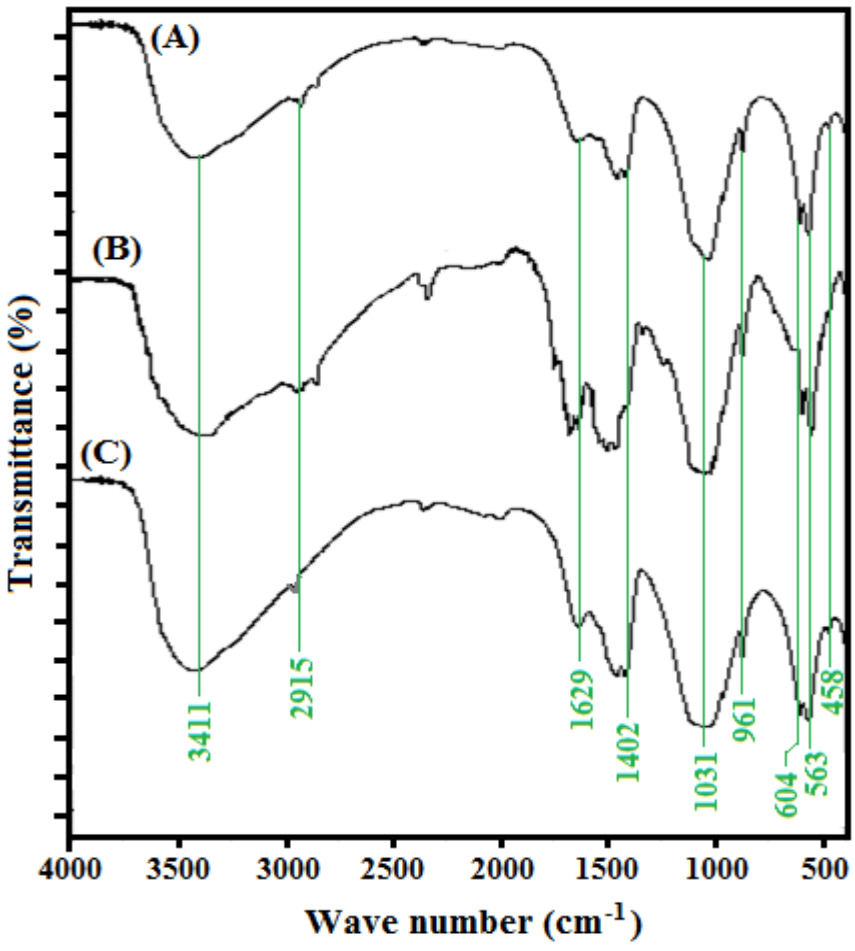

Figure 5.25. FTIR analyses of: (A) CH4, (B) CH3 and (C) CH2.

5.3.5. Catalyst reusability

At optimal process conditions, the CH2 catalyst could be reused upto fifth consecutive batch cycle (total 150 min reaction time) without any noticeable decrease in FAME yield. After fifth batch, the catalysts were washed by methanol and afterwards dried at 105 °C for 2 h and finally calcined over 1 h at 200 °C for regeneration. The resultant FAME yield (employing the regenerated catalyst) was observed to decrease from 96.85% to 95.56%. This could be ascribed to reduced catalytic activity due to leaching of Cr^{+3} ions into reaction mix as confirmed by ICP analysis.

5.3.6. Properties of B10 and B20 fuels produced from UFMO

Table 5.12. Fuel properties of B10 and B20 blends

Properties	**Specification of B6 − B20 (ASTM D7467-10)**	**B10**	**B20**
Flash point (°C)	52 (min)	98	112
Cetane number	40 (min)	45	51
Cloud point (°C)	report[a]	-1	1
Pour point (°C)	-3	-7	-10
Acid value (mg KOH/g)	0.3 (max)	0.14	0.19
Density	810 – 818	812	814
Kinematic viscosity (40 °C, mm²/s)	1.9 – 4.1	3.31	3.40

a Cloud point depends on place and time of year, and is not specified in ASTM D7467-10.

5.3.7. Engine performance tests

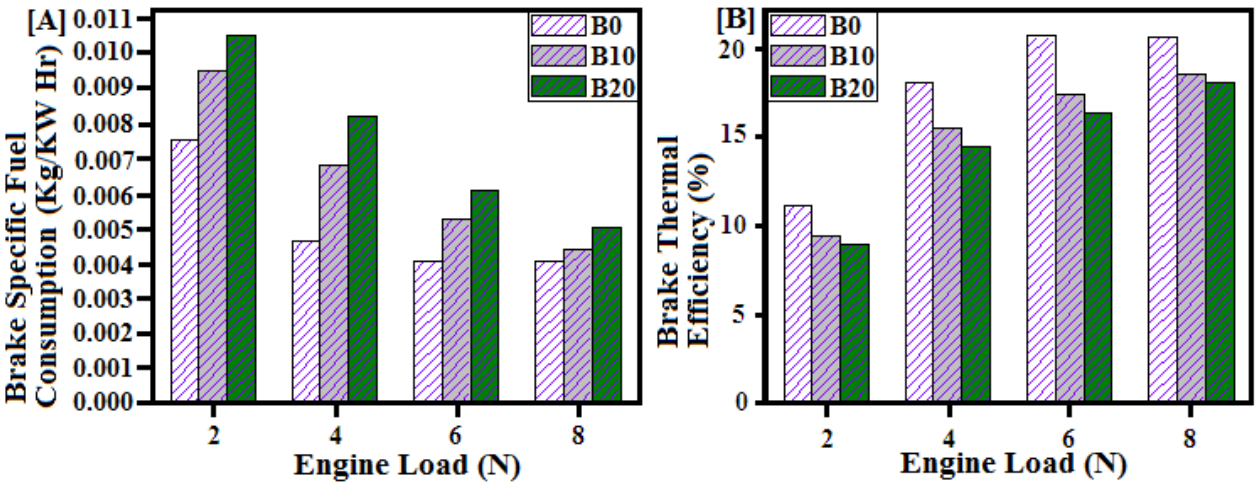

Figure 5.26. (A) Brake Specific Fuel Consumption and (B) Brake thermal efficiency as functions of Engine load.

Engine functioning tests were conducted for B0 (100 vol.% petrodiesel) and different blends of petrodiesel-biodiesel i.e. B10 (90 vol.% petrodiesel) and B20 (80 vol.% petrodiesel).

In Figure 5.26.(A) and (B), 'brake specific fuel consumption' (BFSC) and 'brake thermal efficiency' (BTE) respective patterns are compared amongst B0, B10 and B20. It was evident that, with increase in biodiesel proportion in the blended fuels, BSFC was found to increase while BTE was observed to decrease gradually. B0 exhibited the maximum BTE at different loadings, while B10 demonstrated 11.48% less BTE than B0 and B20 displayed 5.83% less BTE than B10 at the maximum load (8 N). This trend was more or less followed in all other loading conditions. Figure 5.26.A indicates gradual decrease in BFSC while Figure 5.26.B shows continuing increment in BTE with increase in engine load for all blends. It might also be noted that the difference in BFSC (Figure 5.26.A) among the different fuels became smaller at higher engine load. Thus, at higher engine loads, difference in engine performance

among B0, B10 and B20 became smaller. Hence, it may be concluded that at higher engine loads the blended fuels exhibit comparable engine performance with petro-diesel.

Figure 5.27.A and Figure 2.27.B respectively indicate that both engine exhaust temperature (EET) and fuel consumption (FC) increase with augmentation of engine load. Significantly, Figure 5.27.A implies a reduction in EET with increment in biodiesel proportion in the blended fuel. However, Figure 5.27.B suggests a modest enhancement in FC with increase in biodiesel part. Thus, the product biodiesel could partially substitute B0 (towards lessening dependence on B0) owing to favourable lower engine exhaust temperature. Moreover, considering the fact that the biodiesel was prepared from UFMO, a slightly higher value of fuel consumption could possibly be justified when considering from the perspective of waste valorisation. Notably, the reduction in EET due to blending of biodiesel, is a promising feature towards mitigation of global warming and climate change.

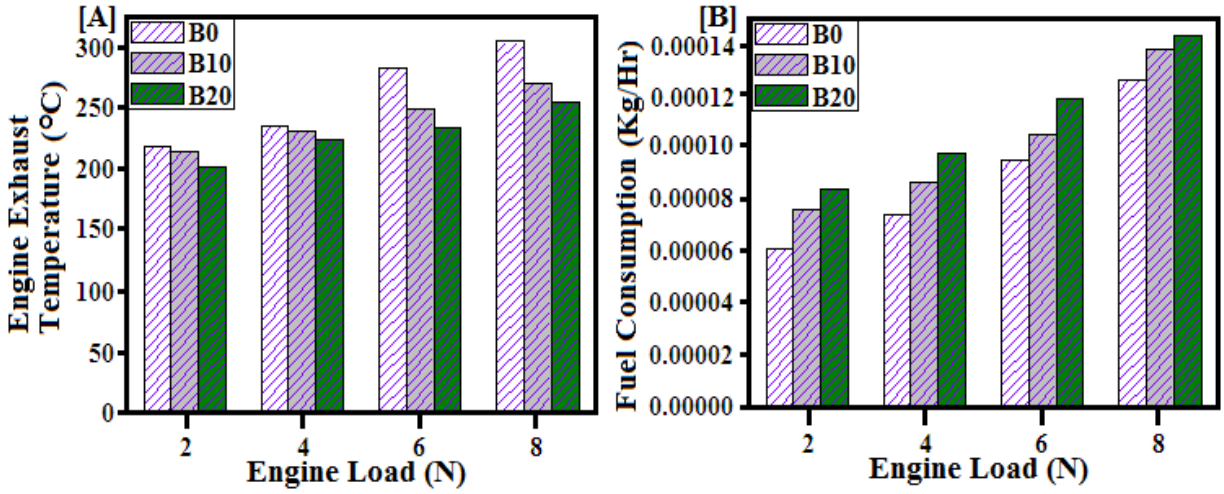

Figure 5.27. (A) Engine exhaust temperature and (B) Fuel consumption as functions of Engine load.

5.3.8. Emission Quality tests

CO emissions (Figure 5.28.A) were observed to gradually decrease with increase in biodiesel proportion and higher reduction in CO emission (for a specific fuel) was found at greater engine load over the entire range considered in the present study. On the other hand (Figure 5.28.B), CO_2 emission was observed to gradually increase with increase in biodiesel proportion and also with increment in engine load (for specific fuel). These observations clearly indicated that the fuel with higher biodiesel content, rendered more complete combustion and lower emission of toxic CO. Figure 5.28.C depicts somewhat higher O_2 emissions for biodiesel rich fuel at all engine load conditions (Prasad et al., 2012 and Chattopadhyay and Sen, 2013). This could be ascribed to the higher O_2 content of biodiesel in comparison with petrodiesel. Moreover, hydrocarbon (HC) emission was found to decrease (Figure 5.29A) while NO_X emission was noticed to increase (Figure 5.29B) with augmentation of biodiesel proportion in the blended fuel for a constant engine load. Notably, both HC and NOx emissions were found to increase with rise in engine load for any given fuel. Thus, use of biodiesel could be beneficial in terms of reduction of CO and HC emissions along with increase in O_2 emission. Nevertheless, suitable fuel additives could possibly be employed to reduce NOx emission.

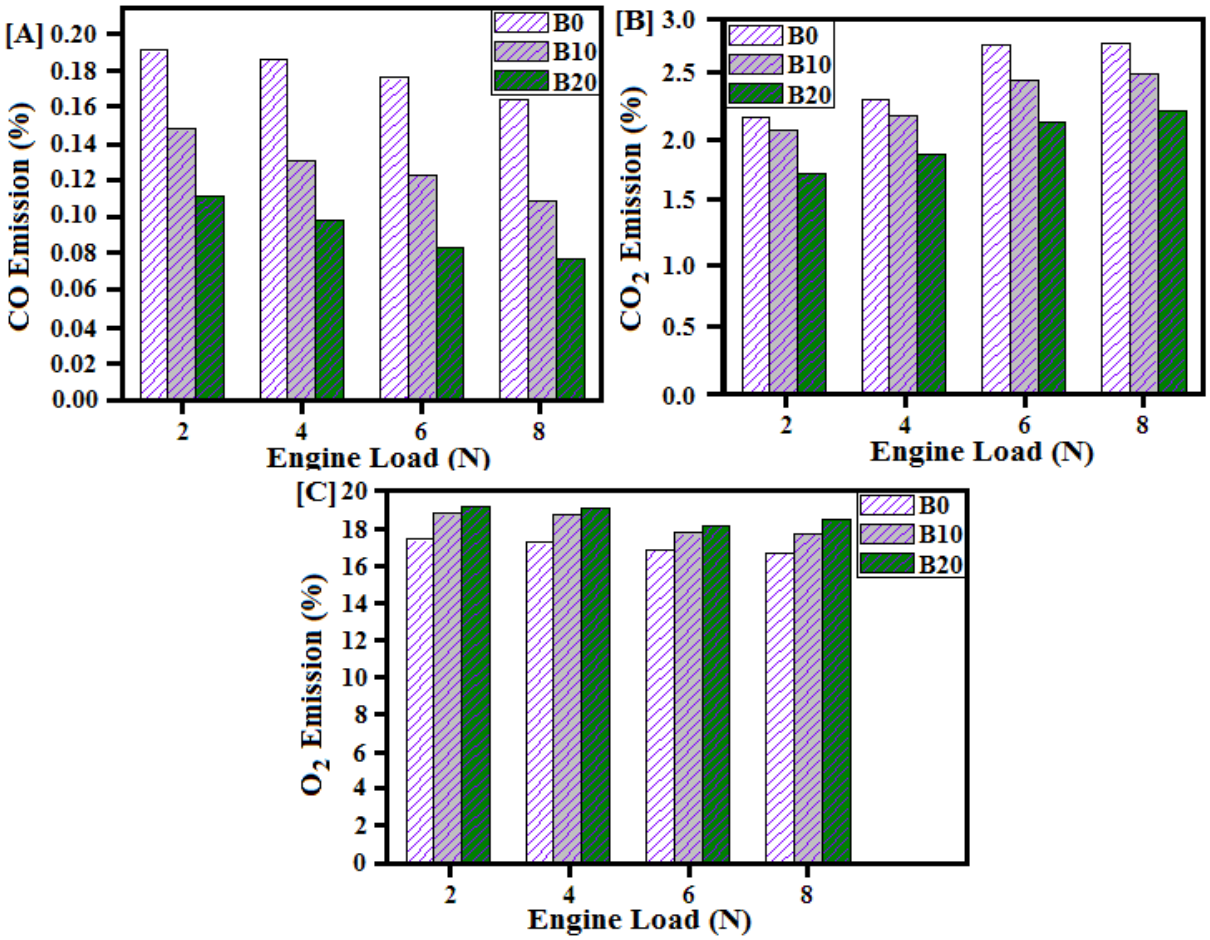

Figure 5.28. (A) CO (B) CO_2 and (C) O_2 emissions as functions of engine load.

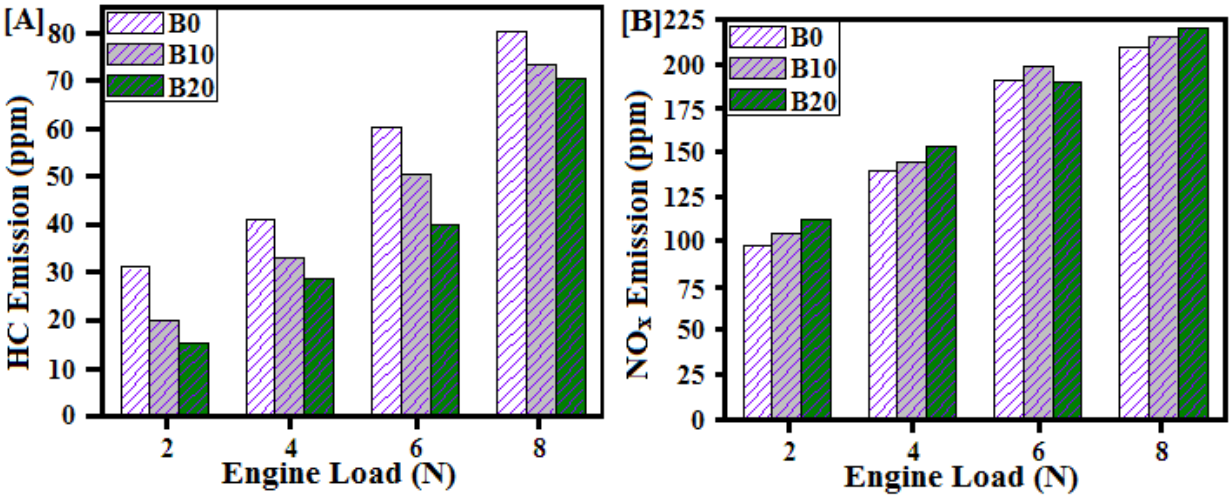

Figure 5.29. (A) HC and (B) NO_X emissions as functions of engine load.

References

Antolın, G., Tinaut, F.V., Briceno, Y., Castano, V., Perez, C. and Ramırez, A.I., 2002. Optimisation of biodiesel production by sunflower oil transesterification. Bioresource technology, 83(2), pp.111-114.

Bari, S. and Saad, I., 2014. Effect of guide vane height on the performance and emissions of a compression ignition (CI) engine run with biodiesel through simulation and experiment. Applied Energy, 136, pp.431-444.

Biju, V. and Khadar, M.A., 2003. Fourier transform infrared spectroscopy study of nanostructured nickel oxide. Spectrochimica Acta Part A: Molecular and Biomolecular Spectroscopy, 59(1), pp.121-134.

Chakraborty, R., Bepari, S. and Banerjee, A., 2011. Application of calcined waste fish (Labeo rohita) scale as low-cost heterogeneous catalyst for biodiesel synthesis. Bioresource technology, 102(3), pp.3610-3618.

Chakraborty, R. and Das, S.K., 2012. Optimization of biodiesel synthesis from waste frying soybean oil using fish scale-supported Ni catalyst. Industrial & Engineering Chemistry Research, 51(25), pp.8404-8414.

Chakraborty, R. and RoyChowdhury, D., 2013. Fish bone derived natural hydroxyapatite-supported copper acid catalyst: Taguchi optimization of semibatch oleic acid esterification. Chemical engineering journal, 215, pp.491-499.

Chakraborty, R., Das, S., Pradhan, P. and Mukhopadhyay, P., 2014. Prediction of Optimal Conditions in the Methanolysis of Mustard Oil for Biodiesel Production Using Cost-Effective Mg-Solid Catalysts. Industrial & Engineering Chemistry Research, 53(51), pp.19681-19689.

Chattopadhyay, S. and Sen, R., 2013. Fuel properties, engine performance and environmental benefits of biodiesel produced by a green process. Applied energy, 105, pp.319-326.

El-Naggar, M.R., El-Kamash, A.M., El-Dessouky, M.I. and Ghonaim, A.K., 2008. Two-step method for preparation of NaA-X zeolite blend from fly ash for removal of cesium ions. Journal of Hazardous Materials, 154(1-3), pp.963-972.

Engin, A.B., Özdemir, Ö., Turan, M. and Turan, A.Z., 2008. Color removal from textile dyebath effluents in a zeolite fixed bed reactor: Determination of optimum process conditions using Taguchi method. Journal of hazardous materials, 159(2-3), pp.348-353.

Fan, Y., Zhang, F.S. and Feng, Y., 2008. An effective adsorbent developed from municipal solid waste and coal co-combustion ash for As (V) removal from aqueous solution. Journal of hazardous materials, 159(2-3), pp.313-318.

Fuks, H., Kaczmarek, S.M. and Bosacka, M., 2010. EPR and IR investigations of some chromium (III) phosphate (V) compounds. Rev. Adv. Mater. Sci, 23, pp.57-63.

Ghobadian, B., Rahimi, H., Nikbakht, A.M., Najafi, G. and Yusaf, T.F., 2009. Diesel engine performance and exhaust emission analysis using waste cooking biodiesel fuel with an artificial neural network. Renewable energy, 34(4), pp.976-982.

Grosvenor, A.P., Biesinger, M.C., Smart, R.S.C. and McIntyre, N.S., 2006. New interpretations of XPS spectra of nickel metal and oxides. Surface Science, 600(9), pp.1771-1779.

Ismail, H.M., Ng, H.K., Gan, S. and Lucchini, T., 2013. Computational study of biodiesel–diesel fuel blends on emission characteristics for a light-duty diesel engine using OpenFOAM. Applied energy, 111, pp.827-841.

Jain, D., Khatri, C. and Rani, A., 2011. Synthesis and characterization of novel solid base catalyst from fly ash. Fuel, 90(6), pp.2083-2088.

Jain, D. and Rani, A., 2011. MgO enriched coal fly ash as highly active heterogeneous base catalyst for Claisen-Schmidt condensation reaction. Journal of the American Chemical Society, 1(2), pp.37-49.

Kusmiyati, K. and Sugiharto, A., 2010. Production of biodiesel from oleic acid and methanol by reactive distillation. Bulletin of Chemical Reaction Engineering & Catalysis, 5(1), pp.1-6.

Li, Y., Zhang, F.S. and Xiu, F.R., 2009. Arsenic (V) removal from aqueous system using adsorbent developed from a high iron-containing fly ash. Science of the total environment, 407(21), pp.5780-5786.

Mahmoudi, M., Simchi, A., Imani, M. and Hafeli, U.O., 2009. Superparamagnetic iron oxide nanoparticles with rigid cross-linked polyethylene glycol fumarate coating for application in imaging and drug delivery. The Journal of Physical Chemistry C, 113(19), pp.8124-8131.

Man, Y.C. and Setiowaty, G., 1999. Application of Fourier transform infrared spectroscopy to determine free fatty acid contents in palm olein. Food chemistry, 66(1), pp.109-114.

Mekala, M. and Goli, V.R., 2014. Comparative kinetics of esterification of methanol–acetic acid in the presence of liquid and solid catalysts. Asia-Pacific Journal of Chemical Engineering, 9(6), pp.791-799.

Palash, S.M., Kalam, M.A., Masjuki, H.H., Arbab, M.I., Masum, B.M. and Sanjid, A., 2014. Impacts of NOx reducing antioxidant additive on performance and emissions of a multi-cylinder diesel engine fueled with Jatropha biodiesel blends. Energy Conversion and Management, 77, pp.577-585.

Prasad, S.G., De, A. and De, U., 2011. Structural and optical investigations of radiation damage in transparent PET polymer films. International Journal of Spectroscopy, 2011.

Prasad, L., Pradhan, S., Das, L.M. and Naik, S.N., 2012. Experimental assessment of toxic phorbol ester in oil, biodiesel and seed cake of Jatropha curcas and use of biodiesel in diesel engine. Applied Energy, 93, pp.245-250.

Rahman, S.A., Masjuki, H.H., Kalam, M.A., Abedin, M.J., Sanjid, A. and Sajjad, H., 2013. Production of palm and Calophyllum inophyllum based biodiesel and investigation of blend performance and exhaust emission in an unmodified diesel engine at high idling conditions. Energy Conversion and Management, 76, pp.362-367.

Rohman, A. and Man, Y.C., 2010. Fourier transform infrared (FTIR) spectroscopy for analysis of extra virgin olive oil adulterated with palm oil. Food research international, 43(3), pp.886-892.

Sanli, H., Canakci, M., Alptekin, E., Turkcan, A. and Ozsezen, A.N., 2015. Effects of waste frying oil based methyl and ethyl ester biodiesel fuels on the performance, combustion and emission characteristics of a DI diesel engine. Fuel, 159, pp.179-187.

Sing, K.S., 1985. Reporting physisorption data for gas/solid systems with special reference to the determination of surface area and porosity (Recommendations 1984). Pure and applied chemistry, 57(4), pp.603-619.

Singh, A.K. and Fernando, S.D., 2008. Transesterification of soybean oil using heterogeneous catalysts. Energy & Fuels, 22(3), pp.2067-2069.

Sreeprasanth, P.S., Srivastava, R., Srinivas, D. and Ratnasamy, P., 2006. Hydrophobic, solid acid catalysts for production of biofuels and lubricants. Applied Catalysis A: General, 314(2), pp.148-159.

Sun, J., Caton, J.A. and Jacobs, T.J., 2010. Oxides of nitrogen emissions from biodiesel-fuelled diesel engines. Progress in Energy and Combustion Science, 36(6), pp.677-695.

Venkatesan, G., Kulasekharan, N., Muthukumar, V. and Iniyan, S., 2015. Regression analysis of a curved vane demister with Taguchi based optimization. Desalination, 370, pp.33-43.

Yu, L., Xiao, H. and Cheng, Y., 2008. Influence of magnesia on the structure and properties of MgO-Al2O3-SiO2-F− glass-ceramics. Ceramics International, 34(1), pp.63-68.

CHAPTER: 6

CONCLUSION

6. CONCLUSION

6.1. Fly ash supported Ni—Fe solid acid catalyst for efficient production of diesel additive: intensification through far-infrared radiation

Fly ash, a waste generated from coal based thermal power plant has been efficiently employed as a support for development of Ni—Fe solid acid cost-effective catalyst. The eco-friendly catalyst demonstrated superior performance in OA-methanol esterification in comparison with homogeneous H_2SO_4 catalyst and chemically prepared hydroxyapatite supported Fe solid acid catalyst. The prepared FA supported Ni—Fe $_{catalyst}$ displayed appreciable reusability attributes and thus, can be employed for a long reaction time suitable for continuous catalytic reactor application. Moreover the high acidity and appreciable morphological properties of the prepared catalyst indicates its suitability for application in other fatty acid esterification process. The application of far-infrared (FIR) radiation exhibited energy efficient, appreciable enhancement of OA conversion compared to conventional heating protocol. The energy efficient FIR radiation can possible applied to large scale similar reaction system pilot scale/ commercial scale development. Moreover FIR radiation can possible be applicable to other esterification reaction involving carbonic acids/ fatty acid and single chain or branch chain alcohol for productions of fuel additives and fine chemicals. A conversion compared to conventional heating protocol. The every efficient far infrared Thus, an efficient, cost-effective and reusable solid catalyst could be developed using FA, paving a greener pathway for effective management of such abundant industrial waste. The use of FA for preparation of highly proficient solid heterogeneous catalyst can be considered as a promising and attractive avenue for commercial purpose.

6.2. Optimization of fast and energy-efficient biodiesel production under infrared radiated from waste mustard oil catalysed by Amberlyst 15: Engine performance and emission quality assessments

It can be conclusively stated that far infrared (FIR) radiation could demonstrate significantly accelerated biodiesel yield from waste mustard oil in comparison with the conventional heating protocol under optimal process conditions derived through application of taguchi orthogonal design (TOD). The rapid production of biodiesel through the FIR-assisted route can save considerable amount of energy requirement, man-hour and thus, overall production cost making the process economically attractive. It can be expected that the outcome of this research will be benificial in developing efficient heterogeneous reactors for economical production of biodiesel. The engine performance results elucidate a trend indicating improved quality of blended fuel at particular proportions of biodiesel that can render superior engine performance and emission qualities conforming to Euro-VI standards. Thus, the accelerated biodiesel production through this novel energy-efficient and environment-friendly route facilitates achieving improved engine performance and emission norms while facilitating waste valorization for making a greener and cleaner world.

6.3 Optimal efficient biodiesel synthesis from used oil employing low-cost ram bone supported Cr catalyst: engine performance and exhaust assessment

The present work explores preparation of a cost-effective, waste ram bone supported Cr heterogeneous mesoporous (19.3 nm modal pore diameter) green catalyst possessing 98.45 m^2/g BET area and 0.78 mmol NH_3/g catalyst acid-site concentration with appreciable efficacy and reusability characteristics for sustainable synthesis of biodiesel from used frying mustard oil with high acid value of 5.3 mg KOH/g oil. The interaction effects among process factors and the optimal parametric values (4 wt.% catalyst concentration, 8.0 methanol/UFMO molar ratio and 200 °C catalyst calcination temperature) corresponding to maximum FAME yield were predicted precisely using D-optimal method. At the optimal conditions, the far infrared radiated heating system (FIRRHS) could render 96.85% FAME yield within only 30 min reaction time, which was remarkably higher than 40.22% FAME yield employing conventional heating system. Moreover, The FIRRHS demonstrated an energy-efficient protocol for biodiesel production as it consumed only 1/4th of the energy required in conventional heating system. The blends of product biodiesel and its blends with petro-diesel demonstrated promising engine performance by means of reduction in engine exhaust temperature while exhibiting acceptable brake specific fuel consumption and brake thermal efficiency at higher engine loads. Biodiesel rich fuel could advantageously reduce CO and HC concentrations while increasing O_2 content in engine exhaust emissions; thus, conforming to Euro-VI standards.

Table 6.1. Overview of properties and performance of the prepared catalysts

Activity	**1. Fly ash supported Ni—Fe solid acid catalyst for efficient production of diesel additive: intensification through far-infrared radiation**	**2. Optimal efficient biodiesel synthesis from used oil employing low-cost ram bone supported Cr catalyst: engine performance and exhaust assessment**
XRD	Fe_2O_3, Al_2SiO_5, Ni_2O_3 and NiS	$Cr_3(PO_4)_2$, Cr_2O_3, HAp and $Ca_{10}(PO_4)_6O$
BET	27.64m^2/g	98.45m^2/g
Pore volume	0.0233 cc/g	0.0586 cc/g
Mesopores	88.79%	71.53%
Reusability	Up to ninth times	Up to fifth times
Performance	98.37% oleic acid conversion	96.85% FAME yield
Optimal conditions	15:1 methanol/OA molar ratio, 1:15:2 nickel nitrate: ferric sulphate:FA (wt. ratio), 4 wt.% (of OA) catalyst concentration, 60 °C temperature under conventional heating and reaction time 1 h.	4 wt.% catalyst concentration, 8.0 methanol/UFMO molar ratio, 200 °C catalyst calcination temperature, 60 °C reaction temperature using energy-proficient infrared radiation and 30 min reaction time.

NOMENCLATURE

FFA = Free fatty acid

TG = Triglycerides

B100 = Pure biodiesel

GoI = Government of India

NBM = National Biodiesel Mission

FAME = Fatty acid methyl ester

HVO = Hydrogenated vegetable oil

UCO = Used cooking oil

FA = Fly ash

HAp = Hydroxyapatite

FIR = Far-infrared radiation

WCO = Waste cooking oil

OA = Oleic acid

CI = Compression-ignition

XRD = X-ray diffraction

BET = Brunner – Emmett –Teller

BJH = Barret, Joyner, Halenda

SEM = Scanning electron microscope

EDX = Energy-dispersive X-ray

XPS = X-ray photoelectron spectroscopy

RSM = Response surface methodology

FCCD = Face centered central composite design

MO = Methyl oleate

CHR = Conventionally heated reactor

SG = Silica gel

MS = Molecular sieve

FIRRR = Far-infrared radiated reactor

WMO = Waste mustard oil

TOD = Taguchi Orthogonal Design

FTIR = Fourier Transform Infrared

TGA = Thermo gravimetric Analysis

TPD = Temperature-programmed desorption

ANOVA = Analysis of variance

GC–MS = Gas chromatography–mass spectrometry

CTE = Concurrent transesterification-esterification

P_{FAME} = Purity of FAME

W_b = Weight (g) of biodiesel

W_O = Weight (g) of WMO;

Y_{FAME} = FAME yield of the product biodiesel

WRB = Waste ram bone

UFMO = Used fried mustard oil

Q_{MR} = Methanol/OA molar ratio

Q_L = $Fe_2(SO_4)_3.H_2O$ loading

Q_C = Catalyst concentration

N_{CT} = Calcination temperature

N_{CC} = Catalyst concentration

N_{MR} = Methanol/UFMO molar ratio

γ_{OA} = OA conversion (%)

λ_{MO} = WMO molar ratio

λ_{CC} = Catalyst concentration

λ_{SS} = Stirrer speed

Y_{FAME} = FAME Yield (%)

ψ_{FAME} = FAME content

S/N = Signal to noise ratio

$\overline{S/N}$ = Mean of the S/N ratio

AV_{OA} = Acid value of oleic acid

W_{UFMO} = Weight (g) of UFMO

SCOPE OF FUTURE WORK

SCOPE OF FUTURE WORK

- Investigations are required to explore the effects of impregnation of some noble metals such as Rh, Ru, Ti as promoter(s) for preparation of natural-HAp or FA supported multi-metallic catalyst(s) for more efficient biodiesel and diesel additive(s) production. This noble metal catalyst viz. supported TiO_2 will have photo catalytic effect which will help in promoting superior catalytic activity under electromagnetic radiation. This noble metal catalyst can have better reusability attributes and longer catalyst life span.
- Instead of using commercially available reagent grade silica and alumina, FA was employed as a cheap resource of silica and alumina. The use of FA could render the cost-effective of solid, reusable catalyst. Thus, metals viz. Cd, Ti, Zn –can be impregnated on FA to prepare cost-effective nano- photocatalyst for further study.
- Scale-up of the laboratory scale batch reactors for pilot scale batch production. The infrared batch reactor used in the present investigation can be used for bench scale/pilot scale process through following standard scale up principles by using large impellers and reactor vessel along with application of enhanced power of infrared radiator, keeping the power to volume ratio constant.
- Determination of heterogeneous reaction kinetics of esterification and transesterification reactions pertaining to conversion of waste cooking oil/animal fat to biodiesel under conventional heating as well energy-efficient electromagnetic radiation. The heterogeneous catalytic reaction kinetics can be evaluated according to Eley-Ridel(ER) model. Besides Pseudo homogeneous higher order or 1^{st} order (considering high amount of excess alcohol in the

reaction mixture) reaction rate equation may be developed for specific reaction condition together with evaluation of reaction activation energy.

- Design and development of laboratory and pilot/commercial scale flow reactor(s) e.g. catalytic packed bed reactor using the evaluated kinetic parameters (for augmentation of biodiesel production capacity). The solid heterogeneous power catalyst can be formed into pellets or other standard shapes for utilization in fixed bed catalytic reactor for production of biodiesel/fuel additives in continuous mode to active enhanced manufacturing capacity. Residence time distribution (RTD) analysis for the packed bed reactor should be performed to predict the real performance of the packed bed flow reactor using standard models i.e, dispersion model.
- Investigations may be conducted to explore the usefulness of new low-cost inedible vegetable oil(s)/animal fat(s) as potential feedstock for biodiesel production. Besides using low cost heterogeneous acid catalyst, further investigation are required to utilized new inedible vegetable oil and animal fats from different resources for cost effective biodiesel production coupled with sustainable waste management. However, the supply chain management of such waste derived fat o
- r oily feedstock should be explored with the help of different stake holder i.e., upper local body (ULB) and other government and private organizations.
- Sustainable syntheses of useful fatty acid esters are required for improvement in biodiesel properties. Branched chain monohydric alcohol can be used with commonly available Fatty acid i.e. oleic, stearic acid , linoleic acid, linolenic acid etc. to produce esters with better cold flow property for blending with biodiesel/ diesel for improving lubricity, pore point and cloud point.